ADAPTIVE SECOND ORDER SLIDING MODE CONTROL STRATEGIES FOR UNCERTAIN SYSTEMS

SANJOY MONDAL

ADAPTIVE SECOND ORDER SLIDING MODE CONTROL STRATEGIES FOR UNCERTAIN SYSTEMS

A

Thesis Submitted

in Partial Fulfilment of the Requirements

for the Degree of

DOCTOR OF PHILOSOPHY

By

SANJOY MONDAL

Department of Electronics and Electrical Engineering

Indian Institute of Technology Guwahati

Guwahati - 781 039, INDIA.

July, 2012

Certificate

This is to certify that the thesis entitled "**ADAPTIVE SECOND ORDER SLIDING MODE CONTROL STRATEGIES FOR UNCERTAIN SYSTEMS**", submitted by **Sanjoy Mondal** (08610202), a research scholar in the *Department of Electronics and Electrical Engineering, Indian Institute of Technology Guwahati*, for the award of the degree of **Doctor of Philosophy**, is a record of an original research work carried out by him under my supervision and guidance. The thesis has fulfilled all requirements as per the regulations of the Institute and in my opinion has reached the standard needed for submission. The results embodied in this thesis have not been submitted to any other University or Institute for the award of any degree or diploma.

Dated:

Guwahati.

Dr. Chitralekha Mahanta
Professor
Dept. of Electronics and Electrical Engg.
Indian Institute of Technology Guwahati
Guwahati - 781039, India.

To the memory of my father Ashok Kumar Mondal

Acknowledgement

First and foremost, I feel it as a great privilege in expressing my deepest and most sincere gratitude to my supervisor Dr. Chitralekha Mahanta, for her excellent guidance. Her kindness, dedication, friendly accessibility and attention to details have been a great inspiration to me. My heartfelt thanks to my supervisor for the unlimited support and patience shown to me. I would particularly like to thank for all her help in patiently and carefully correcting all my manuscripts.

I am also very thankful to my doctoral committee members Prof. R. Bhattacharjee, Prof. S. Majhi and Prof. S. K. Dwivedy for sparing their precious time to evaluate the progress of my work. Their suggestions have been valuable. I would also like to thank other faculty members of EEE Dept. for their kind help during my academic work. I am grateful to all the members of the research and technical staff of the department without whose help I could not have completed this thesis.

Thanks go out to all my friends in the Control and Instrumentation Laboratory. They have always been around to provide useful suggestions, companionship and created a peaceful research environment.

My friends at IITG made my life joyful and were constant source of encouragement. Among my friends, I would like to extend my special thanks to Ali, Senthil, Utkal, Kuntal, Om Prakash, Nagesh, Asish, Rajib Panigharhi, Sayantan, Rajib Jana and Sanjeev. My work definitely would not have been possible without their love and care which helped me to enjoy my new life in IITG. Special thanks also go to Dola Govind Pradhan, Bajrangbali, Mandar, Mridul, Madhulika, Tausif, Basudev and Arghya for their help during my stay.

My deepest gratitude goes to my family for the continuous love and support showered on me throughout. The opportunities that they have given me and their unlimited sacrifices are the reasons for my being where I am and what I have accomplished so far.

Abstract

The main objective of this thesis is to develop robust sliding mode control strategies for uncertain systems. More specifically, the aim of this thesis is to develop sliding mode control schemes which are successful in controlling systems affected by both matched and mismatched types of uncertainty. One major drawback suffered by conventional sliding mode controllers is the presence of high frequency oscillations in the control input known as chattering. Because of the discontinuous control action in sliding mode controllers, chattering becomes an inherent undesired phenomenon. Apart from chattering, another disadvantage faced by conventional sliding mode controllers is their design prerequisite of advance knowledge about the upper bound of the system uncertainty. This thesis is an attempt to provide solution for these two main limitations of conventional first order sliding mode controllers. The central focus of this thesis is to improve upon the existing sliding mode control techniques with the prime objective of chattering mitigation. An adaptive gain tuning mechanism which can estimate the uncertainty adaptively is proposed in this thesis. Hence prior knowledge about the upper bound of system uncertainty is no longer a necessary requirement in the proposed adaptive sliding mode controller. The basic idea of the proposed adaptive sliding mode controller is that the discontinuous sign function is made to act on the time derivative of the control input and the actual control signal obtained after integration is continuous and hence chattering is removed. The adaptive gain tuning strategy ensures that the controller gain is not overestimated. Based upon the core idea of adaptive sliding mode, various classes of sliding mode controllers are proposed in this thesis. In order to ensure smooth control action throughout the entire operating range, this thesis proposes an adaptive integral sliding mode controller. The integral sliding mode (ISM) algorithm eliminates the reaching phase. Therefore, invariance towards matched disturbances can be ensured from the very beginning by using this method. The proposed adaptive sliding mode control methodology is used to control nonlinear multiple input multiple output (MIMO) systems which are highly cross-coupled. The proposed con-

troller is used for stabilization as well as trajectory tracking of coupled MIMO systems affected by both matched and mismatched uncertainty. Experimental studies are conducted on a single degree of freedom (DOF) vertical take-off and landing (VTOL) aircraft system to study the real time performance of the proposed adaptive sliding mode (SM) controller. The design prerequisite of the proposed controller is complete knowledge about the state vector which is not available in this example. Hence unavailable states of the 1 DOF VTOL are estimated by using an extended state observer (ESO). It is a well established fact that finite time convergence of terminal sliding mode (TSM) control exists and can be proved if a detailed mathematical analysis of its behaviour near the singularities is available. However, TSM suffers from the drawback of chattering like in conventional first order sliding mode. The proposed adaptive sliding mode strategy is used to design a terminal sliding mode controller for linear and nonlinear uncertain systems. To improve the transient performance of uncertain systems, a nonlinear sliding surface based adaptive chattering free sliding mode controller is proposed. The nonlinear sliding surface changes the system's closed loop damping ratio from its initial low value to a final high value in accordance with the error magnitude. Hence fast initial response and gradually diminishing overshoot are ensured. This thesis extends the nonlinear sliding surface based integral sliding mode (ISM) controller to the discrete domain also where the controller consists of a nominal control and ISM based discontinuous control. The nominal control is designed based on composite nonlinear feedback (CNF) which varies the damping ratio of the closed loop system to ensure good transient performance. The discontinuous control component rejects the matched disturbances and model mismatches. Simulation studies are conducted involving linear and nonlinear, SISO and MIMO systems affected by both matched and mismatched types of uncertainty and their results demonstrate the effectiveness of the proposed adaptive chattering free sliding mode controller.

Contents

List of Figures

List of Tables

List of Acronyms

CNF	Composite nonlinear feedback
DC	Direct current
DISM	Discrete integral sliding mode
DSM	Discrete time sliding mode
DSMC	Discrete time sliding mode control
HOSM	Higher order sliding mode
HS	Horizontal subsystem
IAE	Integral absolute error
ISM	Integral sliding mode
LTI	Linear time invariant
MIMO	Multiple input multiple output
NTSM	Nonsingular terminal sliding mode
PI	Proportional integral
PID	Proportional integral derivative
SISO	Single input single output
SMC	Sliding mode control
SOSM	Second order sliding mode
SOTSM	Second order terminal sliding mode
TRMS	Twin rotor MIMO system
TV	Total variation
VS	Vertical subsystem
VSC	Variable structure control
VTOL	Vertical take-off and landing

List of Symbols

A	System matrix of continuous time LTI system
$a_{11}, a_{12}, a_{21}, a_{22}$	System matrices in regular form
B	Input matrix of continuous time LTI system
T_r	Transformation matrix
C, C_1	Output matrix
c_1, c_2	Sliding surface parameters
c^T	Switching surface parameters
e	Error between actual and desired values
$f(x), g(x)$	Uncertain nonlinear functions
$\epsilon, \varepsilon, \gamma, \kappa, \eta, \nu, \varrho$	Small positive constant
τ	Sampling time
I	Identity matrix
ϕ	System matrix of discrete time LTI system
Γ	Input matrix of discrete time LTI system
n	Number of states of an LTI system model
P, W	Positive definite matrices
Q, K	Positive definite diagonal matrices
F, G, L, B_g, W_g, B^+	Matrices
Υ	Nonlinear function
s, σ	Sliding surface
R^n	Real vector space of dimension n
$R^{n\times m}$	Real vector space of dimension $n \times m$
u	Control input
V, V_1	Lyapunov function

x	System state
m	Number of inputs of an LTI system model
$\|\| \cdot \|\|$	Euclidian norm for vectors and spectral norm for matrices
$sign(\cdot)$	Signum function
y	System output
z_d	Desired output
z	State vector in regular form
ρ, d	System uncertainty/disturbance
ξ	Damping ratio
$K^{\dagger}, \alpha, \beta$	Positive constant/matrix
ω_n	Natural frequency of oscillations

List of Publications

Refereed Journals

1. S. Mondal and C. Mahanta, "Adaptive Second order Terminal Sliding Mode Controller for Robotic Manipulators", *Journal of the Franklin Institute, Elsevier*, Accepted.

2. S. Mondal and C. Mahanta, "Chattering Free Adaptive Multivariable Sliding Mode Controller for Systems with Matched and Mismatched Uncertainty", *ISA Transactions, Elsevier*, 52(3), pp. 335-341, 2013.

3. S. Mondal and C. Mahanta, "Adaptive Integral Higher Order Sliding Mode Controller for Uncertain Systems", *Journal of Control Theory Applications, Springer*, 11(1), pp. 61-68, 2013.

4. S. Mondal and C. Mahanta, "Adaptive second-order sliding mode controller for a twin rotor multi-input-multi-output system", *IET Control Theory & Applications*, vol. 6(14), pp. 2157-2167, 2012.

5. S. Mondal and C. Mahanta, "A Fast Converging Robust Controller using Adaptive Second Order Sliding Mode", *ISA Transactions, Elsevier*, vol. 51(6), pp. 713-721, 2012.

6. S. Mondal and C. Mahanta, "Composite Nonlinear Feedback based Discrete Integral Sliding Mode Controller for Uncertain Systems", *Communications in Nonlinear Science and Numerical Simulation, Elsevier*, vol. 17(3), pp. 1320-1331, 2012.

7. S. Mondal and C. Mahanta, "Nonlinear Sliding Surface based Second Order Sliding Mode Controller for Uncertain Linear Systems", *Communications in Nonlinear Science and Numerical Simulation, Elsevier*, vol. 16(9), pp. 3760-3769, 2011.

Conference Proceedings

1. S. Mondal, and C. Mahanta, "Observer based Sliding Mode Control Strategy for Vertical Take-Off and Landing (VTOL) Aircraft System", *8th IEEE Conference on Industrial Electronics and Applications (ICIEA),* pp. 1-5, 19-21 June, 2013, Melbourne, Australia.

2. S. Mondal, T.V. Gokul and C. Mahanta, "Adaptive Second Order Sliding Mode Controller for Vertical Take-off and Landing Aircraft System", *6th International Conference on Industrial and Information Systems (ICIIS),* pp. 1-5, 6-9 August, 2012, IITMadras, India.

3. S. Mondal, T.V. Gokul and C. Mahanta, "Chattering Free Sliding Mode Controller for Mismatched Uncertain System", *6th International Conference on Industrial and Information Systems (ICIIS),* pp. 1-5, 6-9 August, 2012, IITMadras, India.

4. S. Mondal and C. Mahanta, "Improved Adaptive Control of Nonlinear Uncertain Systems Through Second Order Sliding Mode Controller", *Proc. 12th IEEE Workshop on Variable Structure Systems,* pp. 100-104, 12-14 January, 2012, Mumbai, India.

5. S. Mondal and C. Mahanta, "Second Order Sliding Mode Controller for Twin Rotor MIMO System", *Proc. INDICON 2011,* pp. 1-5, 17-18 December, 2011, Hyderabad, India.

6. S. Mondal and C. Mahanta,"Controlling Uncertain Systems with Variable Gain based Second Order Integral Sliding Mode Controller", *Proc. National Systems Conference 2011 (NSC 2011),* 9-11 December, 2011, Bhubaneswar, India.

7. S. Mondal and C. Mahanta, "Nonlinear Feedback Based Discrete Integral Sliding Mode Controller for Linear Uncertain System", *Proc. National Systems Conference 2010 (NSC 2010),* 10-12 December, 2010, Surathkal, India.

8. S. Mondal and C. Mahanta, "Discrete-time Sliding Mode Tracking Control for Uncertain Systems", *Proc. 4th International Conference on Computer Applications in Electrical Engineering Recent Advances*, 19-21 February, 2010, IIT Roorkee, India.

1

Introduction

Contents

1.1 Introduction

In reality, all physical systems are affected by uncertainties occurring due to modeling error, parametric variation and external disturbance. Controlling dynamical systems in presence of uncertainties is extremely difficult as performance of the controller degrades and the system may even be driven to instability. As such, active research is continuing to develop controllers which can work successfully in spite of uncertainties. Robust control techniques such as nonlinear adaptive control [9], model predictive control [10], backstepping [11] and sliding mode control [12, 13] have evolved to deal with uncertainties. These control techniques are capable of achieving the specified control objectives in spite of modeling errors and parametric uncertainties affecting the controlled system. Beginning in the late 1970s and continuing till today, the sliding mode control (SMC) [14, 15] methodology has received wide attention because of its inherent insensitivity to parametric variations and external disturbances. The sliding mode control (SMC) is a particular type of variable structure control system (VSCS) which uses a discontinuous control input. Recently many successful practical applications of sliding mode control (SMC) have established the importance of sliding mode theory. Sliding mode controllers are now-a-days widely used in a variety of application areas like robotics, process control, aerospace and power electronics [16, 17]. The research in this held was initiated by Emel'yanov and his colleagues [14] and the design paradigm now forms a mature and established approach for robust control and estimation. The idea of sliding mode control (SMC) was not known to the control community at large until an article published by Utkin [15] and a book by Itkis [18].

Design of the SMC involves two key steps, viz. (1) the design of a sliding surface in accordance with the desired closed loop performance and (2) the design of a suitable control law. The sliding surface is to be designed optimally to satisfy all constraints and required specifications. The initial phase when the state trajectory is directed towards the sliding surface is called the reaching phase. During the reaching phase, the system is sensitive to all types of disturbances. However, a control law can be designed which ensures finite time reaching of the sliding surface even in the presence of uncertainties and disturbances. For eliminating the non-robust reaching phase, an integral sliding mode was proposed in [19, 20] which naturally allowed SMC to be combined with other techniques. The main advantages of the SMC are the following:

(i) During the sliding mode, the system is insensitive to matched model uncertainties and disturbances [21].

(ii) When the system is on the sliding manifold, it behaves as a reduced order system with respect to the original plant.

However, in spite of the claimed robustness, implementation of the SMC in real time is handicapped by a major drawback known as chattering which is the high frequency bang-bang type of control action. Chattering is caused due to the fast dynamics which are usually neglected in the ideal model of sliding mode. In the ideal sliding mode, the control is assumed to switch with an infinite frequency. However, in actual plants, due to the inertia of actuators and sensors as well as the presence of nonlinearities, the switching occurs with high but finite frequency only. The main consequence is that the sliding mode takes place in a small neighborhood of the sliding manifold, whose dimension is inversely proportional to the control switching frequency. In sliding mode, due to the finite switching of control signal, the states would switch about the sliding surface rather than lie directly on it. This switching can occur at a high frequency and is called chattering. The effect of chattering is that the high frequency components of the control propagate through the system and thereby excite the unmodeled fast dynamics and give rise to undesired oscillations which affect the system output. This can degrade the system performance or may even lead to instability. Moreover, the term chattering has been designated to indicate the bad effect, potentially disruptive, that a switching control can produce on a controlled mechanical plant. Chattering as well as the necessity of discontinuous control are two main criticisms against practical realization of sliding mode control scheme. These drawbacks are more prominent while dealing with mechanical systems since rapidly changing control actions induce stress and wear in mechanical parts and the system may even suffer breakdown in a short time [22].

1.2 Motivation and purpose

In order to overcome the above mentioned drawbacks, efforts are on to find a continuous control action which is robust against uncertainties and guarantees the same control objective as offered by the standard sliding mode approach. Different approaches have been proposed to avoid chattering [21,23]. The main idea of such approaches was to change the dynamics in a small vicinity of the discontinuity surface in order to avoid real discontinuity and, at the same time, to preserve the main properties of the whole system. However, the ultimate accuracy and robustness of the sliding mode are partially lost in this process. The commonly used approach is by using continuous approximations of the sign$(\cdot)$ function (such as the sat$(\cdot)$ function, the tanh$(\cdot)$ function) in the implementation of the control

law. An interesting approach evolved for elimination of chattering was the higher order sliding mode methodology introduced by Arie Levant [24–26]. The higher order sliding modes generalize the basic sliding mode idea by acting directly on the higher order time derivatives of the sliding variable instead of influencing its first time derivative only as it happens in standard sliding modes. Keeping the main advantages of the original approach, higher order sliding modes remove the chattering effect and provide even higher accuracy. A number of higher order sliding mode controllers are proposed in the literature [12, 25–29]. However, the main constraint in implementation of higher order sliding modes is the increasing information demand. In general, any r-th order sliding mode controller requires the knowledge of the time derivatives of the sliding variable up to the (r-1)-th order. The only exceptions are provided by the twisting controller [24], the super twisting controller [24] and the sub-optimal algorithm. Among higher order sliding mode controllers, second order sliding mode controllers are the most widely used because of their simplicity and low information demand. In second order sliding mode methodology, the control action affects directly the sign and the amplitude of the sliding variable and a suitable switching logic guarantees the finite time convergence of the state to the sliding manifold.

Sliding mode control [30] has been extensively used in control systems perturbed by matched uncertainty which enters the system through the input channel. However, designing sliding mode controllers for systems perturbed by the mismatched type of uncertainty, which is due to perturbations in the system parameters, still remains a challenge to the research community. The difficulty lies in the fact that the dynamics of the uncertain system are affected even after reaching the sliding mode. Active research is continuing in the control community for developing sliding mode controllers for systems affected by mismatched type of uncertainty. By designing a sliding mode controller for certain states of the system which are provided as inputs to a reduced order system can take care of mismatched uncertainties. However, the disadvantage of this method is that uncertainties should lie in the range space of certain matrix of the nominal system [30]. A fuzzy logic based sliding mode controller proposed in [31] was successful in achieving quadratic stability for systems with mismatched uncertainty. Even this method could handle mismatched uncertainty of a certain form only provided its bound was known apriori [32, 33]. By introducing two sets of switching surfaces for the subsystems and hence reducing the rank of the uncertainty, asymptotic stability was achieved in [34]. Dynamic output feedback sliding mode controllers were attempted in [35] and nonlinear integral type sliding surface was

used to deal with mismatched uncertainties in [36]. All these works required prior knowledge about the upper bound of the mismatched uncertainty which was in general difficult to obtain. Hence a strategy to obtain the upper bound of the system uncertainty or a method which does not require this knowledge is needed. The adaptive sliding mode controller proposed by Cheng at al. [3,37,38] provided a solution to this problem. However, this adaptive method yielded gains which were overestimated in many cases giving rise to large control efforts and high chattering [39, 40].

Motivated by the above reasons, this thesis attempts to develop suitable sliding mode control strategies which can eliminate chattering. In particular, this thesis aims for designing chattering free sliding mode controllers which can effectively handle systems with uncertainties of both matched and mismatched type, without requiring the prior knowledge about the upper bound of the uncertainty. The effectiveness of the developed sliding mode control scheme is validated by applying the controller to important benchmark control problems like the twin rotor MIMO system (TRMS), the vertical take-off and landing system (VTOL) and the two-link robotic manipulator which are typical examples of highly nonlinear systems affected by severe uncertainties.

1.3 Contributions of this Thesis

The main contribution of this thesis is the design of a chattering free adaptive sliding mode controller for systems affected by both matched and mismatched types of uncertainty. The control law is designed in such a way that the discontinuous sign function acts on the time derivative of the control input. So the actual control obtained after integration is continuous and hence chattering is eliminated. Adaptive tuning mechanism is used to estimate the upper bound of the uncertainty, thereby eliminating the necessity of its prior knowledge. The proposed idea of adaptive chattering free sliding mode is used to design integral and terminal sliding mode controllers. A nonlinear sliding surface based adaptive sliding mode controller is proposed for improving transient performances like overshoot and settling time.

1.4 Organization of the Thesis

This thesis is divided into seven chapters. A brief description about each chapter is presented in this section.

- **Chapter 2:** A few preliminary and basic concepts related to sliding mode control are discussed in Chapter 2.

- **Chapter 3:** In this chapter a chattering free adaptive integral sliding mode controller for uncertain systems is proposed. Instead of a regular control input, the derivative of the control input is used in the proposed control law. The discontinuous sign function in the controller is made to act on the time derivative of the control input. The actual control signal obtained by integrating the derivative control signal is smooth and chattering free. The adaptive tuning law used in the proposed controller eliminates the need of prior knowledge about the upper bound of the system uncertainty.

- **Chapter 4:** In this chapter an adaptive sliding mode controller for coupled multi input multi output (MIMO) systems affected by both matched and mismatched uncertainties is proposed. More specifically, the problem of controlling a twin rotor MIMO system (TRMS) in cross-coupled condition is addressed using adaptive sliding mode control technique. An adaptive mechanism is embedded in the controller as well as the sliding surface to overcome the perturbations. The proposed controller with adaptive sliding surface is implemented for a vertical take-off and landing (VTOL) aircraft system affected by matched and mismatched uncertainties. An adaptive gain tuning mechanism is used to ensure that the gain is not overestimated with respect to the actual unknown value of the uncertainty. A case study was conducted on the laboratory set-up of a 1 degree of freedom VTOL system to investigate the real time performance of the proposed adaptive sliding mode controller.

- **Chapter 5:** In this chapter an adaptive chattering free terminal sliding mode controller is proposed to ensure fast and finite time stabilization of uncertain systems. Instead of the normal control input, its time derivative is used in the proposed controller. An adaptive tuning method is utilized to deal with the system uncertainties whose upper bounds are not required to be known in advance.

- **Chapter 6:** An adaptive sliding mode controller is proposed in this chapter using nonlinear sliding surface which ensures better transient performance over linear sliding surfaces. One major benefit is that chattering is completely removed from the control signal. To improve the performance of discrete time uncertain systems, an algorithm based on integral sliding mode (ISM)

and composite nonlinear feedback (CNF) is proposed. The discrete CNF based ISM method ensures fast rise time and less overshoot as compared to ISM method with linear feedback.

- **Chapter 7:** In this chapter conclusions from the research work are drawn and the scope for future research is outlined.

2

Preliminary Concepts

Contents

2.1 Introduction

In this chapter, preliminary concepts relevant to sliding mode control are discussed briefly. The necessary fundamentals of the sliding mode are explained concisely so that the sliding mode controller design and analysis carried out in the succeeding chapters can be easily followed. Chattering phenomenon which is an undesired phenomenon occurring in conventional sliding mode controller is explained and methods devised for chattering mitigation are introduced. Finite time stability which is an important notion in sliding mode control is described. First and second order sliding modes are explained to highlight the basic difference between the two.

2.2 Variable Structure System and Sliding Mode

A variable structure system (VSS) [15] is a dynamical system whose structure changes according to an appropriate switching logic in order to exploit the desirable properties of these structures. To illustrate, let us consider the following dynamical system

$$\dot{x} = f(t, x, u) \tag{2.1}$$

where $x \in R^n$ are the state variables and $u \in R^m$ is the control input.
Further,

$$u = [u_1(t, x), u_2(t, x), ..., u_m(t, x)]^T \tag{2.2}$$

where

$$u_i = \begin{cases} u_i^+(t, x), & if \quad \sigma_i(x) > 0 \\ u_i^-(t, x), & if \quad \sigma_i(x) < 0 \\ & i = 1, 2, ...m \end{cases} \tag{2.3}$$

Here

$$\sigma(x) = [\sigma_1(x) \quad \sigma_2(x)....\sigma_m(x)]^T \tag{2.4}$$

is the sliding manifold and $\sigma_i(x) = 0 (i = 1, 2, ...m)$ is the i-th sliding surface. The motion on the sliding manifold $\sigma(x) = 0$ is called the sliding mode.

The differential equation (2.1) does not formally satisfy the classical theorem on the existence and

uniqueness of the solution since it has discontinuous right hand side. Moreover, the right hand side is usually not defined on the discontinuity surfaces. Thus, it fails to satisfy conventional existence and uniqueness results of differential equation theory. Nevertheless, an important aspect of sliding mode control design is the assumption that the system state behaves in a unique way when restricted to $\sigma(x) = 0$. Therefore, the problem of existence and uniqueness of differential equations with discontinuous right hand sides is of fundamental importance. Various types of existence and uniqueness theorems are proposed by Utkin [15], Itkis [18], Hajeck [41] and Filippov [42]. The method of Filippov [42] is conceptually straightforward. This method is now briefly recalled to help in understanding variable structure system behaviour on the switching surface.

Let us now consider an n-th order VSS system with a single input as given below,

$$\dot{x} = f(t, x, u) \tag{2.5}$$

with the following general control strategy

$$u = \begin{cases} u^+(t,x), & if \quad \sigma(x) > 0 \\ u^-(t,x), & if \quad \sigma(x) < 0 \end{cases} \tag{2.6}$$

The system dynamics are not directly defined on the manifold $\sigma(x) = 0$. It has been shown by Filippov that the state trajectories of (2.5) with control (2.6) on $\sigma(x) = 0$ are the solutions of the equation

$$\dot{x} = \alpha f^+ + (1-\alpha) f^- = f^0; \quad 0 \leq \alpha \leq 1 \tag{2.7}$$

where $f^+ = f(t, x, u^+)$, $f^- = f(t, x, u^-)$ and f^0 is the resulting velocity vector of the state trajectory while in sliding mode. The term α is a function of the system state and can be specified in such a way that the average dynamic of f^0 is tangent to the surface $\sigma(x) = 0$. The geometric concept is illustrated in Fig. 2.1.

Therefore it may be concluded that, on the average, the solution to (2.5) with control (2.6) exists and is uniquely defined on $\sigma(x) = 0$. This solution is called solution in the Filippov sense. It may be noted that this technique can be used to determine the behaviour of the plant in a sliding mode.

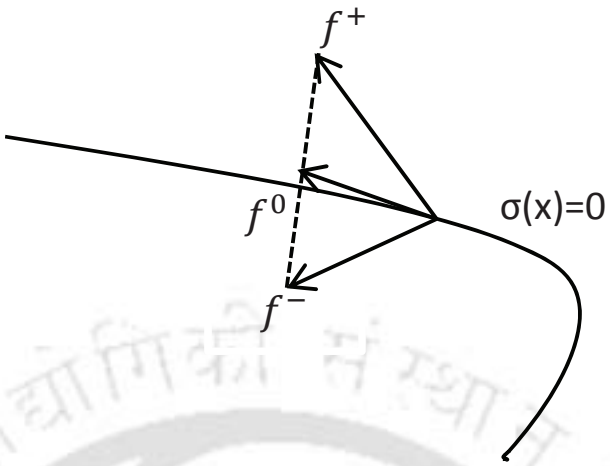

Figure 2.1: Illustration of Filippov method

2.3 Stability of the Sliding mode

The objective of sliding mode control is to ensure sliding motion in finite time from an arbitrary initial condition. The system state must approach the sliding surface at least asymptotically. The largest such neighborhood is called the region of attraction. Stability of the sliding surface requires to choose a generalized Lyapunov function $V(t,x)$ which is positive definite and has a negative time derivative in the region of attraction. Unfortunately, there are no standard methods to find Lyapunov functions for arbitrary nonlinear systems.

For all single input systems, a suitable Lyapunov function can be chosen as

$$V(t,x) = \frac{1}{2}\sigma^2(x) \tag{2.8}$$

which clearly is globally positive definite.

If

$$\dot{V}(t,x) = \sigma(x)\dot{\sigma}(x) < 0 \tag{2.9}$$

in the domain of attraction, then the state trajectory converges to the sliding surface and is restricted to the surface for all subsequent time. This latter condition is called the reaching or reachability condition [12] [22] [30] [43] and it ensures that the sliding manifold is reached asymptotically.

A strong condition for finite time reaching is given as follows

$$\dot{V}(t,x) = \sigma(x)\dot{\sigma}(x) \leq -\eta|\sigma(x)| \tag{2.10}$$

for some $\eta > 0$, known as η reachability condition in the literature. For a general m input system, it is not necessary to ensure sliding mode on each discontinuity surface but sliding mode should exist on the intersection of all discontinuity surfaces. These conditions ascertain that sliding surfaces remain attractive.

2.4 Relative Degree in Sliding Mode

***Definition* 2.1.** *A smooth autonomous single input single output (SISO) system* $\dot{x} = a(t,x) + b(t,x)u$ *with the control* u *and output* σ *is said to have the relative degree* r*, if the Lie derivatives locally satisfy the conditions [44]*

$$L_b\sigma = L_aL_b\sigma = ... = L_a^{r-2}L_b\sigma = 0, \quad L_a^{r-1}L_b\sigma \neq 0. \tag{2.11}$$

It can be shown that the equality of the relative degree to r actually means that $\sigma, \dot{\sigma}, ..., \sigma^{(r-1)}$ do not depend on control and can be taken as a part of new local coordinates and $\sigma^{(r)}$ linearly depends on u with the nonzero coefficient $L_a^{r-1}L_b\sigma$.

2.5 Order of the sliding mode

The standard sliding mode can be implemented only if the relative degree of the sliding variable is 1, i.e. control has to appear in its first total time derivative $\dot{\sigma}$. Another problem of the standard sliding mode is that the high frequency switching in the control may cause dangerous vibrations called chattering. The sliding mode order approach [24] addresses both these issues of relative degree restriction and chattering while preserving the features of the sliding mode. The sliding order characterizes the dynamics smoothness degree in the vicinity of the sliding mode and can be defined as given below:

***Definition* 2.2.** *Let us consider a discontinuous differential equation* $\dot{x} = f(t,x)$ *understood in the Filippov sense [42] and* $\sigma(x)$ *is a smooth function. Then, provided that*

1. $\sigma, \dot{\sigma}, ..., \sigma^{(r-1)}$ are continuous functions of x,

2. the set

$$\sigma = \dot{\sigma} = \ddot{\sigma} = ... = \sigma^{(r-1)} = 0 \tag{2.12}$$

is a non-empty integral set,

the motion on set (2.12) is said to exist in r-sliding (rth-order sliding) mode [24] [45]. The set (2.12) is called r-sliding set. It is said that the sliding order is strictly r, if the next derivative $\sigma^{(r)}$ is discontinuous or does not exist as a single-valued function of x.

2.6 Finite time stability

The standard sliding mode used in the traditional VSSs is of the first order (σ is continuous and $\dot{\sigma}$ is discontinuous). The standard sliding mode design suggests choosing a new auxiliary sliding variable of the first relative degree. That variable is usually a linear combination of the sliding variable σ and its successive total time derivatives [23], which leads to only exponential stabilization of σ. The finite time stabilization corresponds to the high order sliding mode (HOSM) approach [24] [27]. Asymptotically stable HOSMs arise in systems with traditional sliding mode control, if the relative degree of the sliding variable σ is higher than 1. An important property which concerns asymptotic stability is finite time stability (FTS), i.e. the solutions of a system which reach the equilibrium point in finite time. Finite time stability is preferable, since it offers higher robustness and higher accuracy in presence of small sampling noises and delays. The concept of finite time stability corresponding to high order sliding mode (HOSM) is explicitly discussed in [46] [47] [48] [49] [50] [51]. A simple definition of finite time stability as given in [47] is stated below:

The main idea of finite time stability lies in assigning infinite eigenvalue to the closed loop system at the origin and therefore the right hand side of the ordinary differential equation can not be locally Lipschitz at the origin. Also there exists the settling time function $T(x_0)$ where x_0 is the initial condition that determines time for a solution to reach the equilibrium. This settling time function (in general) depends on the initial condition of a solution.

Let us consider the following example [49] [50] [51]

$$\dot{x} = -|x|^a sgn(x) \qquad x \in R^n, \tag{2.13}$$

for which the solutions are ($a \in]0, 1[$):

$$x(t, x_0) = \begin{cases} s(t, x_0), \ if \quad 0 \leq t \leq \frac{|x_0|^{1-a}}{1-a} \\ 0, \qquad\quad if \quad t > \frac{|x_0|^{1-a}}{1-a} \end{cases} \tag{2.14}$$

with $s(t, x_0) = sgn(x_0)(|x_0|^{1-a} - t(1-a))^{\frac{1}{1-a}}$ and they reach the origin in finite time. The time required for the solutions to reach the equilibrium is called the settling time which depends on the initial condition of the solution.

***Definition* 2.3.** *Finite time stability of continuous autonomous systems [49] [50] [51]*

Let us consider the continuous autonomous system

$$\dot{x} = f(x), \qquad x \in R^n \tag{2.15}$$

The origin of the system (2.15) is finite time stable (on an open neighbourhood $\mathcal{V} \subset R^n$) if [52]:

- there exits a function $T : \mathcal{V} \setminus \{0\} \to R_{\geq 0}$ such that if $x_0 \in \mathcal{V} \setminus \{0\}$ then $\Phi^{x_0}(t)$ is defined (and in particular is unique) on $[0, T(x_0))$, $\Phi^{x_0}(t) \in \mathcal{V} \setminus \{0\}$ for all $t \in [0, T(x_0))$ and $\lim_{t \to T(x_0)} \Phi^{x_0}(t) = 0$. The quantity T is called settling time function of system (2.15).
- for all $\epsilon > 0$, there exists a function $\delta(\epsilon) > 0$, for every $x_0 \in (\delta(\epsilon)B^n \setminus \{0\}) \bigcap \mathcal{V}$, $\Phi^{x_0}(t) \in \epsilon B^n$ for all $t \in [0, T(x_0))$

where B is the unit open ball in R^n centered at the origin and $\Phi^{x_0}(t)$ denotes a solution of system (2.15) starting from $x_0 \in R^n$ at $t = 0$.

***Definition* 2.4.** *Finite time stability of discontinuous systems [52]*

Let us consider the differential inclusion

$$\dot{x} \in F(x), \ x \in R^n \tag{2.16}$$

where F is a set valued function on R^n, $\dot{x}$ denotes the right derivative of x. The origin of (2.16) is finite time stable if

- the origin of the system (2.16) is stable : if for all $\epsilon > 0$, there is $\delta(\epsilon) > 0$ such that if $x_0 \in \delta(\epsilon)B^n$, then any solution ϕ^{x_0} starting at x_0 is defined for all $t \geq 0$ and $\phi^{x_0}(t) \in \epsilon B^n$ for all $t \geq 0$,
- there exists $T_0 : \mathcal{S} \to R_{\geq 0}$, such that for all solutions $\phi^{x_0} \in S(x_0)$, $\phi^{x_0}(t) = 0$ for all $t \geq T_0(\phi^{x_0})$. T_0 is the settling time of the solution ϕ^{x_0}.

Here $\phi^{x_0}(t)$ represents a solution of system (2.16) starting from x_0, $S(x_0)$ is the set of all solutions ϕ^{x_0} and space $S = \bigcup_{x_0 \in R^n} S(x_0)$.
If $T(x) = \sup_{\phi^x \in S(x)} T_0(\phi^x) < +\infty$, then $T(x)$ is the time for the solution ϕ^x to reach the origin called the settling time function of system (2.16).

2.7 Chattering

In real life applications, it is not reasonable to assume that the control signal can switch at infinite frequency. Due to the presence of inertia in actuators and sensors, surrounding noise and exogenous disturbances, actually the control signal commutes at a very high though finite frequency. The control signal's oscillation frequency turns out to be not only finite but also almost unpredictable. Its main consequence is that the sliding mode takes place in a small neighbourhood of the sliding manifold whose width is inversely proportional to the control switching frequency [12] [22] [30].
The notions of ideal and real sliding mode are adopted here to distinguish the sliding motion that occurs ideally on the sliding manifold (assuming ideal control devices) from a sliding motion that, due to the non-idealities of the control law implementation, takes place in a vicinity of the sliding manifold, which is called the boundary layer (illustrated in Fig. 2.2).
The effect of the finite switching frequency of the control is referred in the literature as chattering [53] [54] [55]. Basically, the high frequency components of the control propagate through the system, thereby exciting the unmodeled fast dynamics resulting in undesired oscillations which affect the system output. This phenomenon degrades the system performance or may even lead to instability. The term chattering has also been designated to indicate the potentially disruptive affect that a switching control force or torque can produce on a controlled mechanical plant [23] [27] [55] [56]. Chattering and high control activity are the major drawbacks of the sliding mode approach in the practical realization of sliding mode control schemes. Active research is continuing to realize a continuous control action which can overcome these drawbacks and ensure robustness against uncertainties

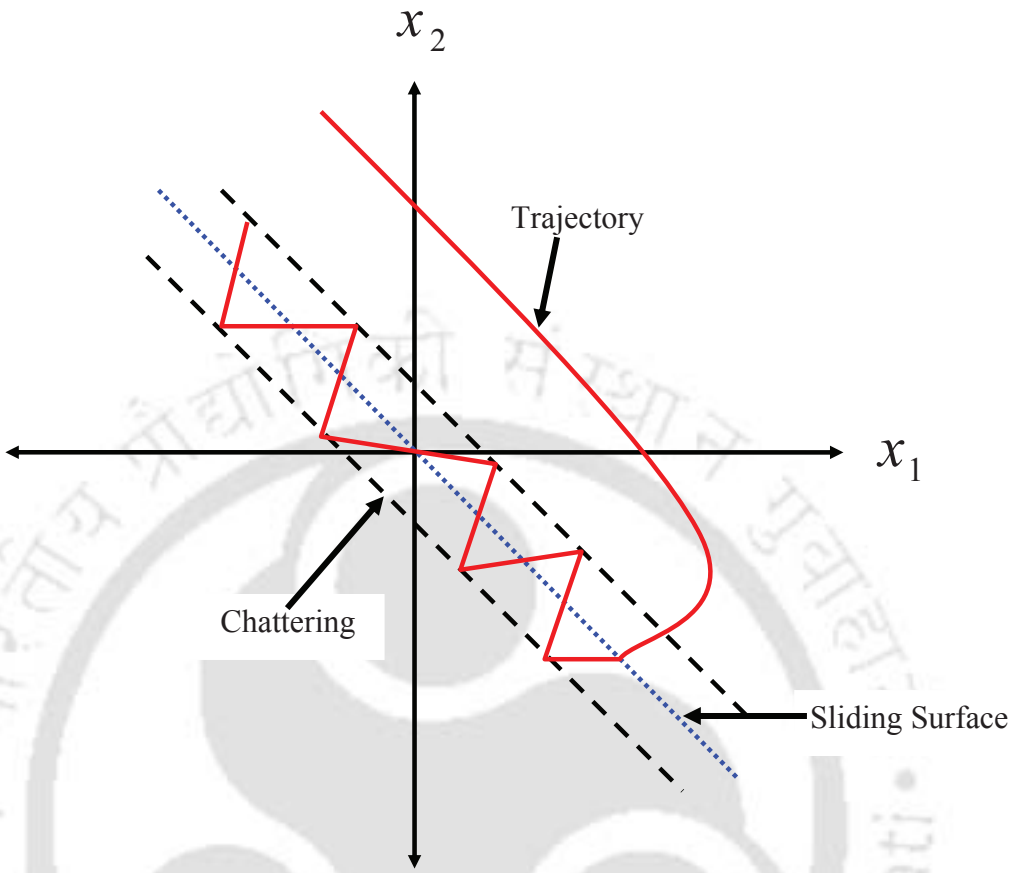

Figure 2.2: The chattering effect

and disturbances and at the same time achieve the same control objective of the standard sliding mode approach [24] [28] [57].

The most practised approach for chattering mitigation is based on the use of continuous approximations of the sign() function (such as the sat() function, the tanh()function) in the implementation of the control law. However, by using this method, the insensitivity feature of sliding mode control is lost. In this method, the system possesses robustness that is a function of the boundary layer width. It is pointed out in [23] [58] that this methodology is highly sensitive to the unmodeled fast dynamics and in some cases it may lead to unacceptable performance. An interesting class of smoothing functions, characterized by time varying parameters, was proposed in [59] while attempting to find a compromise between chattering mitigation and possible excitation of the unmodeled dynamics. In summary, continuation approaches eliminate high frequency chattering at the price of losing invariance

towards uncertainty. One effective approach for chattering elimination is by using the second order sliding mode methodology [24] [27].

2.8 Summary

In this chapter, basic concepts and properties of sliding modes have been discussed concisely. The main advantages of the sliding mode control technique are the simplicity in both implementation and design and the inherent robustness with respect to matched internal and external uncertainties and disturbances.

3

Adaptive Integral Sliding Mode Controller

Contents

3.1 Introduction

Sliding mode control (SMC), developed from the variable structure system theory, has gained much more attention for its robustness against parameter variations and external disturbances under matching conditions [30, 43, 60]. In sliding mode control (SMC), the system states are moved from their initial states towards a chosen manifold in the state space, called the sliding surface [30, 43]. After reaching the sliding manifold, the system becomes totally insensitive to parametric uncertainties and external disturbances. The motion of the trajectory from the initial condition towards the sliding surface until it hits the sliding surface is called the reaching phase. During the reaching phase, the system is not robust and even matched uncertainty can affect the system performance. To solve this problem, an integral sliding mode (ISM) concept was proposed in [19].

In integral sliding mode control method, an integral term was incorporated in the sliding manifold which guaranteed that the system trajectories would start in the manifold itself from the initial time and thus the reaching phase was totally eliminated. Hence the system became invariant towards the matching uncertainty right from the beginning.

Although the ISM controller guarantees robustness against system uncertainty, the crucial part is the control discontinuity leading to chattering as explained in Chapter 2. Another difficulty faced by the ISM controller is the necessity of prior knowledge about the upper bound of the system uncertainty. In real time application it is very difficult to get the upper bound of the uncertainty and often this bound is overestimated yielding to excessive gain.

For circumventing the above difficulties, this chapter proposes an integral sliding surface based chattering free sliding mode controller which uses an adaptive tuning law. The main attributes of the proposed controller are robustness and smooth control signal. An adaptive tuning law is used for the controller to estimate the unknown but bounded system uncertainties. As such the upper bounds of the system uncertainties are not required to be known in advance. Moreover, the chattering in the control input is eliminated by using the proposed controller.

The brief outline of this chapter is as follows. Section 3.2 briefly discusses the design problem and the assumptions made. In Section 3.3, the proposed adaptive integral sliding mode control method is described. Section 3.4 presents simulation examples to demonstrate the efficiency and advantages of the proposed controller. A brief summary of the chapter is presented in Section 3.5.

3.2 Problem Definition

A class of nonlinear dynamic system is considered as follows:

$$\begin{aligned} \dot{x} &= f(x) + g(x)u \\ y &= \sigma(x) \end{aligned} \tag{3.1}$$

where $x \in R^n$ are the state variables, $u \in R$ is the control input and $\sigma(x) \in R$ is the measured output function known as the sliding variable. It is assumed that $f(x)$ and $g(x)$ are smooth functions.

Let the system have a relative degree r with respect to the output variable σ which means that Lie derivatives $L_g\sigma; L_f L_g\sigma; ...; L_f^{r-2} L_g\sigma$ are equal to zero identically in the vicinity of a given point and $L_f^{r-1} L_g\sigma$ is not zero at the point. The equality of the relative degree to r means, in a simplified way, that u first appears explicitly only in the r-th total time derivative of σ.

***Remark* 3.1** *For simplicity, the relative degree of the system (3.1) is assumed to be equal to the order of the sliding surface.*

***Assumption* 3.1** *The relative degree r of the system (3.1) is known a priori.*

***Assumption* 3.2** *An exact robust differentiator is available for exactly measuring or estimating the derivative of variables.*

The aim of the first order sliding mode control is to force the state trajectories to move along the sliding manifold $\sigma(x) = 0$. In the higher order sliding mode control, the purpose is to move the states along the switching surface $\sigma(x) = 0$ and to keep its $(r-1)$ successive time derivatives viz $\dot{\sigma}, \ddot{\sigma}, ..., \sigma^{(r-1)}$ to zero by using a suitable discontinuous control action [24]. The r-th order derivative of $\sigma(x)$ satisfies the following equation,

$$\sigma^{(r)}(x) = a(x) + b(x)u \tag{3.2}$$

where r is the relative degree, $a(x) = L_f^r \sigma(x)$ and $b(x) = L_f^{r-1} L_g \sigma(x)$. Here L_f and L_g are the Lie derivatives [25] of the smooth functions in (3.1).

The r-th order sliding mode control of the system (3.1) with respect to the sliding variable $\sigma(x)$ can be expressed as [61],

$$\begin{aligned} \dot{z}_i &= z_{i+1} \\ \dot{z}_r &= a(x) + b(x)u \end{aligned} \tag{3.3}$$

where $1 \leq i \leq r-1$ and $[z_1, z_2, ..., z_r]^T = [\sigma(x), \dot{\sigma}(x), ..., \sigma^{(r-1)}(x)]^T$

***Assumption* 3.3.** *Matrices $a(x)$ and $b(x)$ consist of the nominal parts ($\bar{a}(x)$, $\bar{b}(x)$) which are known apriori and uncertain parts ($\Delta a(x)$, $\Delta b(x)$) which are bounded and unknown [62].*

Thus the following can be written,

$$\begin{aligned} a(x) &= \bar{a}(x) + \Delta a(x) \\ b(x) &= \bar{b}(x) + \Delta b(x) \end{aligned} \tag{3.4}$$

$$\begin{aligned} \sigma^{(r)}(x) &= (\bar{a} + \Delta a)(x) + (\bar{b} + \Delta b)(x)u \\ &= \bar{a}(x) + \bar{b}(x)u + \Delta F(x,t) \end{aligned} \tag{3.5}$$

where $\Delta F(x,t) = \Delta a(x) + \Delta b(x)u$ includes all the uncertain parameters and external disturbance. Using (3.4) and (3.5) with z as the state variable, the r-th order sliding mode control for the system (3.1) can be written as,

$$\begin{aligned} \dot{z}_i &= z_{i+1} \\ \dot{z}_r &= \bar{a}(z) + \bar{b}(z)u + \Delta F(z,t) \end{aligned} \tag{3.6}$$

In the regular form, the above can be written as,

$$\dot{z} = \bar{A}(z) + \bar{B}(z)u + \Delta F(z,t) \tag{3.7}$$

where $z = [z_1 \;\; z_2 ... z_i .. z_r]^T$, and $\bar{A}(z)$, $\bar{B}(z)$ are matrices with proper dimension. The uncertainties in the system due to modeling error and parameter variation are denoted by $\Delta F(z,t)$ which is assumed to be differentiable with respect to time. In this problem, the uncertainties in the system (3.6) are assumed to meet the matching conditions. Then $\Delta F(z,t) \in span\{\bar{B}(z)\}$ [30] meaning that $\Delta F(z,t)$ is a matched uncertainty.

3.3 Design of adaptive integral sliding mode controller

The design procedure for the overall control signal is carried out in two parts, design of the nominal control w_{nom} and then design of the overall control law u. At first, the nominal control law w_{nom} is designed that guarantees finite time stabilization of the chain of integrators in absence of uncertainties.

Then the reaching law based overall control law is designed to reject the uncertainties and maintain the sliding mode.

3.3.1 Finite time stabilization of an integrator chain system

Let us consider the nominal system which is represented by the single input single output (SISO) integrator chain as described below,

$$\begin{aligned} \dot{z}_1 &= z_2 \\ \dot{z}_2 &= z_3 \\ &\cdot \\ \dot{z}_r &= w_{nom} \end{aligned} \tag{3.8}$$

The control objective is to drive the states of (3.8) to $z = 0$ at the fixed finite time [63].

***Theorem* 3.1**. *Let $k_1, k_2, ...k_n > 0$ be such that the polynomial $\phi(\lambda) = \lambda^n + k_n\lambda^{n-1} + ... + k_2\lambda + k_1$ is Hurwitz. For the system (3.8), there exists a value $\varepsilon \in (0, 1)$ such that for every $\alpha_i \in (1 - \varepsilon, 1)$, $i = 1, 2, ...n$, the origin is a globally stable equilibrium in finite time under the feedback*

$$w_{nom}(z) = -k_1 sign(z_1)|z_1|^{\alpha_1} - k_2 sign(z_2)|z_2|^{\alpha_2} - ... - k_n sign(z_n)|z_n|^{\alpha_n} \tag{3.9}$$

where $\alpha_1, ...\alpha_n$ satisfy

$\alpha_{i-1} = \frac{\alpha_i\alpha_{i+1}}{2\alpha_{i+1} - \alpha_i}$, $i = 2, ..., n$ with $\alpha_{n+1} = 1$ [63].

3.3.2 Design of integral sliding mode controller

However, when the system is perturbed or uncertain, the finite time stabilization is not ensured [63]. In this section a reaching law based discontinuous control law is developed which rejects the uncertainties of the system and ensures that the control objectives are fulfilled [62].

Let us consider an integral sliding surface,

$$s(z) = z_n - z_n(0) - \int w_{nom}(z)dt \tag{3.10}$$

The initial condition of the system is defined by $z_n(0)$. The nominal control w_{nom} ensures the convergence of the chain of integrators in finite time as given in Theorem 3.1.

By taking the time derivative of (3.10), the following is obtained,

$$\begin{aligned} \dot{s}(z) &= \dot{z}_n - w_{nom} \\ &= \bar{a}(z) + \bar{b}(z)u + \Delta F(z,t) - w_{nom} \end{aligned} \tag{3.11}$$

Using (3.11) and the constant rate reaching law $\dot{s}(z) = -Gsign(s(z))$ [30] such that it satisfies the reachability condition $s(z)\dot{s}(z) \leq -\eta|s(z)|$ where η being a positive constant yields,

$$-Gsign(s(z)) = \bar{a}(z) + \bar{b}(z)u - w_{nom} \tag{3.12}$$

Here G is the switching gain. The control law described above ensures finite time stabilization of the system states and also rejects the uncertainties if $G > |\Delta F(z,t)|$. Hence the overall control law can be obtained as [62],

$$u = \bar{b}(z)^{-1}\{-\bar{a}(z) + w_{nom} - Gsign(s(z))\} \tag{3.13}$$

However, the high frequency chattering is always present in the control signal.

In order to remove the undesired chattering in the control input, an adaptive integral chattering free sliding mode controller is developed. In the proposed controller, the time derivative of the control input, $\dot{u}$ would be designed to act on the higher order derivatives of the sliding variable [64,65]. Hence instead of the actual control u, the time derivative of the control, $\dot{u}$ would be used as the control input. The new control $v = \dot{u}$ would be designed as a discontinuous signal, but its integral (the actual control u) would be continuous thereby eliminating the high frequency chattering.

Now taking the first order time derivative of (3.11) yields,

$$\ddot{s}(z) = \ddot{z}_n - \dot{w}_{nom} \tag{3.14}$$

Using (3.2), (3.14) can be written as,

$$\begin{aligned} \ddot{s}(z) &= \frac{d}{dt}(\bar{a}(z) + \bar{b}(z)u) - \dot{w}_{nom} \\ &= \dot{\bar{a}}(z) + \dot{\bar{b}}(z)u + \bar{b}(z)\dot{u} - \dot{w}_{nom} \\ &= \dot{\bar{a}}(z) + \dot{\bar{b}}(z)u + \bar{b}(z)\dot{u} - \dot{w}_{nom} + \Delta\dot{F}(z,t) \end{aligned} \tag{3.15}$$

Assuming $y_1 = s(z)$ and $y_2 = \dot{s}(z)$, the system dynamics can be written as [66, 67],

$$\begin{aligned} \dot{y}_1 &= y_2 \\ \dot{y}_2 &= \Phi[z,u] + \Psi[z]v \end{aligned} \tag{3.16}$$

where $v = \dot{u}$ and $\Phi[z,u]$ collects all the uncertain terms not involving $\dot{u}$, i.e. $\Phi[z,u] = \dot{\bar{a}}(z) + \dot{\bar{b}}(z)u - \dot{w}_{nom} + \Delta\dot{F}(z,t)$ and $\Psi[z] = \bar{b}(z)$. Thus the system (3.16) becomes a chain of integrators controlled by the input v. So a sliding mode controller for the above system can be designed to keep the system trajectories on the sliding manifold by using the control input v. To design an SMC for the system (3.16), the sliding function is considered as,

$$\sigma = y_2 + \kappa y_1 \tag{3.17}$$

where κ is a positive constant. The derivative of (3.17) is obtained as,

$$\dot{\sigma} = \dot{y}_2 + \kappa \dot{y}_1 \tag{3.18}$$

Using (3.18) and (3.15) yields,

$$\dot{\sigma} = \dot{\bar{a}}(z) + \dot{\bar{b}}(z)u + \bar{b}(z)\dot{u} - \dot{w}_{nom} + \Delta\dot{F}(z,t) + \kappa(\dot{z}_n - w_{nom}) \tag{3.19}$$

Using the μ reaching law [68] yields,

$$\dot{\sigma} = -\rho sign(\sigma) \tag{3.20}$$

where $\rho > |\Delta\dot{F}(z,t)|$ to satisfy the reaching law condition $\sigma\dot{\sigma} \leq -\eta|\sigma|$ where η is a positive constant [56]. Using (3.19) and (3.20), the control law is obtained as,

$$\dot{u} = -\bar{b}(z)^{-1}\{\dot{\bar{a}}(z) + \dot{\bar{b}}(z)u - \dot{w}_{nom} + \kappa(\dot{z}_n - w_{nom}) + \rho sign(\sigma)\} \tag{3.21}$$

3.3.3 Design of adaptive integral chattering free sliding mode controller

In practice, the upper bound of the system uncertainty is often unknown in advance and hence the error term $|\Delta\dot{F}(z,t)|$ is difficult to find. So an adaptive tuning law is proposed to estimate ρ. Then the control law (3.21) can be written as

$$\dot{u} = -\bar{b}(z)^{-1}\{\dot{\bar{a}}(z) + \dot{\bar{b}}(z)u - \dot{w}_{nom} + \kappa(\dot{z}_n - w_{nom}) + \hat{T} sign(\sigma)\} \tag{3.22}$$

where $\hat{T}$ estimates the value of ρ. Defining the adaptation error as $\tilde{T} = \hat{T} - T$, the parameter $\hat{T}$ will be estimated by using the adaptation law [40] [69, 70] as given below,

$$\dot{\hat{T}} = \nu|\sigma| \tag{3.23}$$

where ν is a positive constant. A Lyapunov function V is selected as $V = \frac{1}{2}\sigma^2 + \frac{1}{2}\gamma\tilde{T}^2$ whose time derivative is as follows,

$$\begin{aligned}
\dot{V} &= \sigma\dot{\sigma} + \gamma\tilde{T}\dot{\tilde{T}} \\
&\quad \text{Using (3.19) yields,} \\
\dot{V} &= \sigma[\dot{\bar{a}}(z) + \dot{\bar{b}}(z)u + \bar{b}(z)\dot{u} - \dot{w}_{nom} + \Delta\dot{F}(z,t) + \kappa(\dot{z}_n - w_{nom})] + \gamma(\hat{T} - T)\dot{\hat{T}} \\
&\quad \text{Using (3.22) and (3.23) yields,} \\
\dot{V} &= \sigma[\Delta\dot{F}(z,t) - \hat{T}sign(\sigma)] + \gamma(\hat{T} - T)\nu|\sigma| \\
&\quad \text{The above equation can be written as} \\
\dot{V} &\leq |\Delta\dot{F}(z,t)||\sigma| - \hat{T}|\sigma| + T|\sigma| - T|\sigma| + \gamma(\hat{T} - T)\nu|\sigma| \\
&\leq (|\Delta\dot{F}(z,t)| - T)|\sigma| - (\hat{T} - T)|\sigma| + \gamma(\hat{T} - T)\nu|\sigma| \\
&\leq -(-|\Delta\dot{F}(z,t)| + T)|\sigma| - (\hat{T} - T)(-\gamma\nu|\sigma| + |\sigma|) \\
&\leq -\beta_\sigma\sqrt{2}|\sigma|/\sqrt{2} - \beta_\nu\sqrt{2\gamma}(\hat{T} - T)/\sqrt{2\gamma} \\
&\quad \text{where } \beta_\sigma = (T - |\Delta\dot{F}(z,t)|) \text{ and } \beta_\nu = (|\sigma| - \gamma\nu|\sigma|) \\
&\quad \text{So, } \dot{V} \leq -min\{\beta_\sigma\sqrt{2}, \beta_\nu\sqrt{2/\gamma}\}(|\sigma|/\sqrt{2} + \tilde{T}\sqrt{\gamma/2}) \\
&\leq -\beta V^{1/2}
\end{aligned} \tag{3.24}$$

where $\beta = min\{\beta_\sigma\sqrt{2}, \beta_\nu\sqrt{2/\gamma}\}$ with $\beta > 0$. The above inequality holds if $\dot{\hat{T}} = \nu|\sigma|$, $\beta_\sigma > 0, \beta_\nu > 0$, $T > |\Delta\dot{F}(z,t)|$ and $\gamma < \frac{1}{\nu}$. Therefore, finite time convergence to a domain $\sigma = 0$ is guaranteed from any initial condition [40, 62].

***Remark* 3.2.** *Practically, $|\sigma|$ cannot become exactly zero in finite time and thus the adaptive parameter $\dot{\hat{T}}$ may increase boundlessly [40]. A simple way of overcoming this disadvantage is to modify the adaptive tuning law (3.23) by using the dead zone technique [30, 40] as*

$$\dot{\hat{T}} = \begin{cases} \nu|\sigma|, & |\sigma| \geq \epsilon \\ 0, & |\sigma| < \epsilon \end{cases} \tag{3.25}$$

where ϵ is a small positive constant.

As is evident from (3.22), $\dot{u}$ is discontinuous but integration of $\dot{u}$ yields a continuous control law u. Hence the undesired high frequency chattering of the control signal is alleviated. Thus the above adaptive integral sliding mode control method offers two main advantages. Firstly, the knowledge

about the upper bound of the system uncertainties is not required. Secondly, the chattering in the control input is eliminated.

3.4 Simulation Examples

The proposed adaptive integral chattering free sliding mode controller is applied to two examples of uncertain system. Both the examples are simulated by using ODE 5 solver in the MATLAB - Simulink platform with a fixed step size of 0.005 sec.

3.4.1 Adaptive integral chattering free sliding mode controller for the triple integrator system

The triple integrator system [62] having parametric uncertainty is described below,

$$\begin{aligned} \dot{x}_1 &= x_2 \\ \dot{x}_2 &= x_3 \\ \dot{x}_3 &= u + p(x), \quad y = x_1 \end{aligned} \tag{3.26}$$

where $p(x) = \sin(10x_1)$ is the bounded uncertainty, y is the output and the initial condition of the system is assumed as $\boldsymbol{x}(0) = [1 \quad 0 \quad -1]^T$. Stabilization of the above system is investigated and simulation is performed with $k_1 = 1, k_2 = 1.5, k_3 = 1.5$ (3.9) and $G = 1.5$ (3.13). For designing the adaptive integral SM controller, same controller parameters as used by Defoort et al. [62] are chosen. The adaptive tuning law (3.23) is designed as $\dot{\hat{T}} = 0.8|\sigma|$ with $T_0 = 0.5$. The sliding manifold coefficient κ (3.17) is selected as 2.

Figs. 3.1 - 3.4 show the states, the control input, the sliding surface and the estimated adaptive gain obtained by using the proposed controller. It is obvious from Fig.3.1 that the proposed controller converges the system states quickly to the origin. From Figs. 3.2 - 3.3 it is evident that the control input is smooth having no chattering and the sliding surface is also chatterless. The convergence of the estimated adaptive gain $\hat{T}$ is confirmed in Fig.3.4. Notably, prior knowledge about the upper bound of the system uncertainty is not a necessary requirement. The proposed controller adaptively estimates the system uncertainty and hence is suitable for practical applications where the bounds of uncertainty are difficult to be determined.

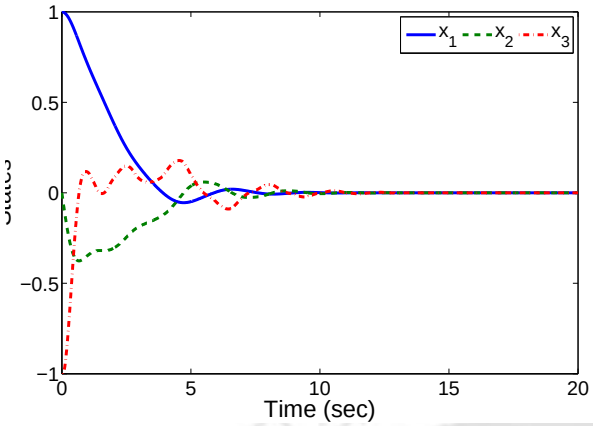

Figure 3.1: State response with the proposed control law (3.22)

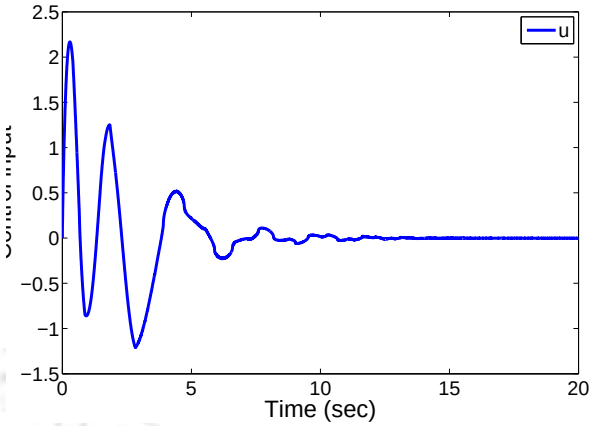

Figure 3.2: Control input with the proposed control law (3.22)

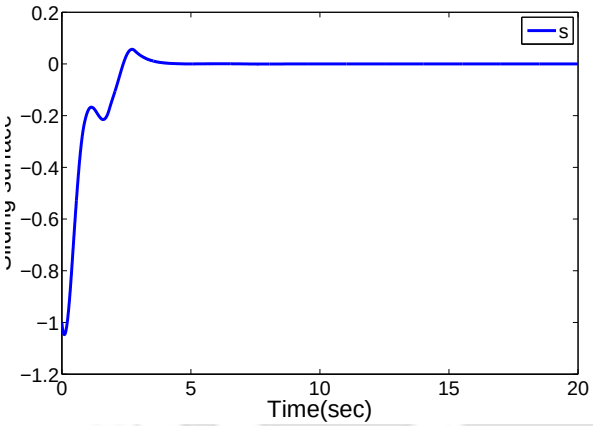

Figure 3.3: Sliding surface with the proposed control law (3.22)

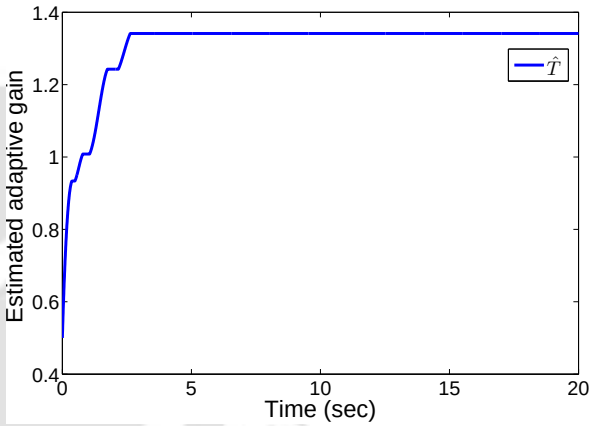

Figure 3.4: Estimated adaptive gain with the proposed control law (3.22)

3.4.2 Adaptive integral chattering free sliding mode controller for the single inverted pendulum

The dynamic equations of the single inverted pendulum are stated below [13, 71],

$$\begin{aligned} \dot{x}_1 &= x_2 \\ \dot{x}_2 &= \frac{g\sin x_1 - (mlx_2^2\cos x_1 \sin x_1/m_c + m)}{l[4/3 - (m\cos^2 x_1/m_c + m)]} + \frac{\cos x_1/m_c + m}{l[4/3 - (m\cos^2 x_1/m_c + m)]}u + \Delta \\ y &= x_1 \end{aligned} \tag{3.27}$$

where Δ is the system perturbation defined by $\Delta = 7\sin(10x_1) + \cos x_2$.

The parameters of the single inverted pendulum are tabulated in Table 3.1.

Table 3.1: Parameters of the single inverted pendulum

Variable name	Description	Values
g	gravitational constant	$9.8ms^{-2}$
m_c	mass of the cart	1kg
m	mass of the pendulum	0.1kg
l	effective length of the pendulum	0.5m
x_1	swing angle	state
x_2	swing speed	state

The objective is to design an adaptive integral sliding mode controller such that the system output y (3.27) tracks the desired reference trajectory given by $x_d = \sin(0.5\pi t)$. The sliding variable is defined as $s = x_1 - x_d$ and the proposed control law (3.22) is used. For our proposed controller (3.22), the model used by Defoort et al. [62] is chosen with $n = 2$, $\alpha_1 = 3/4$, $k_1 = 3$, $\alpha_2 = 3/5$, $k_2 = 2.5$, $G = 10$ and w_{nom} (3.9) is calculated. The sliding manifold parameter (3.17) is selected as $\kappa = 30$. The adaptive tuning law is designed as $\dot{\hat{T}} = 5.5|\sigma|$ with $T_0 = 0$. Figs. 3.5 - 3.8 show the system output, the control input, the sliding manifold and the estimated adaptive gain obtained by using the proposed controller. It is evident from these figures that apart from ensuring the desired tracking performance, the proposed control scheme is able to eliminate the undesired high frequency chattering in the control input.

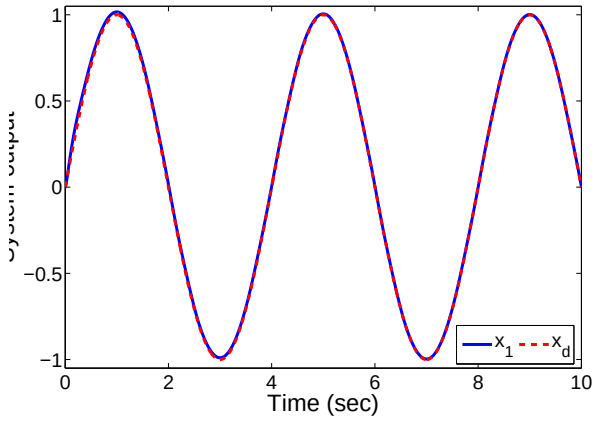

Figure 3.5: System output with the proposed control law (3.22)

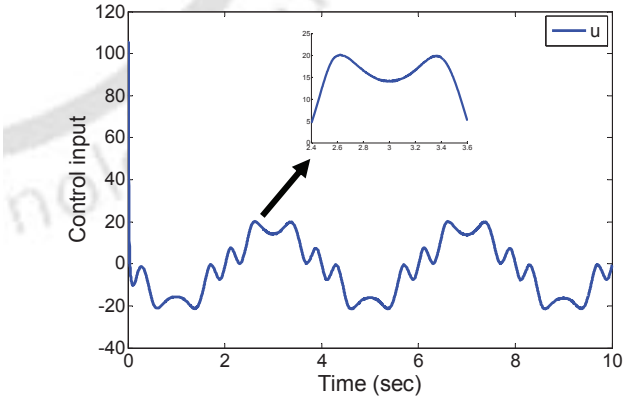

Figure 3.6: Control input with the proposed control law (3.22)

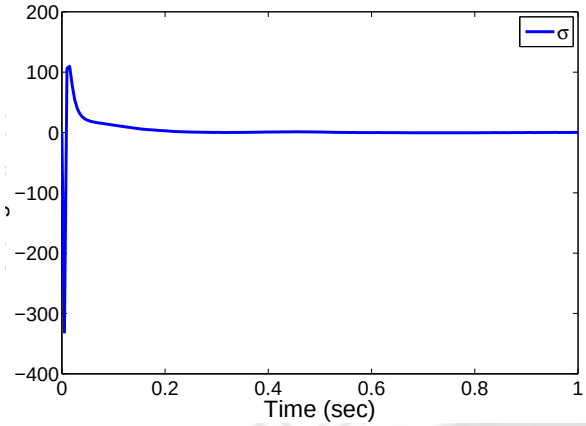

Figure 3.7: Sliding manifold with the proposed control law (3.22)

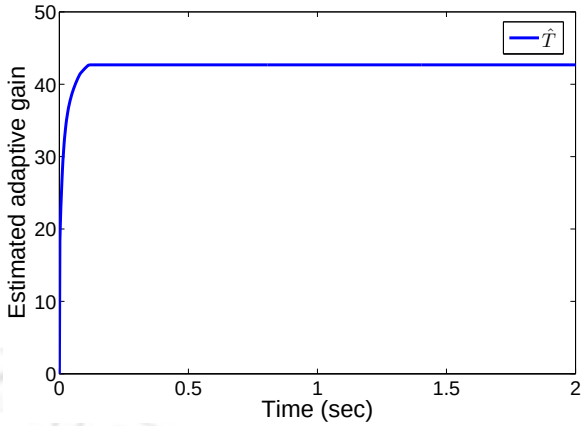

Figure 3.8: Estimated adaptive gain with the proposed control law (3.22)

3.5 Summary

An adaptive integral chattering free sliding mode controller for uncertain systems is proposed in this chapter. A tuning rule is designed to deal with the unknown bounded system uncertainty. The upper bound of the system uncertainty is not required to be known apriori as is the case with most existing sliding mode controllers. Stabilization of the triple integrator system and tracking control of the single inverted pendulum are investigated. It is observed that the proposed control law is capable of achieving the control objective while eliminating the high frequency oscillations in the control input. Hence the proposed controller promises to be highly suitable for practical applications. The stability of the controlled system is proved by using Lyapunov stability criterion. Simulation results demonstrate the efficacy and advantages of the proposed controller.

4

Adaptive Sliding Mode Controller for Multiple Input Multiple Output (MIMO) Systems

Contents

4.1 Introduction

It is evident from the discussion so far that the sliding mode control (SMC) is a robust control strategy which is insensitive to matched uncertainty affecting a dynamic system [43]. However, in presence of mismatched perturbations, the property of asymptotical stability is, in general, hard to achieve by using the traditional SMC technique [59]. One significant research finding is that the stability of the system is guaranteed if the system trajectory is driven to a bounded region [31, 72, 73]. Hence when the system contains mismatched perturbations, the information about the upper bound of perturbations is needed in order to achieve asymptotical stability [32, 74, 75]. A technique was developed in [38] where asymptotic stability could be achieved without requiring the information about the upper bound of the system uncertainties. Here adaptive mechanism was embedded in the controller as well as in the sliding surface, but the control input obtained by using the above-mentioned method was not smooth and high frequency chattering was present which made the algorithm substantially difficult to apply practically.

In this chapter, a chattering free sliding mode control scheme for multiple input multiple output (MIMO) systems with both matched and mismatched uncertainties is proposed. A tuning rule based sliding mode is used to design the proposed controller in order to mitigate chattering and adaptive tuning mechanism is employed for estimating the upper bound of the system uncertainty. The twin rotor multi input multi output system (TRMS), which is a typical example of a coupled MIMO system with mismatched uncertainty, is considered for design and validation purpose. The TRMS is divided into a horizontal and a vertical subsystem and an adaptive sliding mode controller is designed for each of the subsystems. Next the adaptive sliding mode controller is applied for stabilization of the vertical take-off and landing (VTOL) aircraft system which is affected by both matched and mismatched types of uncertainty. To show the effectiveness of the proposed control law, experimental studies are conducted on a single degree of freedom (DOF) vertical take-off and landing (VTOL) aircraft system to study the real time performance of the proposed adaptive sliding mode (SM) controller. The design prerequisite of the sliding mode controller is complete knowledge about the state vector which is not available in this example. Hence unavailable states of the 1 DOF VTOL are estimated by using an extended state observer (ESO).

The outline of this chapter is as follows. Section 4.2 discusses the design procedure of the adaptive sliding mode controller. The design strategy is demonstrated by taking the TRMS into consideration

in Section 4.3. In Section 4.4, effectiveness of this adaptive sliding mode controller is validated by applying it for stabilization of the VTOL system. Experimental results obtained by applying the adaptive sliding mode controller on the laboratory set-up QNET which is the prototype of VTOL aircraft system are presented in Section 4.5. A brief summary of the chapter is presented in Section 4.6.

4.2 Adaptive sliding mode controller

Let us consider the following uncertain system

$$\dot{x} = Ax + Bu + f(x,t) \tag{4.1}$$

where $x \in R^n$ is the state vector, $u \in R^m$ is the control input and the continuous function $f(x,t)$ represents matched and mismatched uncertainties together. Let us assume that the above system is in the regular form requiring no transformation. Thus the system can be written as,

$$\begin{aligned} \dot{x}_1 &= a_{11}x_1 + a_{12}x_2 + f_u(x,t) \\ \dot{x}_2 &= a_{21}x_1 + a_{22}x_2 + B_2u + B_2f_m(x,t) \end{aligned} \tag{4.2}$$

where $x_1 \in R^{n-m}$, $x_2 \in R^m$, $f_u(x,t)$ is the mismatched perturbation and $f_m(x,t)$ is the matched one. Let us consider the sliding surface given by

$$\begin{aligned} s &= cx \\ &= c_1x_1 + c_2x_2 \end{aligned} \tag{4.3}$$

where c_1, c_2 are matrices with proper dimension.

4.2.1 Stability during the sliding mode

During the sliding mode $s = 0$ and therefore (4.3) can be written as,

$$\begin{aligned} s &= cx = c_1x_1 + c_2x_2 = 0 \\ or, x_2 &= -c_2^{-1}c_1x_1 \end{aligned} \tag{4.4}$$

where c_2 is invertible.

Using (4.4) in the state space model (4.2) yields,

$$\begin{aligned}\dot{x}_1 &= a_{11}x_1 - a_{12}c_2^{-1}c_1x_1 + f_u \\ &= (a_{11} - a_{12}c_2^{-1}c_1)x_1 + f_u \\ &= a_sx_1 + f_u \end{aligned} \tag{4.5}$$

where $a_s = (a_{11} - a_{12}c_2^{-1}c_1)$. Furthermore, f_u is the uncertainty satisfying the condition $||f_u|| \leq \tilde{\lambda}||x_1||$ [8] where $\tilde{\lambda}$ is a bounded positive constant.

***Remark* 4.1.** *The above assumption is a limitation on the uncertainties that can be tolerated by the system. From the work in [74] [76] [77], these assumptions are fundamental and reasonable. The structural requirement on the interconnection bounds is not essential because it can be easily extended to a more general case (for example, [78] can be referred to).*

It is to be noted that c_1 and c_2 are designed in such a way that the eigenvalues of a_s lie in the left half of the s-plane and there exits a positive definite matrix P [74] such that

$$a_s^TP + Pa_s = -R \tag{4.6}$$

where R is also a positive definite matrix. Let a Lyapunov function for the system be defined as $V_2 = x_1^TPx_1$. The time derivative of V_2 is obtained as,

$$\begin{aligned}\dot{V}_2 &= \dot{x}_1^TPx_1 + x_1^TP\dot{x}_1 \\ &= x_1^Ta_s^TPx_1 + f_u^TPx_1 + x_1^TPa_sx_1 + x_1^TPf_u \\ &= x_1^T(a_s^TP + Pa_s)x_1 + f_u^TPx_1 + x_1^TPf_u \\ &= -x_1^TRx_1 + 2x_1^TPf_u \end{aligned} \tag{4.7}$$

It is known that [74] [75],

$$x_1^TRx_1 \geq \lambda_{min}(R)x_1^Tx_1 = \lambda_{min}(R)||x_1||^2 \tag{4.8}$$

where λ_{min} is the minimum eigen value and so,

$$\dot{V}_2 \leq -\lambda_{min}(R)||x_1||^2 + 2x_1^TPf_u \tag{4.9}$$

If there exists a bounded positive constant $\tilde{\lambda}$ such that $\tilde{\lambda} < 0.5\lambda_{min}(R)/||P||$, then

$$2x_1^T P f_u \leq 2\tilde{\lambda}||P||||x_1||^2 < \lambda_{min}(R)||x_1||^2 \tag{4.10}$$

and

$$\dot{V}_2 \leq -\lambda_{min}(R)||x_1||^2 + 2x_1^T P f_u < 0 \tag{4.11}$$

Hence the stability in the sliding mode is proved.

4.2.2 Design of the control law

The time derivative of sliding surface

$$\begin{aligned} \dot{s} &= \frac{d}{dt}(cx) \\ &= c\dot{x}(t) \\ &= c(Ax + Bu + f(x,t)) \end{aligned} \tag{4.12}$$

$$\begin{aligned} \ddot{s} &= cA\dot{x} + cB\dot{u} + c\dot{f}(x,t) \\ &= cA^2x + cABu + cB\dot{u} + (cAf(x,t) + c\dot{f}(x,t)) \end{aligned} \tag{4.13}$$

Assuming $s = y_1(x)$ and $\dot{s} = y_2(x)$, the system dynamics can be written as,

$$\begin{aligned} \dot{y}_1(x) &= y_2(x) \\ \dot{y}_2(x) &= \Phi[x,u] + \Psi[x]v \end{aligned} \tag{4.14}$$

where $v = \dot{u}$ and $\Phi[x,u]$ collects all the uncertain terms not involving $\dot{u}$. So a sliding mode controller for the above system can be designed to keep the system trajectories on the sliding manifold using the control input $\dot{u} = v$. Let the sliding function be considered as,

$$\sigma = y_2(x) + \kappa y_1(x) \tag{4.15}$$

where κ is a positive constant. Differentiating (4.15) yields,

$$\dot{\sigma} = \dot{y}_2(x) + \kappa \dot{y}_1(x) \tag{4.16}$$

Using (4.12), (4.13) and (4.16) yields,

$$\begin{aligned}\dot{\sigma} &= cA^2x + cABu + cB\dot{u} + (cAf(x,t) + c\dot{f}(x,t)) \\ &\quad +\kappa c(Ax + Bu + f(x,t)) \\ &= cA^2x + \kappa cAx + (cAB + \kappa cB)u + cB\dot{u} \\ &\quad +c(Af(x,t) + \dot{f}(x,t) + \kappa f(x,t)) \end{aligned} \tag{4.17}$$

Using the constant plus proportional reaching law gives rise to,

$$\dot{\sigma} = -k_1\sigma - k_2 sign(\sigma) \tag{4.18}$$

Using (4.17) and (4.18), the control law is obtained as,

$$\begin{aligned}\dot{u} &= -(cB)^{-1}((cA^2 + \kappa cA)x + (cAB + \kappa cB)u \\ &\quad +k_1\sigma + k_2 sign(\sigma)) \end{aligned} \tag{4.19}$$

where $k_1 \geq 0$ and $k_2 > c(Af(x,t)+\dot{f}(x,t)+\kappa f(x,t)) = c\nabla F = Q$ to satisfy the reaching law condition $\sigma\dot{\sigma} \leq -\eta||\sigma||$, where η is a positive constant.

Proof : A Lyapunov function is defined as $V = \frac{1}{2}\sigma^2$ and using the control law it is easy to find that,

$$\begin{aligned}\dot{V} &= \sigma\dot{\sigma} \\ &= \sigma[c\nabla F - k_1\sigma - k_2 sign(\sigma)] \\ &= \sigma[Q - k_1\sigma - k_2 sign(\sigma)] \\ &\leq Q||\sigma|| - k_2||\sigma|| \leq -\eta||\sigma|| \end{aligned} \tag{4.20}$$

Clearly, (4.20) implies that if $k_1 \geq 0$ and $k_2 > Q$, control law (4.19) forces the sliding manifold σ to zero in finite time.

4.2.3 Design of the adaptive tuning law

In practice, the uncertain term ∇F is often difficult to know. Hence an adaptive tuning law is designed to determine k_2. So (4.18) can be written as

$$\dot{\sigma} = -k_1\sigma - \hat{T} sign(\sigma) \tag{4.21}$$

where $\hat{T}$ estimates the value of k_2.

Using (4.19) and (4.21), the control law is obtained as,

$$\begin{aligned} \dot{u} &= -(cB)^{-1}((cA^2 + \kappa cA)x + (cAB + \kappa cB)u \\ &\quad + k_1\sigma + \hat{T}sign(\sigma)) \end{aligned} \tag{4.22}$$

Defining the adaptation error as $\tilde{T} = \hat{T} - T$, the parameter $\hat{T}$ is estimated by using the adaptation law [39, 69, 79]

$$\dot{\hat{T}} = \frac{1}{\gamma}||\sigma|| \tag{4.23}$$

where γ is a positive constant. A Lyapunov function is defined as $V = \frac{1}{2}\sigma^2 + \frac{1}{2}\gamma\tilde{T}^2$ and it is easy to find that,

$$\begin{aligned} \dot{V} &= \sigma\dot{\sigma} + \gamma\tilde{T}\dot{\tilde{T}} \\ &= \sigma[c\nabla F - k_1\sigma - \hat{T}sign(\sigma)] + \gamma(\hat{T} - T)\dot{\hat{T}} \\ &= \sigma[Q - k_1\sigma - \hat{T}sign(\sigma)] + \gamma(\hat{T} - T)\dot{\hat{T}} \\ &\leq Q||\sigma|| - T||\sigma|| \leq -\eta||\sigma|| \end{aligned} \tag{4.24}$$

The above inequality holds if $\dot{\hat{T}} = \frac{1}{\gamma}||\sigma||$, $\eta > 0$ and $T > Q$. This ensures the convergence of σ and guarantees that the states converges to equilibrium asymptotically.

***Remark* 4.2.** *Practically, $||\sigma||$ cannot become exactly zero in finite time and thus the adaptive parameter $\dot{\hat{T}}$ may increase boundlessly. A simple way of overcoming this disadvantage is to modify the adaptive tuning law (4.23) by using the dead zone technique [30] as*

$$\dot{\hat{T}} = \begin{cases} \frac{1}{\gamma}||\sigma||, & ||\sigma|| \geq \epsilon \\ 0, & ||\sigma|| < \epsilon \end{cases} \tag{4.25}$$

where ϵ is a small positive constant.

As is evident from (4.19), $\dot{u}$ is free from any discontinuous part and so integration of $\dot{u}$ yields a continuous control law u. Hence the undesired high frequency chattering of the control signal is eliminated.

Thus the above adaptive SM control method offers two main advantages. Firstly, the knowledge about

the upper bound of the system uncertainties is not required. Secondly, the chattering in the control input is removed.

4.3 The twin rotor MIMO System

In this section the problem of controlling the twin rotor MIMO system (TRMS), which is the prototype of a helicopter, is addressed. The above-mentioned control law is used for the TRMS affected by mismatched uncertainty.

The TRMS has been the object of research for control theorists for many years. The TRMS resembles a nonlinear system with heavy cross coupling effects. Hence controlling the TRMS is quite challenging and has gained a lot of research interest [8, 80–83]. An evolutionary computation based proportional integral derivative (PID) controller has been proposed for addressing the tracking control problem in the TRMS [84]. A fuzzy logic based linear quadratic regulator (LQR) control has been developed to stabilize the TRMS in presence of high cross coupling [1]. In [1] the phase portrait technique has been used for rule reduction and obtaining the model. In [85] a robust dead beat controller has been designed for controlling the TRMS. Here the system was decoupled into two single input single output (SISO) models and the cross coupling was considered as disturbance for each other.

In this section, a sliding mode (SM) controller is proposed for position control of the TRMS. In the proposed design methodology, the mathematical model of the TRMS is pseudo decoupled into a horizontal and a vertical subsystem. The cross coupling effect between the main rotor and the tail rotor is considered as the uncertainty in the pseudo decoupled TRMS. An adaptive tuning law is adopted to deal with the system uncertainty. The main benefit offered by this adaptive sliding mode controller is that apriori knowledge about the upper bound of the system uncertainty is not needed. A proportional integral (PI) sliding surface is designed for the vertical subsystem to remove the offset in the pitch angle. Simulation results illustrate that our proposed adaptive sliding mode controller shows better tracking performance with lesser control effort as compared to PID controllers [84]. Even the presence of an external disturbance in the horizontal as well as the vertical subsystem does not degrade the performance of the proposed adaptive sliding mode controller.

4.3.1 TRMS Description

The TRMS is a laboratory setup resembling a flight control system as shown in Fig. 4.1. The TRMS is a highly coupled nonlinear multi input multi output (MIMO) system. The TRMS consists

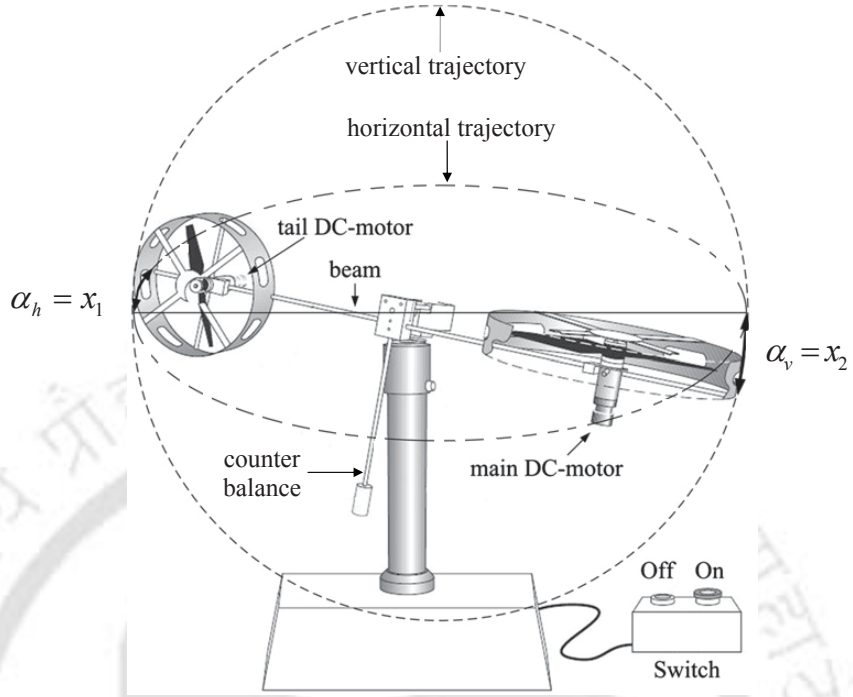

Figure 4.1: The twin rotor MIMO system (TRMS) [1]

of two rotors which are perpendicular to each other and are joined by a beam pivoted on its base in such a way that it can rotate freely in both the horizontal and the vertical planes. The main rotor produces a lifting force allowing the beam to rise vertically (pitch angle) while the tail rotor is used to control the beam to turn to the left or the right (yaw angle). Both the rotors are driven by similar independent D.C. motors which produce the aerodynamic forces. A counterbalance arm with a weight at its end is fixed to the beam at the pivot to stabilize the TRMS. Tacho-generators are attached to the D.C. motors to measure the angular velocities of the two rotors.

4.3.2 System Modeling

Approximate mathematical model of the twin rotor MIMO system is obtained by using Newton's second law of motion and is converted into the state space form [8, 84] as given below:

$$\dot{x}_1 = x_3$$

$$\dot{x}_2 = x_4$$

$$
\begin{aligned}
\dot{x}_3 &= \frac{1}{j_h}[l_t S_f F_h(w_t) cos x_2 - k_h x_3 - x_3 x_4 (D-E) sin 2x_2 - j_{mr} w_m(x_6) x_4 sin x_2 \\
&\quad + \frac{j_{mr}}{T_{mr}}(u_v - x_6)\frac{dw_m(x_6)}{dx_6} cos x_2] \\
\dot{x}_4 &= 9.1[l_m S_f F_v(w_m) - g(0.0099 cos x_2 + 0.0168 sin x_2) - k_v x_4] \\
&\quad + 9.1[-0.0252 x_3^2 sin 2x_2 + \frac{j_{tr}}{T_{tr}}(u_h - x_5)\frac{dw_t(x_5)}{dx_5}] \\
\dot{x}_5 &= \frac{1}{T_{tr}}(u_h - x_5) \\
\dot{x}_6 &= \frac{1}{T_{mr}}(u_v - x_6)
\end{aligned} \tag{4.26}
$$

With $u_v(u_h)$ being the input voltage of the DC motor for the main (tail) propeller, the armature current $i_v(i_h)$ can be obtained by solving the following differential equations

$$
\begin{aligned}
\frac{di_v}{dt} &= \frac{1}{T_{mr}}(u_v - i_v) \\
\frac{di_h}{dt} &= \frac{1}{T_{tr}}(u_h - i_h)
\end{aligned} \tag{4.27}
$$

where $x_1 = \alpha_h$ is the yaw angle, $x_2 = \alpha_v$ is the pitch angle, $x_3 = \Omega_h$ is the angular velocity around the horizontal axis, $x_4 = \Omega_v$ is the angular velocity around the vertical axis, $x_5 = i_h$ is the armature current of the tail propeller subsystem, $x_6 = i_v$ is the armature current of the main propeller subsystem. Furthermore, $l_m(l_t)$ is the main (tail) length of the beam, $j_{mr}(j_{tr})$ is the moment of inertia for the main (tail) propeller subsystem, $T_{mr}(T_{tr})$ is the time constant of the main (tail) motor-propeller system and $\omega_m(\omega_t)$ is the rotational speed of the main (tail) rotor DC motor. Moreover, $k_v(k_h)$ is the friction constant of the main (tail) propeller subsystem, S_f is the balanced scale and $u_v(u_h)$ is the control input for the main (tail) DC motor. The propulsive force to move the joined beam in the vertical (horizontal) direction is denoted by $F_v(F_h)$ which is approximately described by a nonlinear function of the angular velocity $\omega_m(\omega_t)$. Gravitational acceleration is symbolized as g and D, E, G are constants. Furthermore,

$$
\begin{aligned}
j_h &= D sin^2 x_2 + E cos^2 x_2 + G \\
\omega_m(x_6) &= 90.99 x_6^6 + 599.73 x_6^5 - 129.26 x_6^4 - 1283.64 x_6^3 + 63.45 x_6^2 + 1283.41 x_6 \\
\omega_t(x_5) &= 2020 x_5^5 - 194.69 x_5^4 - 4283.15 x_5^3 + 262.27 x_5^2 + 3768.83 x_5
\end{aligned}
$$

$$
\begin{aligned}
F_v(w_m) &= -3.48\times10^{-12}\omega_m^5 + 1.09\times10^{-9}\omega_m^4 + 4.123\times10^{-6}\omega_m^3 - 1.632\times10^{-4}\omega_m^2 \\
&\quad +9.544\times10^{-2}\omega_m \\
F_h(w_t) &= -3\times10^{-14}\omega_t^5 - 1.595\times10^{-11}\omega_t^4 + 2.511\times10^{-7}\omega_t^3 - 1.808\times10^{-4}\omega_t^2 \\
&\quad +8.01\times10^{-2}\omega_t
\end{aligned} \tag{4.28}
$$

Table 4.1 lists the physical parameters of the TRMS and their values.

Table 4.1: Physical parameters of the TRMS [8]

Symbol	Definition	value
l_m	Length of the main part of the beam	0.236m
l_t	Length of the tail part of the beam	0.25m
k_v	Friction coefficient of the vertical axis	0.0095
k_h	Friction coefficient of the horizontal axis	0.0054
j_{mr}	Moment of inertia of the DC motor main propeller	$1.6543\times10^{-5}kgm^2$
j_{tr}	Moment of inertia of the DC motor tail propeller	$2.65\times10^{-5}kgm^2$
T_{mr}	Time constant of the main rotor	1.432 sec
T_{tr}	Time constant of the tail rotor	0.3842 sec
D	Mechanical related constant	$1.6065\times10^{-3}kgm^2$
E	Mechanical related constant	$4.90092\times10^{-2}kgm^2$
G	Mechanical related constant	$6.3306\times10^{-3}kgm^2$
S_f	Balance scale	8.43318×10^{-4}
g	Gravitational constant	$9.81m/s^2$

The nonlinear state equations of the TRMS in (4.26)-(4.28) can be represented as,

$$
\begin{aligned}
&\dot{X} = f(X, u_h, u_v), \text{where} \quad X = [x_1, x_2, ..., x_6]^T, \text{and} \\
&f(X, u_h, u_v) = [f_1(X, u_h, u_v), f_2(X, u_h, u_v)...., f_6(X, u_h, u_v)]^T
\end{aligned} \tag{4.29}
$$

In order to reduce the complexity of the position controller, the complex TRMS model is divided into a horizontal subsystem (HS) and a vertical subsystem (VS) following the approach in [1] [8]. While designing the controller for the subsystem, a linear part is added to and the same is then subtracted from the nonlinear part for facilitating pseudo-separation whereas the overall system remains the same. The state equations are then written as,

$$
\begin{aligned}
\dot{x}_h &= \bar{A}_h x_h + \bar{B}_h u_h + \Delta F_h \\
\dot{x}_v &= \bar{A}_v x_v + \bar{B}_v u_v + \Delta F_v
\end{aligned} \tag{4.30}
$$

For the above horizontal and vertical subsystems, the states and parameters are defined as, $x_h = [x_1, x_3, x_5]^T$, $\Delta F_h = [0,\ \Delta f_h(x_h, x_v, u_v),\ 0]^T$ and $x_v = [x_2, x_4, x_6]^T$, $\Delta F_v = [0,\ \Delta f_v(x_v, x_h, u_h),\ 0]^T$.

Here,

$$\bar{A}_h = \begin{bmatrix} a_{h11} & a_{h12} & a_{h13} \\ a_{h21} & a_{h22} & a_{h23} \\ a_{h31} & a_{h32} & a_{h33} \end{bmatrix} = \begin{bmatrix} \frac{\partial f_1}{\partial x_1} & \frac{\partial f1}{\partial x_3} & \frac{\partial f_1}{\partial x_5} \\ \frac{\partial f_3}{\partial x_1} & \frac{\partial f_3}{\partial x_3} & \frac{\partial f_3}{\partial x_5} \\ \frac{\partial f_5}{\partial x_1} & \frac{\partial f_5}{\partial x_3} & \frac{\partial f_5}{\partial x_5} \end{bmatrix}_{X=0} = \begin{bmatrix} 0 & 1 & 0 \\ 0 & -\frac{k_h}{E+G} & \frac{301.88 l_t S_f}{E+G} \\ 0 & 0 & -T_{tr}^{-1} \end{bmatrix} \quad (4.31)$$

$$\bar{B}_h^T = \begin{bmatrix} b_{h11} & b_{h21} & b_{h31} \end{bmatrix} = \begin{bmatrix} \frac{\partial f_1}{\partial u_h} & \frac{\partial f_3}{\partial u_h} & \frac{\partial f_5}{\partial u_h} \end{bmatrix} = \begin{bmatrix} 0 & 0 & T_{tr}^{-1} \end{bmatrix} \quad (4.32)$$

$$\bar{B}_v^T = \begin{bmatrix} b_{v11} & b_{v21} & b_{v31} \end{bmatrix} = \begin{bmatrix} \frac{\partial f_2}{\partial u_v} & \frac{\partial f_4}{\partial u_v} & \frac{\partial f_6}{\partial u_v} \end{bmatrix} = \begin{bmatrix} 0 & 0 & T_{mr}^{-1} \end{bmatrix} \quad (4.33)$$

$$\begin{aligned} \bar{A}_v &= \begin{bmatrix} a_{v11} & a_{v12} & a_{v13} \\ a_{v21} & a_{v22} & a_{v23} \\ a_{v31} & a_{v32} & a_{v33} \end{bmatrix} = \begin{bmatrix} \frac{\partial f_2}{\partial x_2} & \frac{\partial f_2}{\partial x_4} & \frac{\partial f_2}{\partial x_6} \\ \frac{\partial f_4}{\partial x_2} & \frac{\partial f_4}{\partial x_4} & \frac{\partial f_4}{\partial x_6} \\ \frac{\partial f_6}{\partial x_2} & \frac{\partial f_6}{\partial x_4} & \frac{\partial f_6}{\partial x_6} \end{bmatrix}_{X=0} \\ &= \begin{bmatrix} 0 & 1 & 0 \\ -0.153g & -9.1k_v & 1114.65 l_m S_f \\ 0 & 0 & -T_{mr}^{-1} \end{bmatrix} \end{aligned} \quad (4.34)$$

$$\begin{aligned} \Delta f_h(x_h, x_v, u_v) &= \frac{1}{j_h}[l_t S_f F_h(w_t) cos x_2 - k_h x_3 - x_3 x_4 (D-E) sin 2x_2 - j_{mr} w_m(x_6) x_4 sin x_2 \\ &\quad + \frac{j_{mr}}{T_{mr}}(u_v - x_6)\frac{dw_m(x_6)}{dx_6} cos x_2] - a_{h21} x_1 - a_{h22} x_3 - a_{h23} x_5 \\ \Delta f_v(x_v, x_h, u_h) &= 9.1[l_m S_f F_v(w_m) - g(0.0099 cos x_2 + 0.0168 sin x_2) - k_v x_4 \\ &\quad - 0.0252 x_3^2 sin 2x_2 + \frac{j_{tr}}{T_{tr}}(u_h - x_5)\frac{dw_t(x_5)}{dx_5}] - a_{v21} x_2 - a_{v22} x_4 - a_{v23} x_6 \end{aligned} \quad (4.35)$$

In (4.30), ΔF_h and ΔF_v are considered as the uncertainty in the TRMS. The system (4.30) can be partitioned into the regular form,

$$\begin{aligned} \dot{z}_{1h} &= a_{11h} z_{1h} + a_{12h} z_{2h} + f_{1h} \\ \dot{z}_{2h} &= a_{21h} z_{1h} + a_{22h} z_{2h} + b_{h31} u_h + f_{2h} \end{aligned} \quad (4.36)$$

where $z_{1h} = [x_1 \quad x_3]^T$, $z_{2h} = x_5$, $a_{11h} = \begin{bmatrix} a_{h11} & a_{h12} \\ a_{h21} & a_{h22} \end{bmatrix}$, $a_{12h} = \begin{bmatrix} a_{h13} \\ a_{h23} \end{bmatrix}$, $a_{21h} = [a_{h31} \quad a_{h32}]$, $a_{22h} = a_{h33}$.

Here,

$$f_{1h} = \begin{bmatrix} 0 \\ \Delta f_h(x_h, x_v, u_v) \end{bmatrix}, \; f_{2h} = 0.$$

Therefore the state space model of the TRMS-HS can be expressed as,

$$\begin{bmatrix} \dot{z_{1h}} \\ \dot{z_{2h}} \end{bmatrix} = A_h \begin{bmatrix} z_{1h} \\ z_{2h} \end{bmatrix} + \begin{bmatrix} 0 \\ B_{2h} \end{bmatrix} u_h + \begin{bmatrix} \Delta\tilde{F}_h \\ 0 \end{bmatrix} \tag{4.37}$$

where $A_h = \begin{bmatrix} a_{11h} & a_{12h} \\ a_{21h} & a_{22h} \end{bmatrix}$, $B_{2h} = b_{h31}$, $\Delta\tilde{F}_h = f_{1h} = \begin{bmatrix} 0 \\ \Delta f_h(x_h, x_v, u_v) \end{bmatrix}$.

Similarly the TRMS-VS can be expressed as,

$$\begin{aligned} \dot{z}_{1v} &= a_{11v} z_{1v} + a_{12v} z_{2v} + f_{1v} \\ \dot{z}_{2v} &= a_{21v} z_{1v} + a_{22v} z_{2v} + b_{v31} u_v + f_{2v} \end{aligned} \tag{4.38}$$

where $z_{1v} = [x_2 \;\; x_4]^T$, $z_{2v} = x_6$, $a_{11v} = \begin{bmatrix} a_{v11} & a_{v12} \\ a_{v21} & a_{v22} \end{bmatrix}$, $a_{12v} = \begin{bmatrix} a_{v13} \\ a_{v23} \end{bmatrix}$,

$a_{21v} = [a_{v31} \;\; a_{v32}]$, $a_{22v} = a_{v33}$.

Here, $f_{1v} = \begin{bmatrix} 0 \\ \Delta f_v(x_h, x_v, u_h) \end{bmatrix}$, $f_{2v} = 0$.

Therefore the state space model of the TRMS-VS can be expressed as,

$$\begin{bmatrix} \dot{z_{1v}} \\ \dot{z_{2v}} \end{bmatrix} = A_v \begin{bmatrix} z_{1v} \\ z_{2v} \end{bmatrix} + \begin{bmatrix} 0 \\ B_{2v} \end{bmatrix} u_v + \begin{bmatrix} \Delta\tilde{F}_v \\ 0 \end{bmatrix} \tag{4.39}$$

where $A_v = \begin{bmatrix} a_{11v} & a_{12v} \\ a_{21v} & a_{22v} \end{bmatrix}$, $B_{2v} = b_{v31}$, $\Delta\tilde{F}_v = f_{1v} = \begin{bmatrix} 0 \\ \Delta f_v(x_v, x_h, u_h) \end{bmatrix}$. Let the desired reference vector be $r_{iv}(r_{ih})$ for $z_{iv}(z_{ih})$, $i = 1, 2$. Then $r_{1v} = [r_{xv} \;\; 0]^T$, $r_{2v} = 0$ and $r_{1h} = [r_{xh} \;\; 0]^T$, $r_{2h} = 0$. Hence the error vectors $e_{iv}(e_{ih})$ are obtained as,

$$\begin{aligned} e_{1v} = z_{1v} - r_{1v}, \quad e_{2v} = z_{2v} - r_{2v} \\ e_{1h} = z_{1h} - r_{1h}, \quad e_{2h} = z_{2h} - r_{2h} \end{aligned} \tag{4.40}$$

Without loss of generality the desired vectors are assumed to be zero [8], hence the error state space

model becomes,

$$\dot{E}_v = A_v E_v + B_v u_v + \Delta F_v \tag{4.41}$$

$$\dot{E}_h = A_h E_h + B_h u_h + \Delta F_h \tag{4.42}$$

where $E_v(E_h) \in R^3$ is the error state vector and $u_v(u_h) \in R^1$ is the control input. Here $A_v(A_h)$ and $B_v(B_h)$ are known matrices with proper dimensions.

4.3.3 Design of sliding mode controller for the TRMS horizontal subsystem

The main idea behind the proposed sliding mode is to act on the second order derivative of the sliding variable $\sigma(x,t)$ rather than the first derivative as in standard sliding modes. Besides retaining the main benefits of the standard sliding modes, the proposed sliding mode offers the additional advantage of eliminating the chattering effect [64]. Let the sliding surface be chosen as

$$s_h = c_h E_h \tag{4.43}$$

where $c_h = [c_{1h} \;\; c_{2h}]$ are real positive constants. For the proposed sliding mode, the first and second order time derivatives of the sliding surface are obtained as,

$$\begin{aligned} \dot{s}_h &= \frac{d}{dt}(c_h E_h) \\ &= c_h \dot{E}_h = c_h(A_h E_h + B_h u_h + \Delta F_h) \end{aligned} \tag{4.44}$$

$$\begin{aligned} \ddot{s}_h &= c_h A_h \dot{E}_h + c_h B_h \dot{u}_h + c_h \Delta \dot{F}_h \\ &= c_h A_h(A_h E_h + B_h u_h + \Delta F_h) + c_h B_h \dot{u}_h + c_h \Delta \dot{F}_h \\ &= c_h A_h^2 E_h + c_h A_h B_h u_h + c_h B_h \dot{u}_h + (c_h A_h \Delta F_h + c_h \Delta \dot{F}_h) \end{aligned} \tag{4.45}$$

If it is possible to bring s_h and $\dot{s}_h$ to zero in by using a discontinuous control signal $\dot{u}_h$, then the actual input of the system u_h is the integration of the discontinuous signal. Thus u_h is continuous, thereby reducing the undesired high frequency oscillations are always present in the first order sliding mode control. Assuming $y_1(E_h) = s_h$ and $y_2(E_h) = \dot{s}_h$, the system dynamics can be written as,

$$\begin{aligned} \dot{y}_1(E_h) &= y_2(E_h) \\ \dot{y}_2(E_h) &= F[E_h, u_h] + G[E_h, v_h] \end{aligned} \tag{4.46}$$

where $v_h = \dot{u}_h$ and $F[E_h, u_h]$ collects all the uncertain terms not involving $\dot{u}_h$. Thus the horizontal subsystem (4.30) becomes a chain of integrators controlled by the input $\dot{u}_h$. So a sliding mode controller for the above system can be designed to keep the system trajectories in the sliding manifold using the control input v_h. To design a SMC for the system (4.42), the sliding function is considered as,

$$\sigma_h = y_2(E_h) + \kappa_h y_1(E_h) \tag{4.47}$$

where κ_h is a positive constant. Taking the derivative of (4.47) we get,

$$\dot{\sigma}_h = \dot{y}_2(E_h) + \kappa_h \dot{y}_1(E_h) \tag{4.48}$$

From (4.44), (4.45) and (4.46) we have,

$$\begin{aligned} \dot{y}_1(E_h) &= c_h(A_h E_h + B_h u_h + \Delta F_h) \\ \dot{y}_2(E_h) &= c_h A_h^2 E_h + c_h A_h B_h u_h + c_h B_h \dot{u}_h + c_h A_h \Delta F_h + c_h \Delta \dot{F}_h \end{aligned} \tag{4.49}$$

Using (4.48) and (4.49) we have,

$$\begin{aligned} \dot{\sigma}_h &= c_h A_h^2 E_h + c_h A_h B_h u_h + c_h B_h \dot{u}_h + c_h A_h \Delta F_h + c_h \Delta \dot{F}_h + \kappa_h(c_h(A_h E_h + B_h u_h + \Delta F_h)) \\ &= c_h A_h^2 E_h + \kappa_h c_h A_h E_h + (c_h A_h B_h + \kappa_h c_h B_h) u_h + c_h B_h \dot{u}_h \\ &\quad + (c_h A_h \Delta F_h + c_h \Delta \dot{F}_h) + \kappa_h c_h \Delta F_h \end{aligned} \tag{4.50}$$

For designing the adaptive part of the control law, we consider

$$\dot{\sigma}_h = -k_{1h}\sigma_h - k_{2h} sign(\sigma_h) \tag{4.51}$$

Using (4.50) and (4.51), the control law is obtained as,

$$\dot{u}_h = -(c_h B_h)^{-1}((c_h A_h^2 + \kappa_h c_h A_h) E_h + (c_h A_h B_h + \kappa_h c_h B_h) u_h + k_{1h}\sigma_h + k_{2h} sign(\sigma_h)) \tag{4.52}$$

where $k_{1h} \geq 0$ and $k_{2h} > c_h(A_h \Delta F_h + \Delta \dot{F}_h + \kappa_h \Delta F_h) = c_h \nabla F_h = Q_h$ to satisfy the reaching law $\sigma_h \dot{\sigma_h} \leq -\eta_h |\sigma_h|$, where $\eta_h > 0$ [56]. Let us assume that there exits a bounded positive constant $\tilde{\lambda}'_h$ such that, $||\nabla F_h|| \leq \tilde{\lambda}'_h ||E_h||$ [8] and $Q_h = \tilde{\lambda}'_h c_h ||E_h|| \geq 0$.

4.3.4 Design of adaptive tuning law for the horizontal subsystem

In practice the bound of uncertainty is often not known and hence the error term $||E_h||$ is difficult to know. So an adaptive tuning law is designed to determine k_{2h}. Then the time derivative of the control law (4.52) can be written as

$$\dot{u}_h = -(c_h B_h)^{-1}[(c_h A_h^2 + \kappa_h c_h A_h)E_h + (c_h A_h B_h + \kappa_h c_h B_h)u_h + k_{1h}\sigma_h + \hat{T}_h sign(\sigma_h)] \tag{4.53}$$

and consequently the actual control law can be obtained as,

$$u_h = -(c_h B_h)^{-1} \int_0^t [(c_h A_h^2 + \kappa_h c_h A_h)E_h + (c_h A_h B_h + \kappa_h c_h B_h)u_h + k_{1h}\sigma_h + \hat{T}_h sign(\sigma_h)]d\tau \tag{4.54}$$

where $c_h B_h$ is nonsingular, $sign(\sigma_h)$ is the sign function and $\hat{T}_h$ is the unknown bound which will be estimated adaptively.

Defining the adaptation error as $\tilde{T}_h = \hat{T}_h - T_h$, where T_h is the actual gain, the parameter $\hat{T}_h$ will be estimated by using the adaptation law

$$\dot{\hat{T}}_h = \frac{1}{\gamma_h}|\sigma_h| \tag{4.55}$$

and $\gamma_h > 0$ is designed positive constant, $T_h(0)$ is the initial condition. A Lyapunov function is selected as $V_{1h} = \frac{1}{2}\sigma_h^2 + \frac{1}{2}\gamma_h \tilde{T}_h^2$ whose time derivative is as follows,

$$\begin{aligned}
\dot{V}_{1h} &= \sigma_h \dot{\sigma}_h + \gamma_h \tilde{T}_h \dot{\hat{T}}_h \\
&= \sigma_h[c_h \nabla F_h - k_{1h}\sigma_h - \hat{T}_h sign(\sigma_h)] + \gamma_h(\hat{T}_h - T_h)\dot{\hat{T}}_h \\
&= \sigma_h[Q_h - k_{1h}\sigma_h - \hat{T}_h sign(\sigma_h)] + \gamma_h(\hat{T}_h - T_h)\dot{\hat{T}}_h \\
&\leq Q_h|\sigma_h| - T_h|\sigma_h| \\
&\leq -\eta_h|\sigma_h|
\end{aligned} \tag{4.56}$$

The above inequality holds if $\dot{\hat{T}}_h = \frac{1}{\gamma_h}|\sigma_h|$, $\eta_h > 0$ and $T_h > Q_h$. Considering (4.55) and (4.56), it is straightforward to verify that $\dot{V}_{1h} \leq -\eta_h|\sigma_h|$, where $\eta_h > 0$. This ensures the convergence of σ_h and guarantees that the states converge to the equilibrium asymptotically.

The adaptive law (4.55) is modified by using dead zone technique [30] as

$$\dot{\hat{T}}_h = \begin{cases} \frac{1}{\gamma_h}|\sigma_h|, & |\sigma_h| \geq \epsilon_h \\ 0, & |\sigma_h| < \epsilon_h \end{cases} \tag{4.57}$$

where ϵ_h is a small positive constant.

Initially the adaptation gain parameter γ_h is so chosen that it is smaller than the upper bound of the system uncertainties. However, this is not really a restriction of the method since one can freely choose a sufficiently small number.

4.3.5 Stability during the sliding mode

During the sliding mode $s_h = 0$ and therefore (4.43) can be written as,

$$\begin{aligned} s_h &= c_h E_h = c_{1h} e_{1h} + c_{2h} e_{2h} = 0 \\ or, e_{2h} &= -c_{2h}^{-1} c_{1h} e_{1h} \end{aligned} \tag{4.58}$$

where c_{2h} is invertible.

Using (4.58) in the error state space model (4.42), we get

$$\begin{aligned} \dot{e}_{1h} &= a_{11h} e_{1h} - a_{12h} c_{2h}^{-1} c_{1h} e_{1h} + \Delta \tilde{F}_h \\ &= (a_{11h} - a_{12h} c_{2h}^{-1} c_{1h}) e_{1h} + \Delta \tilde{F}_h = a_{hs} e_{1h} + \Delta \tilde{F}_h \end{aligned} \tag{4.59}$$

where $a_{hs} = (a_{11h} - a_{12h} c_{2h}^{-1} c_{1h})$. Furthermore, $\Delta \tilde{F}_h$ is the uncertainty satisfying the condition $||\Delta \tilde{F}_h|| \leq \tilde{\lambda}_h ||e_{1h}||$ [8]. It is to be noted that c_{1h} and c_{2h} are designed in such a way that the eigenvalues of $(a_{11h} - a_{12h} c_{2h}^{-1} c_{1h})$ lie in the left half of the s-plane and there exists a positive definite matrix P_h [74] such that

$$a_{hs}^T P_h + P_h a_{hs} = -R_h \tag{4.60}$$

where R_h is also a positive definite matrix. Let a Lyapunov function for the system be defined as $V_{2h} = e_{1h}^T P_h e_{1h}$. The time derivative of V_{2h} is obtained as,

$$\begin{aligned} \dot{V}_{2h} &= \dot{e}_{1h}^T P_h e_{1h} + e_{1h}^T P_h \dot{e}_{1h} \\ &= e_{1h}^T a_{hs}^T P_h e_{1h} + \Delta \tilde{F}_h^T P_h e_{1h} + e_{1h}^T P_h a_{hs} e_{1h} + e_{1h}^T P_h \Delta \tilde{F}_h \\ &= e_{1h}^T (a_{hs}^T P_h + P_h a_{hs}) e_{1h} + \Delta \tilde{F}_h P_h e_{1h} + e_{1h}^T P_h \Delta \tilde{F}_h \\ &= -e_{1h}^T R_h e_{1h} + 2 e_{1h}^T P_h \Delta \tilde{F}_h \end{aligned} \tag{4.61}$$

It is known that [74] [75],

$$e_{1h}^T R_h e_{1h} \geq \lambda_{min}(R_h) e_{1h}^T e_{1h} = \lambda_{min}(R_h) ||e_{1h}||^2 \tag{4.62}$$

where λ_{min} is the minimum eigen value and so,

$$\dot{V}_{2h} \leq -\lambda_{min}(R_h)||e_{1h}||^2 + 2e_{1h}^T P_h \Delta\tilde{F}_h \tag{4.63}$$

If there exists a bounded positive constant $\tilde{\lambda}_h$ such that $\tilde{\lambda}_h < 0.5\lambda_{min}(R_h)/||P_h||$, then

$$2e_{1h}^T P_h \Delta\tilde{F}_h \leq 2\tilde{\lambda}_h||P_h||||e_{1h}||^2 < \lambda_{min}(R_h)||e_{1h}||^2 \tag{4.64}$$

and

$$\dot{V}_{2h} \leq -\lambda_{min}(R_h)||e_{1h}||^2 + 2e_{1h}^T P_h \Delta\tilde{F}_h < 0 \tag{4.65}$$

Hence the stability in the sliding mode is proved.

4.3.6 Design of sliding mode controller for the TRMS vertical subsystem

As the gravity force affects the dynamics of the vertical subsystem of the TRMS, it is difficult to control the pitch angle at a desired reference location. In order to reduce the offset of the pitch angle, a proportional plus integral sliding surface is designed for the vertical subsystem. Let us consider the error state space model of the vertical subsystem given by (4.41),

$$\dot{E}_v = A_v E_v + B_v u_v + \Delta F_v \tag{4.66}$$

where $E_v \in R^3$ is the error state vector and $u_v \in R^1$ is the control input. Here A_v and B_v are known matrices with proper dimensions. A proportional plus integral sliding surface is chosen as,

$$s_v = c_v E_v + c_{3v}\int_0^t e_{1v} d\tau \tag{4.67}$$

where $c_v = [c_{1v} \;\; c_{2v}]$ are real positive constants and c_{3v} is also a real positive constant whose selection criterion is to be discussed in Section 4.3.8. For the proposed sliding mode, the first and second order time derivatives of s_v need to be considered. Thus we have,

$$\begin{aligned} \dot{s}_v &= \frac{d}{dt}(c_v E_v + c_{3v}\int_0^t e_{1v} d\tau) \\ &= c_v \dot{E}_v + c_{3v} e_{1v} \\ &= c_v(A_v E_v + B_v u_v + \Delta F_v) + c_{3v} e_{1v} \end{aligned} \tag{4.68}$$

$$\begin{aligned}\ddot{s}_v &= c_v A_v \dot{E}_v + c_v B_v \dot{u}_v + c_v \Delta \dot{F}_v + c_{3v}\dot{e}_{1v} \\ &= c_v A_v (A_v E_v + B_v u_v + \Delta F_v) + c_v B_v \dot{u}_v + c_v \Delta \dot{F}_v + c_{3v}\dot{e}_{1v} \\ &= c_v A_v^2 E_v + c_v A_v B_v u_v + c_v B_v \dot{u}_v + c_{3v}\dot{e}_{1v} + c_v(A_v \Delta F_v + \Delta \dot{F}_v) \end{aligned} \tag{4.69}$$

By following a similar procedure as described earlier in Section 4.3.3, the following is obtained in the case of TRMS VS,

$$\begin{aligned}\dot{\sigma}_v &= (c_v A_v^2 + \kappa_v c_v A_v)E_v + (c_v A_v B_v + \kappa_v c_v B_v)u_v + c_v B_v \dot{u}_v + c_{3v}\dot{e}_{1v} \\ &\quad + \kappa_v c_{3v} e_{1v} + c_v(A_v \Delta F_v + \Delta \dot{F}_v) + \kappa_v c_v \Delta F_v \end{aligned} \tag{4.70}$$

where κ_v is a positive constant. For designing the adaptive part of the control law, we consider [68]

$$\dot{\sigma}_v = -k_{1v}\sigma_v - k_{2v} sign(\sigma_v) \tag{4.71}$$

Using (4.70) and (4.71), the control law is obtained as,

$$\begin{aligned}\dot{u}_v &= -(c_v B_v)^{-1}[(c_v A_v^2 + \kappa_v c_v A_v)E_v + (c_v A_v B_v + \kappa_v c_v B_v)u_v \\ &\quad + c_{3v}\dot{e}_{1v} + \kappa_v c_{3v} e_{1v} + k_{1v}\sigma_v + k_{2v} sign(\sigma_v)] \end{aligned} \tag{4.72}$$

where $k_{1v} \geq 0$ and $k_{2v} > c_v(A_v \Delta F_v + \Delta \dot{F}_v) + \kappa_v c_v \Delta F_v = c_v \nabla F_v = Q_v$ to satisfy the reaching law $\sigma_v \dot{\sigma_v} \leq -\eta_v |\sigma_v|$ [56]. Let us assume that there exits a bounded positive constant $\tilde{\lambda}'_v$ such that, $||\nabla F_v|| \leq \tilde{\lambda}'_v ||E_v||$ [8] and $Q_v = \tilde{\lambda}'_v c_v ||E_v|| \geq 0$.

4.3.7 Design of adaptive tuning law for the vertical subsystem

An adaptive tuning law is designed to determine k_{2v} and so (4.72) can be written as [75]

$$\begin{aligned}\dot{u}_v &= -(c_v B_v)^{-1}[(c_v A_v^2 + \kappa_v c_v A_v)E_v + (c_v A_v B_v + \kappa_v c_v B_v)u_v \\ &\quad + c_{3v}\dot{e}_{1v} + \kappa_v c_{3v} e_{1v} + k_{1v}\sigma_v + \hat{T}_v sign(\sigma_v)] \end{aligned} \tag{4.73}$$

where $\hat{T}_v$ estimates the value of k_{2v}. The actual control is obtained as,

$$\begin{aligned}u_v &= -(c_v B_v)^{-1} \int_0^t [(c_v A_v^2 + \kappa_v c_v A_v)E_v + (c_v A_v B_v + \kappa_v c_v B_v)u_v \\ &\quad + c_{3v}\dot{e}_{1v} + \kappa_v c_{3v} e_{1v} + k_{1v}\sigma_v + \hat{T}_v sign(\sigma_v)] d\tau \end{aligned} \tag{4.74}$$

The parameter $\hat{T}_v$ is estimated as [69] [70]

$$\dot{\hat{T}}_v = \frac{1}{\gamma_v}|\sigma_v| \tag{4.75}$$

where γ_v is a positive constant. A Lyapunov function is chosen as $V_{1v} = \frac{1}{2}\sigma_v^2 + \frac{1}{2}\gamma_v \tilde{T}_v^2$ whose time derivative is obtained as,

$$\begin{aligned}
\dot{V}_{1v} &= \sigma_v \dot{\sigma}_v + \gamma_v \tilde{T}_v \dot{\tilde{T}}_v \\
&= \sigma_v[c_v \nabla F_v - k_{1v}\sigma_v - \hat{T}_v sign(\sigma_v)] + \gamma_v(\hat{T}_v - T_v)\dot{\hat{T}}_v \\
&= \sigma_v[Q_v - k_{1v}\sigma_v - \hat{T}_v sign(\sigma_v)] + \gamma_v(\hat{T}_v - T_v)\dot{\hat{T}}_v \\
&\leq Q_v|\sigma_v| - T_v|\sigma_v| \\
&\leq -\eta_v|\sigma_v|
\end{aligned} \tag{4.76}$$

The above inequality holds if $\dot{\hat{T}}_v = \frac{1}{\gamma_v}|\sigma_v|$ and $T_v > Q_v$.

The adaptive law (4.75) is modified using the dead zone technique [30] as

$$\dot{\hat{T}}_v = \begin{cases} \frac{1}{\gamma_v}|\sigma_v|, & |\sigma_v| \geq \epsilon_v \\ 0, & |\sigma_v| < \epsilon_v \end{cases} \tag{4.77}$$

where ϵ_v is a small positive constant.

The above control law (4.74) is free from any discontinuous part and hence chattering is reduced.

4.3.8 Stability of the sliding surface

During the sliding mode $s_v = 0$ and therefore (4.67) can be written as,

$$\begin{aligned}
s_v &= c_{1v}e_{1v} + c_{2v}e_{2v} + c_{3v}\int_0^t e_{1v}d\tau = 0 \\
or, e_{2v} &= -c_{2v}^{-1}(c_{1v}e_{1v} + c_{3v}\int_0^t e_{1v}d\tau)
\end{aligned} \tag{4.78}$$

Using (4.41), we have

$$\begin{aligned}
\dot{e}_{1v} &= a_{11v}e_{1v} - a_{12v}c_{2v}^{-1}(c_{1v}e_{1v} + c_{3v}\int_0^t e_{1v}\,d\tau) + \Delta\tilde{F}_v \\
&= (a_{11v} - a_{12v}c_{2v}^{-1}c_{1v})e_{1v} - a_{12v}c_{2v}^{-1}c_{3v}\int_0^t e_{1v}\,d\tau + \Delta\tilde{F}_v \\
&= a_{vs}e_{1v} - a_{vt}\int_0^t e_{1v}\,d\tau + \Delta\tilde{F}_v
\end{aligned} \tag{4.79}$$

where $a_{vs} = (a_{11v} - a_{12v}c_{2v}^{-1}c_{1v}) = \begin{bmatrix} a_{vs11} & a_{vs12} \\ a_{vs21} & a_{vs22} \end{bmatrix}$ and $a_{vt} = a_{12v}c_{2v}^{-1}c_{1v} = \begin{bmatrix} a_{vt11} & a_{vt12} \\ a_{vt21} & a_{vt22} \end{bmatrix}$

Let $e_{1v} = [e_{11v} \;\; e_{12v}]^T$ and

$$\int_0^t e_{12v}\, d\tau = e_{11v} \tag{4.80}$$

A new state variable χ_1 is defined as $\chi_1 = \int_0^t e_{11v}\, d\tau$ and hence $\dot{\chi}_1 = e_{11v}$. Thus (4.79) can be represented as,

$$\begin{aligned} \dot{\chi} &= \begin{bmatrix} \dot{\chi}_1 \\ \dot{e}_{11v} \\ \dot{e}_{12v} \end{bmatrix} = \begin{bmatrix} 0 & 1 & 0 \\ 0 & 0 & 1 \\ -a_{vt21} & a_{vs21} - a_{vt22} & a_{vs22} \end{bmatrix} \begin{bmatrix} \chi_1 \\ e_{11v} \\ e_{12v} \end{bmatrix} + \begin{bmatrix} 0 \\ \Delta\tilde{F}_v \end{bmatrix} \\ &= a_{vv}\chi + \begin{bmatrix} 0 \\ \Delta\tilde{F}_v \end{bmatrix} = a_{vv}\chi + \Delta F_{vv} \end{aligned} \tag{4.81}$$

where $\Delta F_{vv} = [0 \;\; \Delta\tilde{F}_v]^T$. It is clear that $||\Delta F_{vv}|| = ||\Delta\tilde{F}_v||$. Here c_{1v}, c_{2v} and c_{3v} are designed in such a way that the eigenvalues of $(a_{11v} - a_{12v}c_{2v}^{-1}c_{1v})$ lie in the left half of the s-plane and there exits a positive definite matrix P_v such that

$$a_{vv}^T P_v + P_v a_{vv} = -R_v \tag{4.82}$$

where R_v is also a positive definite matrix. In the TRMS -VS, ΔF_{vv} satisfies $||\Delta F_{vv}|| \leq \tilde{\lambda}_v||\chi||$ with $\tilde{\lambda}_v < 0.5\lambda_{min}(R_v)/||P_v||$. So the TRMS-VS is stable in the sliding mode. Let a Lyapunov function for the system be selected as $V_{2v} = \chi^T P_v \chi$ whose time derivative is obtained as,

$$\begin{aligned} \dot{V}_{2v} &= \dot{\chi}^T P_v \chi + \chi^T P_v \dot{\chi} \\ &= \chi^T a_{vv}^T P_v \chi + \Delta F_{vv}^T P_v \chi + \chi^T P_v a_{vv} \chi + \chi^T P_v \Delta F_{vv} \\ &= \chi^T (a_{vv}^T P_v \chi + P_v a_{vv})\chi + \Delta F_{vv}^T P_v \chi + \chi^T P_v \Delta F_{vv} \\ &= -\chi^T R_v \chi + 2\chi^T P_v \Delta F_{vv} \end{aligned} \tag{4.83}$$

It is known that [8]

$$\chi^T R_v \chi \geq \lambda_{min}(R_v)\chi^T\chi = \lambda_{min}(R_v)||\chi||^2 \tag{4.84}$$

and $\dot{V}_{2v} \leq -\lambda_{min}(R_v)||\chi||^2 + 2\chi^T P_v \Delta F_{vv}$ if $\tilde{\lambda}_v < 0.5\lambda_{min}(R_v)/||P_v||$, then

$$2\chi^T P_v \Delta F_{vv} \leq 2\tilde{\lambda}_v||P_v||||\chi||^2 < \lambda_{min}(R_v)||\chi||^2 \tag{4.85}$$

Therefore, $\dot{V}_{2v} \leq -\lambda_{min}(R_v)||\chi||^2 + 2\chi^T P_v \Delta F_{vv} < 0$. Hence the stability in the sliding mode is proved.

***Remark* 4.3.** *In designing the control law for the horizontal and vertical subsystems, the terms $\dot{s}_h$ and $\dot{s}_v$ are needed. However, these derivative terms can neither be directly obtained nor measured. Direct differentiation on $s_h(s_v)$ is highly undesirable as practical measurement of $s_h(s_v)$ in real time application will contain high frequency noise. The first/higher order Levant's exact differentiator [25] [64] can be used for the estimation of $\dot{s}_h(\dot{s}_v)$. A first order real time differentiator has the form,*

$$\begin{aligned} \dot{z}_0 &= -\lambda_1 |z_0 - s_h(s_v)|^{1/2} sign(z_0 - s_h(s_v)) + z_1 \\ \dot{z}_1 &= -\lambda_2 sign(z_0 - s_h(s_v)) \end{aligned} \tag{4.86}$$

where $\lambda_1 > 0$ and $\lambda_2 > 0$ are the design parameters and the estimators are designed as $\dot{s}_h(\dot{s}_v) = z_1$.

4.3.9 Simulation results

The proposed adaptive sliding mode controller is applied to the TRMS [8] and the performance of the controlled system is studied by carrying out simulations using MATLAB ODE 4 solver with a fixed step size of 0.01sec. The parameters used for the TRMS are as listed in Table 4.1.

4.3.10 Control parameters for the horizontal subsystem

In the horizontal subsystem, the sliding surface parameters $c_h = [c_{1h} \;\; c_{2h}]$ are chosen as $c_{1h} = [11 \;\; 7]$ and $c_{2h} = [7]$ to satisfy the condition (4.60). The values of the reaching mode coefficient k_{1h} and adaptive tuning parameter γ_h are chosen as 1.0 and 10 respectively (4.51, 4.55) by using the condition given in Section 4.3.4. The value of κ_h (4.47) is chosen as 2.0. The adaptive tuning law is formed as $\dot{\hat{T}}_h = 0.1|\sigma_h|$ and $\hat{T}_h(0) = 0.7$ (4.55). The positive definite matrices P_h and R_h satisfying the stability condition are selected as

$$P_h = \begin{bmatrix} 122.27 & 27.28 \\ 27.28 & 53.24 \end{bmatrix}, R_h = \begin{bmatrix} 98.61 & 7.98 \\ 7.98 & 78.29 \end{bmatrix} \tag{4.87}$$

The above values of P_h and R_h are found suitable for the simulation example.

4.3.11 Control parameters for the vertical subsystem

For the vertical subsystem, the PI sliding surface parameters $c_v = [c_{1v} \;\; c_{2v}]$ (4.67) are chosen as $c_{1v} = [11 \;\; 8], c_{2v} = 12$ and $c_{3v} = [7 \;\; 0.5]$ to satisfy the condition mentioned in Section 4.3.5. The values of the reaching mode coefficient k_{1v} and the adaptive tuning parameter γ_v are selected as 1.3 and 1.25

respectively (4.71, 4.75). The value of κ_v is chosen as 2.0. The adaptive tuning law for the TRMS-VS is formed as $\dot{\hat{T}}_v = 0.8|\sigma_v|$ and $\hat{T}_v(0) = 0.5$. The positive definite matrices P_v and R_v satisfying the stability condition as explained in Section 4.3.8 are found as

$$P_v = \begin{bmatrix} 105.10 & 30.49 & 59.89 \\ 30.49 & 288.55 & 28.08 \\ 59.89 & 28.08 & 199.89 \end{bmatrix}, R_v = \begin{bmatrix} 15.50 & 1.50 & 8.30 \\ 1.50 & 35.60 & 1.30 \\ 8.30 & 1.30 & 30.10 \end{bmatrix} \tag{4.88}$$

The TRMS controlled by using our proposed adaptive sliding mode controller is studied for the position as well as the tracking control problem. In the position control example, the initial condition of the TRMS is considered as $x(0) = [0 \quad -0.5 \quad 0 \quad 0 \quad 0 \quad 0]^T$. In order to study the performance of the proposed controller for both the cases of position and tracking control, the simulation is performed by applying three different reference signals: 1) Step input with 1 rad in the horizontal subsystem and step input with 0.2 rad in the vertical subsystem; 2) Sine wave having amplitude 0.5 rad and frequency 0.025 Hz for the horizontal subsystem and sine wave having amplitude 0.2 rad and frequency 0.025 Hz for the vertical subsystem; 3) Square wave having amplitude 0.5 rad and frequency 0.025 Hz for the horizontal subsystem and square wave having amplitude 0.2 rad and frequency 0.025 Hz for the vertical subsystem.

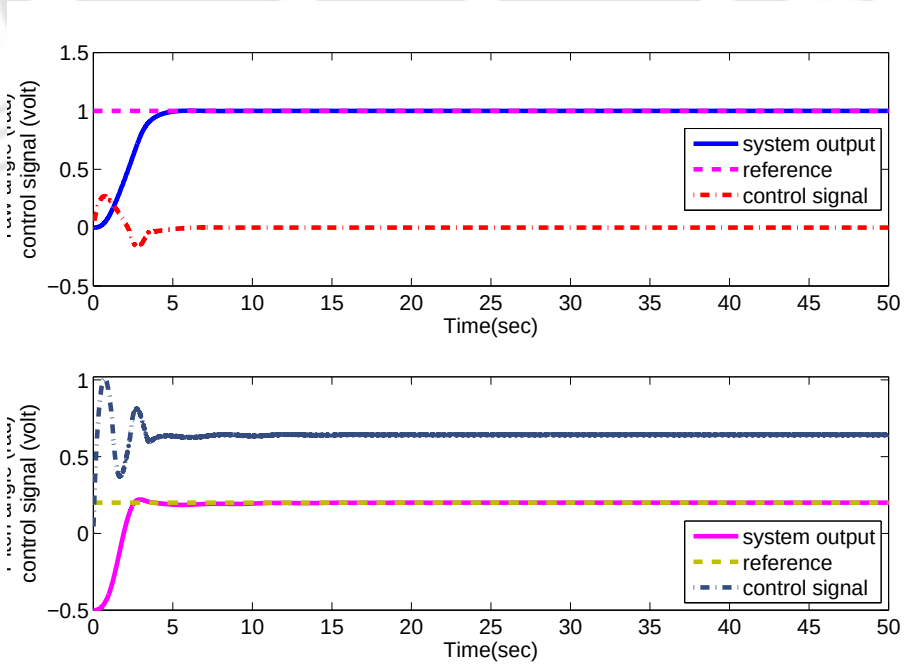

Figure 4.2: Step response of the TRMS using the proposed adaptive SM controller

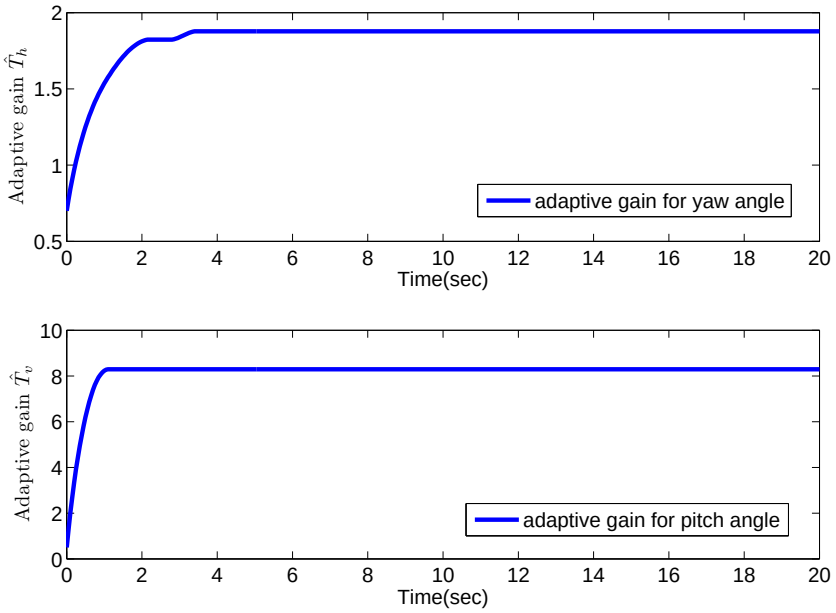

Figure 4.3: Adaptive gain parameter of proposed adaptive SM controller

The desired and the actual step responses of the TRMS along with the control inputs for both the horizontal and the vertical subsystems are plotted in Fig.4.2. The adaptive gain parameters $\hat{T}_h$ and $\hat{T}_v$ for the step response analysis are shown in Fig.4.3.

Table 4.2: Transient performance of the TRMS for step input

Time response parameters					
Reference		Rise time (sec)	Settling time (sec)	Peak time (sec)	Peak overshoot %
Step	H	3.45	4.60	5.50	0
	V	2.45	2.50	2.95	2

Table 4.2 summarises the transient performance of the TRMS using the proposed adaptive sliding mode controller for the step input case. It can be observed from Table 4.2 that for both the horizontal and the vertical subsystems, the TRMS settles quickly to the desired position without much oscillation. In the tracking control example with sine wave, the TRMS settling time is less than 10 sec which was reported in [84]. The actual and the desired trajectory tracking (square and sine) responses as well as the control inputs for both the horizontal and the vertical subsystems are plotted in Figs. 4.4-4.5.

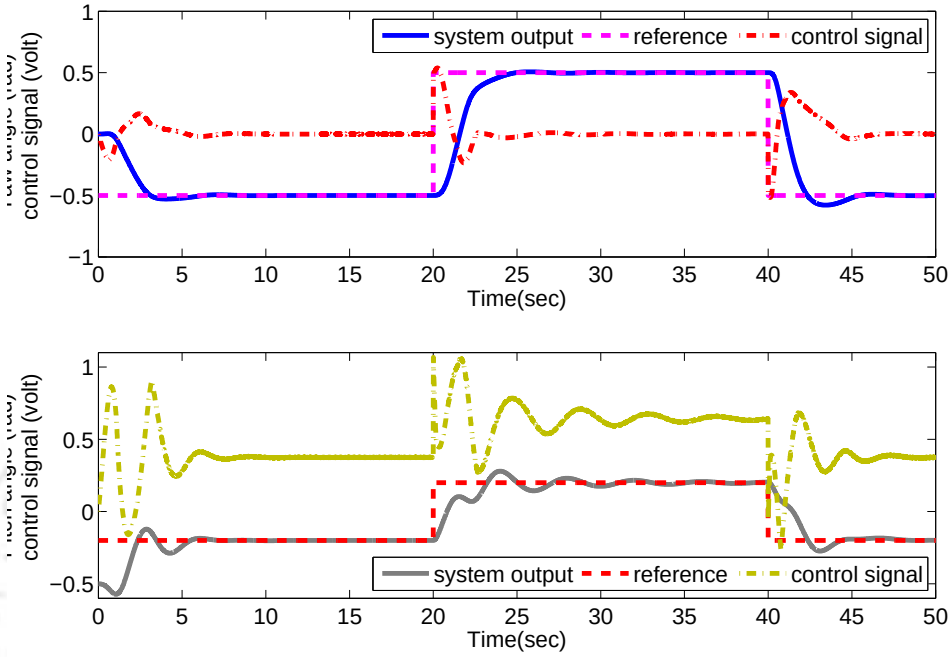

Figure 4.4: Square wave response of the TRMS using the proposed adaptive sliding mode controller

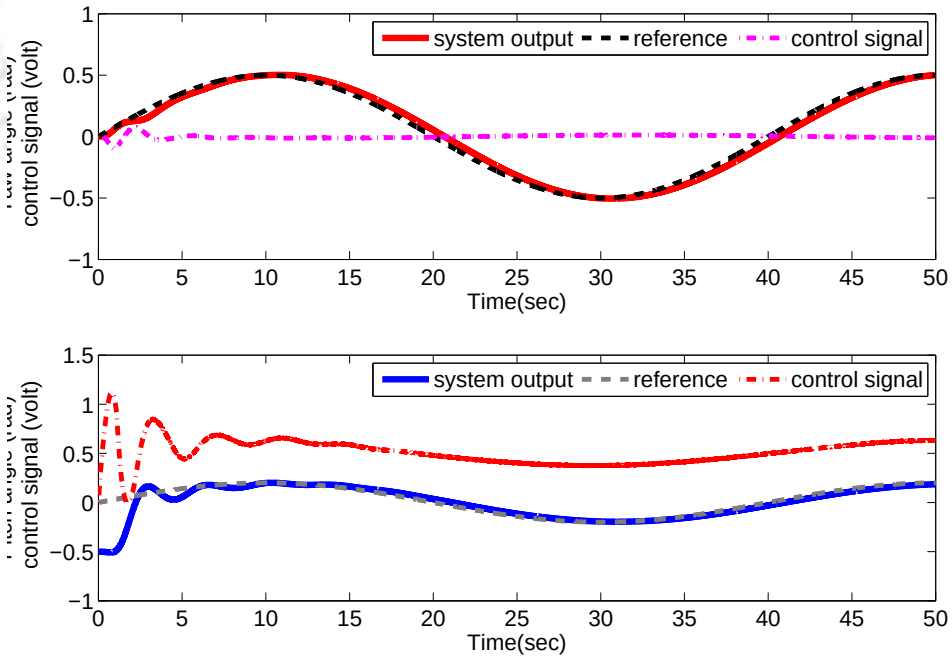

Figure 4.5: Sine wave response of the TRMS using the proposed adaptive sliding mode controller

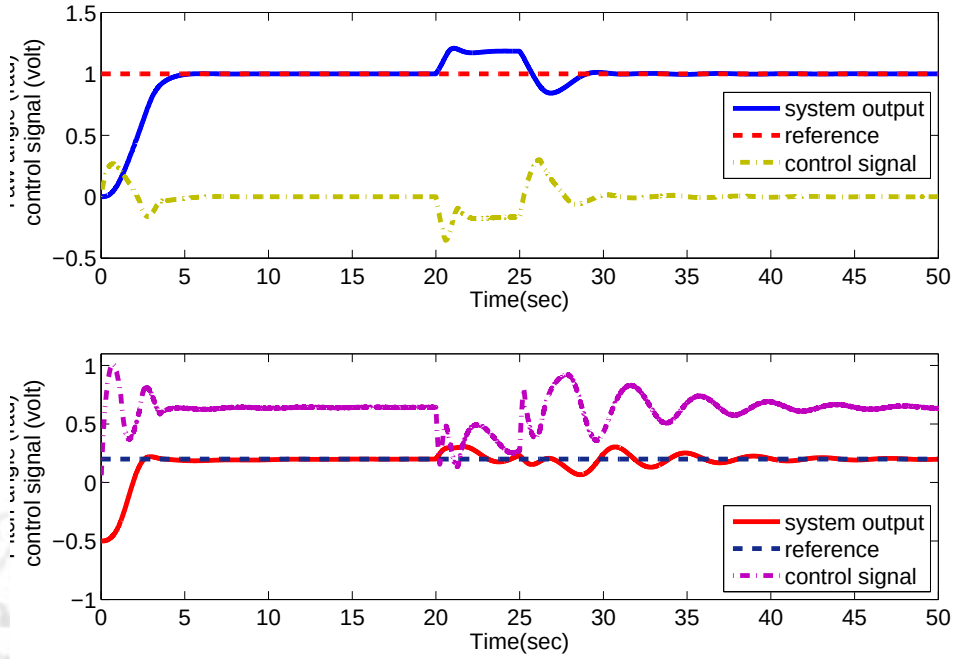

Figure 4.6: Position tracking using the proposed controller subjected to an external disturbance

In order to study the robustness of the adaptive sliding mode controller, an external disturbance $d(t)$ as given below is applied to the TRMS.

$$d(t) = \begin{cases} 0.2, & 20sec \leq t \leq 25sec \\ 0, & otherwise \end{cases} \tag{4.89}$$

Fig. 4.6 illustrates that the TRMS controlled by using the adaptive sliding mode controller stays at the desired position even in the presence of disturbance and thereby proving its robustness.

Juang et al. in [84] illustrated that the proportional integral differential (PID) control with improved RGA (modified real-value-type genetic algorithm (M-RGA)) offered superior control performance than the conventional PID control and conventional realtime GA PID (C-RGA) control. In [84] the performances of the PID, C-RGA and M-RGA controllers are compared by computing the error and control indices which are defined as the sum of their absolute values [8]. In order to study the relative performance of our proposed adaptive sliding mode controller against these afore-mentioned control schemes, the same performance criteria are applied. In our comparison analysis, the error and control indices are calculated from 0 to 50 sec with a sampling period of 0.05 sec and are tabulated in Tables 4.3 and 4.4. The error index is defined as the sum of the absolute values (i.e., error index of HS TRMS=

$\sum_{k=1}^{n} |x_1(k) - x_1^d(k)|$ and error index of VS TRMS= $\sum_{k=1}^{n} |x_2(k) - x_2^d(k)|$ where n is the number of sampling data and $x_1(k)$, $x_1^d(k)$ and $x_2(k)$, $x_2^d(k)$ being the actual and desired states of the HS TRMS and VS TRMS respectively). The control index is defined as the sum of the absolute values of control actions (i.e., control index of HS TRMS = $\sum_{k=1}^{n} |u_h(k)|$ and control index of VS TRMS=$\sum_{k=1}^{n} |u_v(k)|$ where u_h and u_v are the control inputs for the HS TRMS and VS TRMS respectively.

Table 4.3: Comparison of Error Index among different controllers

Error index					
Reference		PID [84]	C-RGA [84]	M-RGA [84]	Adaptive sliding mode
Step	H	81.2	69.09	54.52	45.23
	V	40.11	34.92	27.46	23.08
Sine	H	23.21	19.33	20.92	32.33
	V	65.74	51.78	52.61	42.20
Square	H	150.22	141.52	134.03	83.70
	V	112.85	96.36	90.21	45.80

Table 4.4: Comparison of Control Index among different controllers

Control Index					
Reference		PID [84]	C-RGA [84]	M-RGA [84]	Adaptive sliding mode
Step	H	76.71	51.34	40.47	12.45
	V	812.36	701.23	617.10	645.98
Sine	H	27.41	20.12	18.93	10.68
	V	611.70	500.2	501.78	515.42
Square	H	202	171.28	165.32	42.34
	V	656.37	591.65	551.59	487.29

It is evident from these two tables that the proposed adaptive sliding mode controller exhibits lesser error and requires lesser control action in majority of the cases as compared to the other control methods [84].

4.4 The vertical take-off and landing (VTOL) aircraft

The vertical take-off and landing (VTOL) aircraft is a highly complex nonlinear system whose aerodynamic parameters vary considerably during the flight. Fig.4.7 shows the typical coordinate system for a VTOL aircraft in the vertical plane. The linearized dynamics of this VTOL aircraft in the vertical plane can be described as,

$$\dot{x} = Ax + B[u + \xi(t, x)] + p(t, x) \tag{4.90}$$

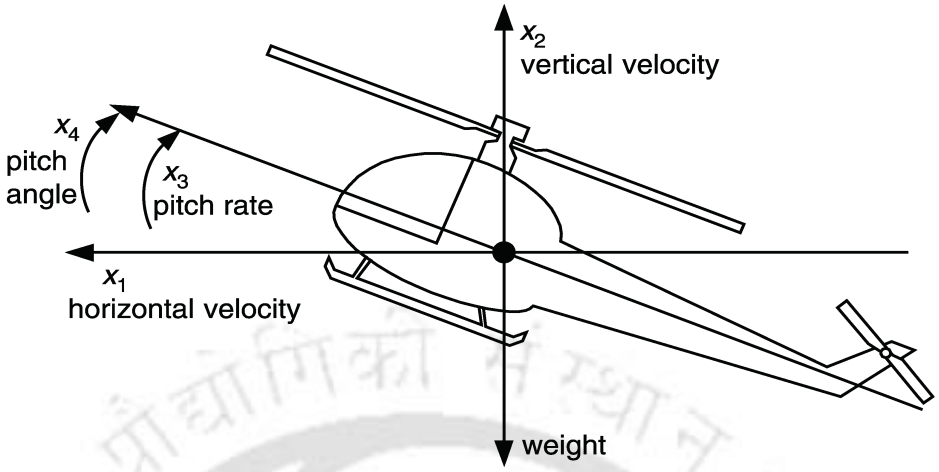

Figure 4.7: A typical sketch of a VTOL aircraft in the vertical plane [2].

where

$$\begin{aligned} x &= [x_1 \;\; x_2 \;\; x_3 \;\; x_4]^T \\ u &= [u_1 \;\; u_2]^T \end{aligned} \tag{4.91}$$

Here x_1 is the horizontal velocity (knots), x_2 is the vertical velocity (knots), x_3 is the pitch rate (degrees per second) and x_4 is the pitch angle (degrees). Furthermore, u_1 is the collective pitch control which alters the pitch angle (angle of attack with respect to air) of the main rotor blades collectively to provide the vertical movement. Moreover, u_2 is the longitudinal cyclic pitch control which tilts the main rotor disc by varying the pitch of the main rotor blades individually to provide the horizontal movement. However, u_1 and u_2 have some cross-effect on the horizontal and vertical velocities, respectively. The matched and mismatched perturbations are $\xi(t,x)$ and $p(t,x)$ respectively [3]. Moreover, A and B are known matrices with proper dimension and B has full rank.

4.4.1 Adaptive sliding mode controller design with PI sliding surface

The sliding surface σ is designed as

$$\sigma = sx \tag{4.92}$$

where $s \in R^{m*n}$ is a constant matrix designed by selecting the eigen values suitably (all negative) to make the system stable [68]. By using the transformation [3] [35] [86] $\begin{bmatrix} z \\ \sigma \end{bmatrix} = Mx$ where the transformation matrix $M = \begin{bmatrix} W_g \\ B_g \end{bmatrix}$, Eq.(4.90) can be transformed to

$$\begin{aligned} \dot{z} &= W_g AWz + W_g AB\sigma + W_g p(t,x) \\ \dot{\sigma} &= B_g AWz + B_g AB\sigma + u + \xi(t,x) + sp(t,x) \end{aligned} \tag{4.93}$$

Here $s = B_g$ and W_g, B_g satisfy $B_g B = I_m$, $B_g W = 0$, $W_g B = 0$, and $W_g W = I_{n-m}$. The matrix W is chosen in such a way that $J = W_g AW$ has the desired eigen values [86] where J is a symmetric matrix. It can be verified that

$$M^{-1} = [W \quad B] \tag{4.94}$$

When the system is in the sliding mode, it satisfies the conditions $\sigma = 0$ and $\dot{\sigma} = 0$. Then the perturbation term in Eq.(4.93) becomes $W_g p(t,x) = W_g p(t, Wz) = p_r(t,z)$. Now the reduced order equation becomes

$$\dot{z} = Jz + p_r(t,z) \tag{4.95}$$

If the mismatched perturbation $p_r(t,z)$ satisfies $||p_r(t,z)|| \leq \phi_r ||z||$ where $\phi_r < -\lambda_{\max}(J)$, $\lambda_{max}(J)$ being the maximum eigen value of the J matrix, then by choosing the Lyapunov function $V = \frac{1}{2}||z||^2$, it can be proved that [3] [38]

$$\dot{V} = z^T Jz + z^T p_r(t,z) \leq \lambda_{\max}(J)||z||^2 + \phi_r ||z||^2 = [\lambda_{\max}(J) + \phi_r]V < 0 \tag{4.96}$$

The above condition means that the system will be asymptotically stable once the sliding mode is reached. However, it is obvious from the above discussion that the sliding surface design requires the bounds of the uncertainties to be known apriori [75] which is extremely difficult practically. Hence the need arises for designing the sliding surface in such a way that prior knowledge about the bounds of the uncertainties is not required.

4.4.2 The adaptive PI sliding surface design

Let us consider the sliding surface

$$\sigma = s(t)x \tag{4.97}$$

The sliding coefficient matrix $s(t) \in R^{m*n}$ can be designed as [3]

$$s(t) = B^{+} + N(t)W_g \tag{4.98}$$

where $B^{+} = (B^T B)^{-1}B^T \in R^{m*n}$ is the Moore-Penrose pseudo inverse [20] of B and $N(t) \in R^{m*n}$ is designed using adaptive technique to be explained later. Let us consider the transformation

$$\begin{bmatrix} z \\ \sigma \end{bmatrix} = \begin{bmatrix} W_g \\ s(t) \end{bmatrix} x = M(t)x \tag{4.99}$$

Now defining $W(t) = W_g^{+} - BN(t) \in R^{n*(n-m)}$ and $W_g^{+} = W_g^T(W_g W_g^T)^{-1} \in R^{n*(n-m)}$, it can be verified that

$$M(t)^{-1} = [W(t) \quad B] \tag{4.100}$$

From Eq.s (4.99) and (4.100), it can be observed that

$$x = W(t)z + B\sigma \tag{4.101}$$

So, Eq.(4.90) gets transformed to

$$\dot{z} = W_g AW(t)z + W_g AB\sigma + W_g p(t,x) \tag{4.102}$$

$$\dot{\sigma} = s(t)AW(t)z + s(t)AB\sigma + u + \dot{N}(t)z + \xi(t,x) + s(t)p(t,x) \tag{4.103}$$

When the system is in the sliding mode, it satisfies the conditions $\sigma = 0$ and $\dot{\sigma} = 0$. Then the perturbation term in Eq.(4.102) becomes $W_g p(t,x) = W_g p(t, W(t)z) = \bar{p}(t,z)$ and Eq.(4.102) transforms into a reduced order equation as,

$$\dot{z} = \bar{A}z + \bar{B}v(t) + \bar{p}(t,z) \tag{4.104}$$

where $\bar{A} = W_g A W_g^+ \in R^{(n-m)*(n-m)}$, $\bar{B} = W_g A B \in R^{(n-m)*m}$ and $v(t) = -N(t)z \in R^m$.

***Theorem* 4.1.** *Let us consider the perturbed dynamic equation (4.104) under the assumption that $n \leq 2m$. Suppose that $\bar{B}$ has full rank and the mismatched perturbations in the domain of interest satisfy $\|\bar{p}(t,z)\| \leq \phi_2||z||$, where ϕ_2 is an unknown positive constant. If the feedback gain $N(t)$ of the controller is designed as [38]*

$$N(t) = K_2 + [\hat{\phi}_2(t) + \rho]\bar{B}^+ \tag{4.105}$$

where ρ is a positive constant, $K_2 = \bar{B}^+\bar{A}$, $\bar{B}^+ = \bar{B}^T(\bar{B}\bar{B}^T)^{-1} \in R^{m*(n-m)}$ and $\hat{\phi}_2(t)$ is an adaptive gain given by

$$\hat{\phi}_2(t) = \int_{t_0}^{t} \theta||z||^2 d\tau + \hat{\phi}_2(t_0) \tag{4.106}$$

with $\theta > 0$ being a positive constant and $\hat{\phi}_2(t_0) = 0$ being the initial condition, then $\hat{\phi}_2(t)$ is bounded and the trajectories z (4.104) and state x will be asymptotically stable in the sliding mode.

Proof. Let us consider the Lyapunov function $V_2(z, \tilde{\phi}_2) = \frac{1}{2}[\|z\|^2 + \theta^{-1}\tilde{\phi}_2(t)^2]$. Here $\tilde{\phi}_2(t)$ is the estimation error of the adaptive gain given by $\tilde{\phi}_2(t) = \hat{\phi}_2(t) - \phi_2(t)$, where $\hat{\phi}_2(t)$ is the estimated adaptive gain and $\phi_2(t)$ is the actual adaptive gain [3]. Then

$$\begin{aligned}
\dot{V}_2(z, \tilde{\phi}_2) &= z^T\bar{A}z + z^T\bar{B}v + z^T\bar{p} + \theta^{-1}\tilde{\phi}_2\dot{\hat{\phi}}_2 \\
&\leq z^T\bar{A}z + z^T\bar{B}v + ||z||||\bar{p}|| + \theta^{-1}\tilde{\phi}_2\dot{\hat{\phi}}_2 \\
&\leq z^T\bar{A}z + z^T\bar{B}v + \phi_2||z||^2 + (\hat{\phi}_2 - \phi_2)||z||^2 \\
&\leq z^T\bar{A}z + z^T\bar{B}v + \hat{\phi}_2||z||^2 \\
&\leq -\rho||z||^2 \leq 0
\end{aligned} \tag{4.107}$$

It is obvious from the above discussion that $z \in L_2 \cap L_\infty$ and $\tilde{\phi}_2(t) \in L_\infty$. Hence from Eq.s (4.104), (4.105) and the fact that $\|\bar{p}(t,z)\| \leq \phi_2\|z\|$, it can be shown that $\dot{z} \in L_\infty$ as well as $\ddot{V}_2 \in L_\infty$. From Barbalat's lemma [30], it is found that $z \to 0$ as $t \to \infty$. The bound of the adaptation law is $0 \leq \phi_2(t) \leq (\|z(t_0)\|^2 + \phi_2^2)/\rho$. Moreover, it can be seen from equation (4.105) that $N(t)$ is bounded since $\tilde{\phi}_2(t) \in L_\infty$ and hence the state $x(t) = W(t)z = [W_g^+ - BN(t)]z$ becomes asymptotically stable as the system reaches the sliding mode.

It can be observed in Fig.4.7 that the VTOL weighs asymmetrically as the main propeller is heavier than the tail propeller, i.e. the horizontal velocity and the vertical velocity would not stay in the

desired states because of gravity. As such, control performance of the VTOL tends to be poor. In order to eliminate the effect of the asymmetrical weight and reduce the offset in control, a proportional plus integral sliding surface is used in the proposed controller. The sliding surface is chosen as,

$$\sigma' = s(t)x - B^{+}(A + BK)\int_0^t x d\tau \tag{4.108}$$

where x is the state vector and $B^{+} = (B^T B)^{-1}B^T \in R^{m*n}$ is the the Moore-Penrose pseudo inverse of B [20]. Moreover, K is the design matrix $\in R^{m*n}$ to satisfy the inequality

$$Re[\lambda_{max}(A + BK) < 0] \tag{4.109}$$

Taking the derivative of σ' and using (4.103) yields

$$\dot{\sigma}' = s(t)AW(t)z + s(t)AB\sigma + u - B^{+}(A + BK)(W(t)z + B\sigma) + d(t, x) \tag{4.110}$$

where,

$$\begin{aligned} d(t,x) &= \dot{N}(t)z + \xi(t,x) + s(t)p(t,x) \\ &= \theta \left\|W_g x\right\|^2 \bar{B}^{+} W_g x + \xi(t,x) + s(t)p(t,x) \end{aligned} \tag{4.111}$$

The second derivative of σ' can be expressed as

$$\begin{aligned} \ddot{\sigma}' &= \dot{s}(t)AW(t)z + s(t)A\dot{W}(t)z + s(t)AW(t)\dot{z} + \dot{s}(t)AB\sigma + s(t)AB\dot{\sigma} \\ &\quad -B^{+}(A + BK)(\dot{W}(t)z + W(t)\dot{z} + B\dot{\sigma}) + \dot{u} + \dot{d}(t,x) \end{aligned} \tag{4.112}$$

In the above equation (4.112), $\dot{d}(t, x)$ is considered as unknown disturbance or perturbation.

***Assumption* 4.1.**: *The disturbance $\dot{d}(t, x)$ in (4.112) is assumed to be bounded and satisfy the following condition:*

$$||\dot{d}(t,x)|| \leq \sum_{i=0}^{r} \bar{B}_i ||x||^i \tag{4.113}$$

where $\bar{B}_i$ are unknown bounds, which are not easily obtained due to the complicated structure of the uncertainties in practical control systems. Furthermore, r is a positive integer determined by the designer in accordance with the knowledge about the order of the perturbations. For example, if the perturbations contain a term x_1^3, then one may choose $r = 3$. However, if x_1^4 exists in the perturbation, then the inequality might not be satisfied for certain domain of x if one still chooses $r = 3$ [38].

Let us define the sliding manifold $l(t)$ such that,

$$\begin{aligned} l(t) &= \dot{\sigma}' + \kappa\sigma' \\ \dot{l}(t) &= \ddot{\sigma}' + \kappa\dot{\sigma}' \end{aligned} \tag{4.114}$$

Using the above equations (4.112), (4.113) and (4.114) yields

$$\begin{aligned} \dot{l}(t) &= \dot{s}(t)AW(t)z + s(t)A\dot{W}(t)z + s(t)AW(t)\dot{z} + \dot{s}(t)AB\sigma + s(t)AB\dot{\sigma} \\ &\quad -B^{+}(A+BK)(\dot{W}(t)z + W(t)\dot{z} + B\dot{\sigma}) + \dot{u} + \dot{d}(t,x) + \kappa\dot{\sigma}' \end{aligned} \tag{4.115}$$

The derivative of the sliding manifold $l(t)$ can be expressed as

$$\dot{l}(t) = \Phi(t,z,u) + \psi(t,z)\dot{u} \tag{4.116}$$

where $\Phi(t,z,u) = \dot{s}(t)AW(t)z+s(t)A\dot{W}(t)z+s(t)AW(t)\dot{z}+\dot{s}(t)AB\sigma+s(t)AB\dot{\sigma}-B^{+}(A+BK)(\dot{W}(t)z+W(t)\dot{z}+B\dot{\sigma}) + \dot{d}(t,x) + \kappa\dot{\sigma}'$ collects all the uncertain terms not involving $\dot{u}$ and $\psi(t,z) = 1$. From equation (4.115), the equivalent control $\dot{u}_{eq}$ for controlling the nominal system can be designed as

$$\begin{aligned} \dot{u}_{eq} &= -[\dot{s}(t)AW(t)z + s(t)A\dot{W}(t)z + s(t)AW(t)\dot{z} + \dot{s}(t)AB\sigma \\ &\quad +s(t)AB\dot{\sigma} - B^{+}(A+BK)(\dot{W}(t)z + W(t)\dot{z} + B\dot{\sigma}) + \kappa\dot{\sigma}'] \qquad \text{if} \quad l(t) \neq 0 \\ &= 0 \qquad \text{otherwise} \end{aligned} \tag{4.117}$$

In practice, the bounds of the system uncertainty are often unknown in advance and hence the error term $\dot{d}(t,x)$ in equation (4.112) is difficult to find. So an adaptive tuning law is proposed to estimate $\dot{d}(t,x)$. Now the proposed adaptive controller for tackling the system uncertainty is designed as [87],

$$\begin{aligned} \dot{u}_{adp} &= -\sum_{i=0}^{r} \hat{\bar{B}}_i ||x||^i sign(l(t)) \qquad \text{if} \quad l(t) \neq 0 \\ &= 0 \qquad \text{otherwise} \end{aligned} \tag{4.118}$$

where $\hat{\bar{B}}_i$ is the adaptive parameter which is tuned using the following adaptive rule,

$$\begin{aligned} \dot{\hat{\bar{B}}}_i &= -\theta_i\rho_i\hat{\bar{B}}_i + \theta_i||l(t)||||x||^i \qquad \text{if} \quad l(t) \neq 0 \\ &= 0 \qquad \text{otherwise} \end{aligned} \tag{4.119}$$

where ρ_i and θ_i are positive constants, $\hat{\bar{B}}_i(0) = 0$ is the initial condition, $0 \leq i \leq r$.

The switching control law $\dot{u}_s$ can be designed as,

$$\begin{aligned} \dot{u}_s &= -\tau l(t) - \eta sign(l(t)) \qquad \text{if} \quad l(t) \neq 0 \\ &= 0 \qquad \text{otherwise} \end{aligned} \tag{4.120}$$

where τ and η are positive constants.

Now the control law $\dot{u}$ can be obtained as,

$$\dot{u} = \dot{u}_{eq} + \dot{u}_{adp} + \dot{u}_s \tag{4.121}$$

where $\dot{u}_{eq}$ is the equivalent control part, $\dot{u}_{adp}$ is the adaptive control part and $\dot{u}_s$ is the switching control.

***Theorem* 4.2.** *Let us consider the system (4.90) with the adaptive sliding surface given by (4.98) and (4.105). The trajectory of the closed loop system (4.90) can be driven onto the sliding manifold $l(t)$ in finite time by using the controller given by*

$$\begin{aligned} \dot{u} &= -[\dot{s}(t)AW(t)z + s(t)A\dot{W}(t)z + s(t)AW(t)\dot{z} + \dot{s}(t)AB\sigma \\ &\quad + s(t)AB\dot{\sigma} - B^{+}(A+BK)(\dot{W}(t)z + W(t)\dot{z} + B\dot{\sigma}) + \kappa\dot{\sigma}'] \\ &\quad - \sum_{i=0}^{r} \hat{\bar{B}}_i ||x||^i sign(l(t)) - \tau l(t) - \eta sign(l(t)) \qquad \text{if} \quad l(t) \neq 0 \\ &= 0 \qquad otherwise \end{aligned} \tag{4.122}$$

Proof. Let us define a Lyapunov function V_0 as follows [40, 87],

$$V_0 = \frac{1}{2} l(t)^T l(t) + \frac{1}{2} \sum_{i=0}^{r} \theta_i^{-1} \tilde{\bar{B}}_i^2 \tag{4.123}$$

where $\tilde{\bar{B}}_i(t) = \hat{\bar{B}}_i(t) - \bar{B}_i$ are the estimation errors of the adaptive gains. The time derivative of V_0 is obtained as,

$$\begin{aligned} \dot{V}_0 &= l(t)^T \dot{l}(t) + \sum_{i=0}^{r} \theta_i^{-1} \tilde{\bar{B}}_i \dot{\tilde{\bar{B}}}_i \\ &= l(t)^T [\dot{s}(t)AW(t)z + s(t)A\dot{W}(t)z + s(t)AW(t)\dot{z} + \dot{s}(t)AB\sigma \\ &\quad + s(t)AB\dot{\sigma} - B^{+}(A+BK)(\dot{W}(t)z + W(t)\dot{z} + B\dot{\sigma}) + \kappa\dot{\sigma}' + \dot{u} + \dot{d}(t,x)] + \sum_{i=0}^{r} \theta_i^{-1} \tilde{\bar{B}}_i \end{aligned}$$

$$
\begin{aligned}
&= l(t)^T[\dot{s}(t)AW(t)z + s(t)A\dot{W}(t)z + s(t)AW(t)\dot{z} + \dot{s}(t)AB\sigma \\
&+s(t)AB\dot{\sigma} - B^+(A+BK)(\dot{W}(t)z + W(t)\dot{z} + B\dot{\sigma}) + \kappa\dot{\sigma}' + \dot{u} + \dot{d}(t,x)] \\
&+\sum_{i=0}^{r}\theta_i^{-1}(\hat{\bar{B}}_i(t) - \bar{B}_i)\theta_i(-\rho_i\hat{\bar{B}}_i + ||l(t)||\,||x||^i) \\
&\text{Using the relations in (4.117-4.120) yields,} \\
\dot{V}_0 \quad &\leq [-\sum_{i=0}^{r}\hat{\bar{B}}_i||x||^i||l(t)|| - \sum_{i=0}^{r}\bar{B}_i||x||^i||l(t)|| - \tau||l(t)|| - \eta||l(t)|| \\
&+\sum_{i=0}^{r}\hat{\bar{B}}_i||x||^i||l(t)|| + \sum_{i=0}^{r}\bar{B}_i||x||^i||l(t)||] - \rho_i(\hat{\bar{B}}_i^2 - \hat{\bar{B}}_i\bar{B}_i) \\
&\leq -\eta l(t)sign(l(t)) - \tau l(t)^2 - \rho_i(\hat{\bar{B}}_i - \frac{1}{2}\bar{B}_i)^2 + \frac{1}{4}\rho_i\bar{B}_i^2 \\
&\leq -\eta||l(t)|| - \tau l(t)^2 + \frac{1}{4}\rho_i\bar{B}_i^2 \qquad (4.124)
\end{aligned}
$$

It is clear that $\dot{V}_0 < 0$ if $l(t) > \sqrt{\frac{\delta_1}{4\tau_{min}}}$ or $||l(t)|| > \frac{\delta_1}{4\eta_{min}}$, where η, τ are positive design parameters and $\delta_1 = \rho_i\bar{B}_i^2$. The decrease of V_0 eventually drives the trajectories of the closed loop system into $l(t) > \sqrt{\frac{\delta_1}{4\tau_{min}}}$ and $||l(t)|| > \frac{\delta_1}{4\eta_{min}}$. Therefore, the trajectories of the closed loop system are bounded ultimately as

$$\lim_{t\to\infty} l(t) \in \left(l(t) > \sqrt{\frac{\delta_1}{4\tau_{min}}}\right) \bigcap \left(||l(t)|| > \frac{\delta_1}{4\eta_{min}}\right) \qquad (4.125)$$

which is a small set containing the origin of the closed loop system. In order to guarantee bounded motion around the sliding surface, the positive parameters η and τ are chosen to be large enough such that $\dot{V}_0 < 0$ when V_0 is out of the bounded region which contains an equilibrium point [40]. It can be observed that $\dot{V}_0 < 0$ is achievable which implies that the sliding manifold $l(t)$ will approach zero in finite time. Therefore, the control law given by (4.122) guarantees that the sliding mode will be reached in finite time and sustained thereafter [87].

***Remark* 4.4.** *Once the sliding mode is established, the proposed gain adaptation law (4.119) allows the gain $\hat{\bar{B}}_i$ to decrease. Thus it is seen that the proposed gain adaptation law, while maintaining the sliding mode, keeps the gain $\hat{\bar{B}}_i$ at the smallest possible level to ensure accuracy.*

Thus the adaptive gain tuning law is modified as,

$$
\begin{aligned}
\dot{\hat{\bar{B}}}_i &= -\theta_i\rho_i\hat{\bar{B}}_i + \theta_i||l(t) - \wp||||x||^i \qquad \text{if} \qquad l(t) \neq 0 \\
&= 0 \qquad \text{otherwise} \qquad (4.126)
\end{aligned}
$$

where $0 \leq i \leq r$ and $\wp$ is a small positive number.

***Remark* 4.5.** *The parameter τ in the controller (4.122) is very crucial as it is one of the parameters responsible for determining the convergence rate of the sliding surface. It is clear that a large value of τ will force the system states to converge to the origin at a high speed. Since a high η will require a very high control input which is not desirable in reality, the parameter η cannot be selected too large. Hence a compromise has to be made between the response speed and the control input.*

***Remark* 4.6.** *The parameters ρ_0 and ρ_1 in (4.126) determine the convergence rate of the estimated bounds $\hat{\bar{B}}_0$ and $\hat{\bar{B}}_1$. Large values of ρ_0 and ρ_1 can be chosen so that the estimated bounds $\hat{\bar{B}}_0$ and $\hat{\bar{B}}_1$ converge quickly to the actual bounds.*

4.4.3 Effectiveness

Let us compare the proposed adaptive sliding mode controller with the adaptive sliding mode controller (SMC) designed by Wen and Cheng [3] and given below:

$$u = u_f + u_{adp} + u_s \tag{4.127}$$

where

$$\begin{aligned} u_f &= -s(t)AW(t)z - s(t)AB\sigma \\ u_{adp} &= -\sum_{i=0}^{r} \hat{\bar{B}}_i ||x||^i \frac{\sigma}{||\sigma||} \qquad \text{if} \quad \sigma \neq 0 \\ &= 0 \qquad \text{otherwise} \\ u_s &= -\eta \frac{\sigma}{||\sigma||} \qquad \text{if} \quad \sigma \neq 0 \\ &= 0 \qquad \text{otherwise} \end{aligned} \tag{4.128}$$

The adaptive parameter $\hat{\bar{B}}_i$ is tuned using the following adaptive rule,

$$\begin{aligned} \dot{\hat{\bar{B}}}_i &= \theta_i ||x||^i \qquad \text{if} \quad \sigma \neq 0 \\ &= 0 \qquad \text{otherwise} \end{aligned} \tag{4.129}$$

where θ_i are positive constants, $\hat{\bar{B}}_i(0) = 0$ is the initial condition, $0 \leq i \leq r$.

Implementation of the adaptive SMC (4.127-4.129) is limited by the obvious drawback of the gain $\hat{\bar{B}}_i$

being susceptible to overestimation and thereby increasing the chattering in the system. Furthermore, this approach is not directly applicable to real systems but requires modifications involving the sign function which needs replacement by a saturation function. However, the width of the boundary layer in the saturation function affects accuracy and robustness of the SMC. Furthermore, no methodology for tuning the boundary layer width is provided in [3].

4.4.4 Simulation Results

The typical load and flight conditions for the VTOL aircraft are considered at the nominal airspeed of 135 knots [3]. The linearized dynamics of this VTOL aircraft in the vertical plane can be described by (4.90 - 4.91) where,

$$\begin{aligned} A &= \begin{bmatrix} -0.0366 & 0.0271 & 0.0188 & -0.4555 \\ 0.0482 & -1.0100 & 0.0024 & -4.0208 \\ 0.1002 & 0.3681 & -0.7070 & 1.4200 \\ 0 & 0 & 1 & 0 \end{bmatrix}, \quad B = \begin{bmatrix} -0.4422 & 0.1761 \\ 3.5446 & -7.5922 \\ -5.52 & 4.49 \\ 0 & 0 \end{bmatrix} \\ \xi(t,x) &= \begin{bmatrix} -5\sin(0.5t) + x_3 \\ 2\cos(0.2x_1)x_2 + 3 \end{bmatrix}, \quad p(t,x) = \begin{bmatrix} \sin(0.1x_2)(0.1x_3 + 0.7x_4) \\ -0.3x_4\cos(0.3x_4 t) \\ -2x_1 - 0.3x_2 \\ (0.2x_1 + 0.4x_4)\sin(0.4x_3) \end{bmatrix} \end{aligned} \tag{4.130}$$

The simulation is carried out in MATLAB Simulink platform by using ODE 4 solver with a fixed step size of 0.001sec. The reference vector is chosen as $x_d = [0\ 0\ 0\ 0]^T$ since all the states are to be driven to zero. For comparison purpose, the associated design parameters of the proposed adaptive sliding mode controller are chosen following [3]. As such W_g is selected as,

$$W_g = \begin{bmatrix} 0.0666 & 0.0076 & 0.0102 & 0.72 \\ 0.8879 & 0.1010 & 0.136 & -0.028 \end{bmatrix} \tag{4.131}$$

Hence $W_g B = 0$ [86]. Next the pseudo control input, the adaptive controller and the adaptive gains are designed in accordance with equations (4.105), (4.106), (4.119) and (4.126) where $\theta = 0.1474$, $\theta_0 = 0.1271$, $\theta_1 = 0.1251$, $\rho = 0.1971$, $\eta = 2$, $\tau = 1$, $\kappa = diag(1.25, 1.25)$, $\rho = 0.1519$ and K is so chosen that the eigen values are placed at $-0.5, -0.7, -15, -25$ [20]. The initial state is assumed as $x(0) = [2 \quad -2 \quad 1 \quad 1]^T$.

The adaptive tuning laws used for stabilization are given by,

$$\begin{aligned}
\dot{\hat{\phi}}_2 &= \theta||z||^2 \\
\dot{\hat{B}}_1 &= -0.151\hat{B}_1 + \theta_1 \ ||l(t) - \wp|| \ ||x|| \\
\dot{\hat{B}}_0 &= -0.151\hat{B}_0 + \theta_0 \ ||l(t) - \wp||
\end{aligned}$$

The initial values of $\hat{\phi}_2$, $\hat{B}_1$ and $\hat{B}_0$ are chosen as $0, 1, 1$ respectively. The small positive constant $\wp$ is chosen as $\wp = 0.01$.

The adaptive first order sliding mode controller proposed by Wen and Cheng [3] (4.127 - 4.129) is applied to the VTOL aircraft system (4.90 - 4.91). The design parameters are chosen as $\theta = 0.3$, $\theta_0 = 0.21$, $\theta_1 = 0.27$, $\eta = 4$ and $\rho = 1$. The initial state is assumed as $x(0) = [2 \quad -2 \quad 1 \quad 1]^T$. From simulation results obtained in Figs. 4.8 - 4.9 it can be observed that although the system states converge to the equilibrium, the control inputs are not smooth and contain excessive chattering.

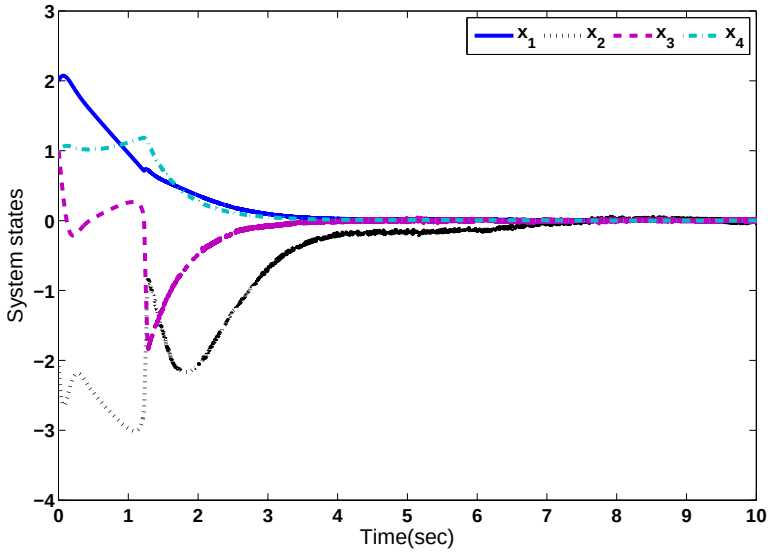

Figure 4.8: State responses with the method proposed by Wen and Cheng [3]

The simulation results obtained by using the proposed adaptive sliding mode controller to the VTOL aircraft system are shown in Figs. 4.10 - 4.13. It is observed from Fig. 4.10 that all the states converge to the origin quickly. Moreover, comparison of Fig. 4.10 with Fig. 4.8 reveals that in the proposed method, the states converge in lesser time as compared to Wen and Cheng [3]. From Fig. 4.9 and Fig. 4.11 it is evident that chattering present in the control inputs obtained by using the proposed adaptive

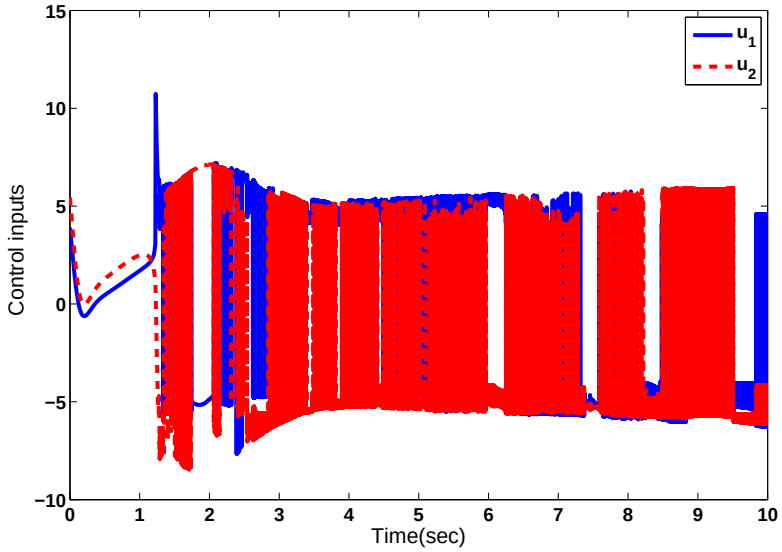

Figure 4.9: Control inputs with the method proposed by Wen and Cheng [3]

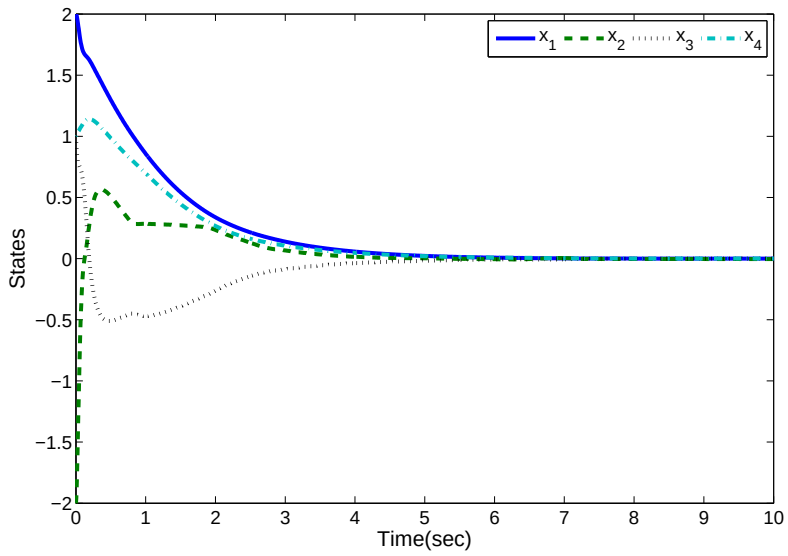

Figure 4.10: State responses using the proposed adaptive sliding mode controller

sliding mode controller is significantly lesser as compared to that in [3]. The bounded convergence of the adaptive gains $\hat{\bar{B}}_0$, $\hat{\bar{B}}_1$ and $\hat{\phi}_2$ are confirmed in Fig. 4.12. From Fig. 4.13 it can be observed that the proportional plus integral sliding surface σ' and the sliding manifold $l(t)$ are smooth and both approach zero quickly.

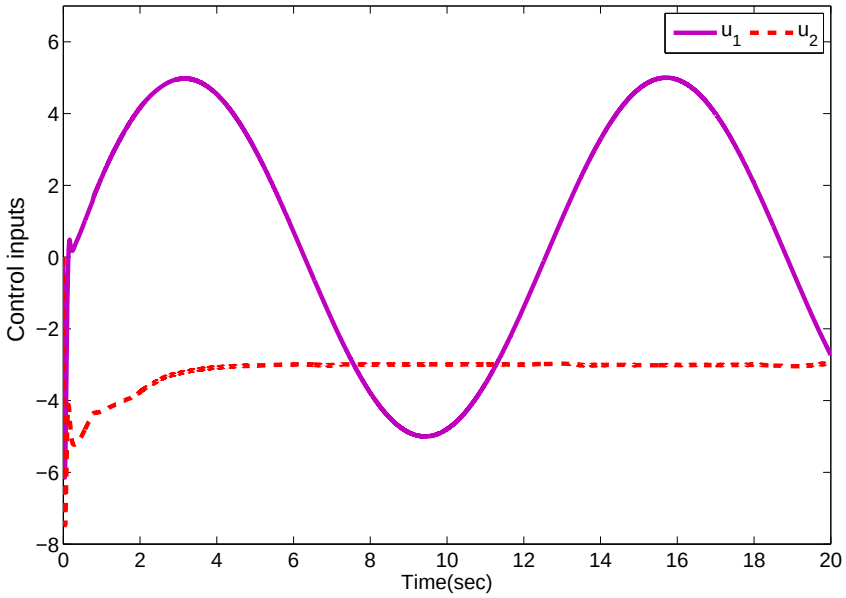

Figure 4.11: Control inputs using the proposed adaptive sliding mode controller

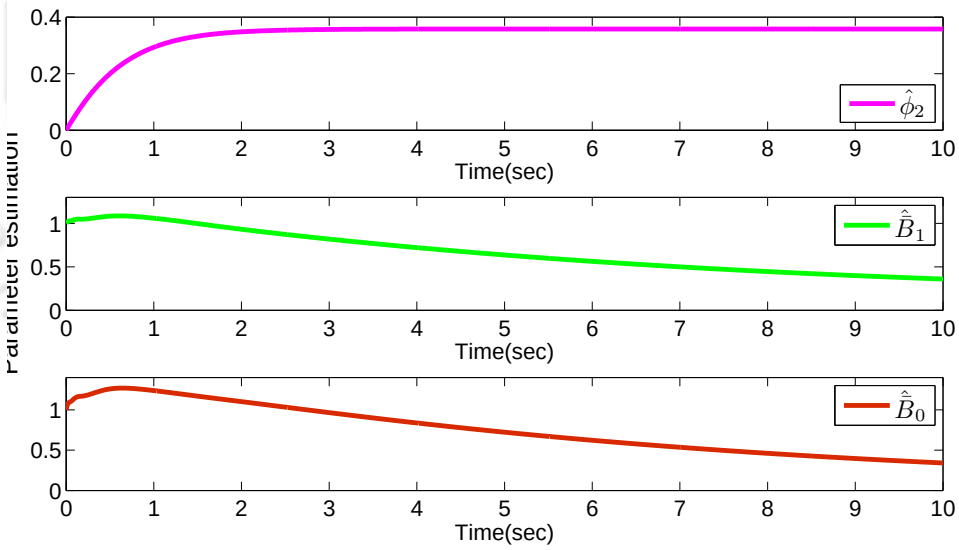

Figure 4.12: Estimated parameters using the proposed adaptive sliding mode controller

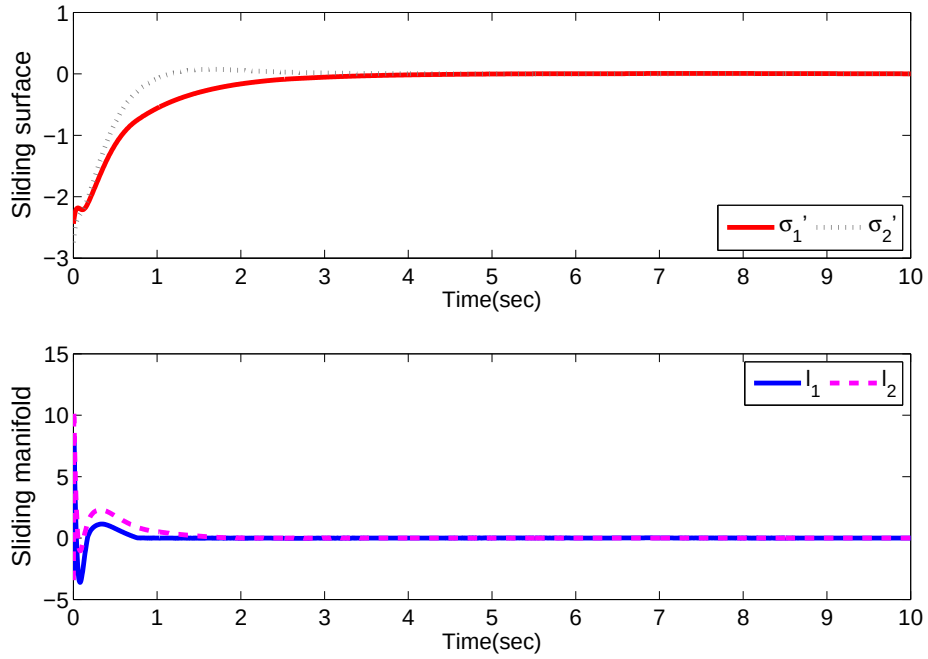

Figure 4.13: Sliding surface and sliding manifold using the proposed adaptive sliding mode controller

4.5 Case study on 1 degree of freedom (DOF) vertical take-off and landing (VTOL) aircraft system

The 1 DOF VTOL system moves vertically up and down about its axis and this motion is called pitch motion. Real world examples of the VTOL aircraft system are aerospace vehicles which comprise of helicopters, rockets, balloons and harrier jets. All aerospace vehicles are difficult to model due to their changing aerodynamic parameters and environmental behavior during flight. Hence VTOL aircraft system is a suitable example of uncertain systems. The vertical take-off and landing (VTOL) system [88] with one degree of freedom (pitch motion) is considered here for practical demonstration of the proposed adaptive sliding mode controller. The modelling of 1 DOF VTOL system is presented in the Appendix A. The design prerequisite of the sliding mode controller is the complete knowledge about the state vector which is practically difficult to get. Hence unavailable states of the VTOL are estimated by using the extended state observer (ESO) [89]. The ESO can estimate the uncertainties along with the states of the system. Unlike traditional (linear or nonlinear) observers, the ESO estimates the uncertainties, unmodeled dynamics and external disturbances as extended states of the original system [90].

4.5.1 Linear extended state observer (LESO) design

The idea of LESO is explained in the following single input single output (SISO) system,

$$\begin{aligned} x^{(n)}(t) &= f(x^{(n-1)}(t), x^{(n-2)}(t), ..., x(t), d(t), t) + bu(t) \\ y &= x(t) \end{aligned} \tag{4.132}$$

where $x(t)$ is the nth order state vector, y is the output, u is the input, b is a constant, $d(t)$ is the external disturbance, $f(\cdot)$ is an unknown function which can be viewed as the total uncertainties or disturbances, both internal and external, acting on the system. Now $v = \frac{df}{dt}$ is introduced such that if the function f is nonsmooth, v denotes the generalized derivative of $f(\cdot)$. Treating the uncertainty f as an extended state of the system (4.132), Eq. (4.132) can be written in the state space form as,

$$\begin{aligned} \dot{x}_1(t) &= x_2(t) \\ \dot{x}_2(t) &= x_3(t) \\ &\cdot \\ &\cdot \\ \dot{x}_{n-1}(t) &= x_n(t) \\ \dot{x}_n(t) &= x_{n+1}(t) + b_0 u \\ \dot{x}_{n+1}(t) &= v(\cdot) \end{aligned} \tag{4.133}$$

where $X = [x_1, x_2, ..., x_n, x_{n+1}]^T \in R^{n+1}$ represents the state of the system and b_0 is best estimate of b(4.132). Now, LESO for estimating both the states and the extended state for the uncertain system (4.132) can be obtained as follows [91]

$$\begin{aligned} \dot{z}_1 &= z_2 - \delta_1 e_1 \\ \dot{z}_2 &= z_3 - \delta_2 e_1 \\ &\cdot \\ &\cdot \\ \dot{z}_{n-1} &= z_n - \delta_{n-1} e_1 \\ \dot{z}_n &= z_{n+1} - \delta_n e_1 + b_0 u \\ \dot{z}_{n+1} &= -\delta_{n+1} e_1 \end{aligned} \tag{4.134}$$

where $Z = [z_1, z_2, ..., z_n, z_{n+1}]^T \in R^{n+1}$, $e_1 = z_1 - x_1$ and $\delta_i (i \in n+1)$ are the states of LESO, the observation error and observer gains, respectively. LESO (4.134) is designed to have the property, $z_i(t) \to x_i(t) (i \in n+1)$.

Writing the extended order system (4.133) in the state space form gives rise to,

$$\dot{X} = AX + Bu + Ev \tag{4.135}$$

where $X = [x_1, x_2, ..., x_n, x_{n+1}]^T$ is the state vector of the extended order system. Here A, B and E matrices are given by,

$$A = \begin{bmatrix} 0 & 1 & .... & 0 & 0 \\ 0 & 0 & 1 & .... & 0 \\ . & & & & \\ . & & & & \\ 0 & 0 & 0 & .... & 1 \\ 0 & 0 & 0 & .... & 0 \end{bmatrix}, B = \begin{bmatrix} 0 \\ 0 \\ . \\ . \\ b_0 \\ 0 \end{bmatrix}, E = \begin{bmatrix} 0 \\ 0 \\ . \\ . \\ 0 \\ 1 \end{bmatrix} \tag{4.136}$$

So (4.134) represents LESO for the system (4.135). The state space model of the LESO dynamics can be written as

$$\dot{Z} = AZ + Bu + L(y - CZ) \tag{4.137}$$

where $L = [\delta_1 \quad \delta_2 .... \delta_n \quad \delta_{n+1}]^T$ is the observer gain vector, y is output vector and $C = [1 \quad 0 \quad 0 .....0]$ is the output matrix.

The parameters are chosen in a special way as $s^{n+1} + \delta_1 s^n + ... + \delta_{n+1} = (s + \omega_0)^{n+1}$, where ω_0 denotes the bandwidth of the LESO (4.134) [92]. It is proved that if f is differentiable with respect to t and $v = \dot{f}$ is bounded, then the LESO (4.134) can estimate $f(t)$ with bounded error and also estimates the unknown states.

***Remark* 4.7.** *In the control law (4.22), the derivative term $\dot{s}$ is needed. However, in real time implementation, direct differentiation will lead to erroneous result as the measurements are often noisy. There are three methods to resolve this issue, namely, the derivative estimator, the suboptimal algorithm and the twisting algorithm. In experimental study of the VTOL system, the first method is utilized. A derivative estimator is designed using the method in [25] [64] and is given below,*

$$\begin{aligned} \dot{z}_0 &= -\lambda_1 |z_0 - s|^{1/2} sign(z_0 - s) + z_1 \\ \dot{z}_1 &= -\lambda_2 sign(z_0 - s) \end{aligned} \tag{4.138}$$

where $\lambda_1 > 0$ and $\lambda_2 > 0$ are the design parameters and the estimators are designed as $\dot{s} = z_1$.

4.5.2 Experimental Results

Experiments are conducted on the laboratory set-up QNET VTOL which was controlled by applying the adaptive sliding mode controller. Figure 4.14 shows the experimental board QNET VTOL trainer on ELVIS II which basically consists of a variable speed fan with a safety guard mounted on an arm. An adjustable counterweight is attached to the other end of the arm. This counterweight allows position of the weight to be changed which in turn affects the system dynamics. A rotary encoder shaft to measure the VTOL pitch position is attached to an arm assembly.

The nominal values of the VTOL parameters are given in the QNET manual [88] as,

Figure 4.14: QNET VTOL trainer on ELVIS II

Table 4.5: Parameters of 1DOF VTOL system

Variable name	Description	Values
L_m	Motor inductance	53.8 mh
R_m	Motor resistance	3 Ω
k_t	Torque thrust constant	0.0108 Nm/A
j	Moment of inertia	0.00347 $kg - m^2$
b_v	Viscous damping	0.002 Nms/rad
k	Stiffness constant	0.0373 Nm/rad

Experiments are carried out on the QNET VTOL ElVIS II board using LABVIEW software for interfacing. Furthermore, Runge Kutta 4 algorithm with step size of 0.1 ms is used in a PC with 2.50

GHz Core I-7 processor having 4GB memory for simulation purpose.

Using the parameter values given above, the transfer function for the 1 DOF VTOL [88] (A.1.12) is obtained as,

$$G(s) = \frac{\theta(s)}{V_m(s)} = \frac{57.78}{s^2 + 0.576s + 10.7} \tag{4.139}$$

where θ is the pitch angle and V_m is the motor voltage. Accordingly, the state space model for the above system (A.1.13) in presence of matched uncertainty can be described as,

$$\begin{bmatrix} \dot{x}_1 \\ \dot{x}_2 \end{bmatrix} = \begin{bmatrix} 0 & 1 \\ -10.7 & -0.576 \end{bmatrix} \begin{bmatrix} x_1 \\ x_2 \end{bmatrix} + \begin{bmatrix} 0 \\ 57.78 \end{bmatrix} u + \begin{bmatrix} 0 \\ 57.78 \end{bmatrix} f_m(x,t) \tag{4.140}$$

and the output matrix $C = [1 \quad 0]$. Here x_1 is the pitch angle and x_2 is the angular velocity. The uncertainty is chosen as,

$$f_m(x,t) = 0.25\sin(0.1x_1) \tag{4.141}$$

The control law (4.22) is applied to the above system where, $\kappa = 0.25$, $k_1 = 5$, $\gamma = 2$ and $c = [5 \quad 1]$. The LESO observer gain parameter is

$$L = \begin{bmatrix} 19.5 & 126.75 & 274.625 \end{bmatrix}^T \tag{4.142}$$

considering $\omega_0 = 6.5$.

The initial condition for the VTOL system is chosen as $[-0.45 \quad 0]^T$ and the initial condition for the observer is also selected as $[-0.45 \quad 0]^T$.

The adaptive tuning law is designed as $\dot{\hat{T}} = 0.5|\sigma|$ with $T_0 = 0$. Boundary layer ϵ is chosen as 0.05. The parameters of the derivative estimator in (4.138) are $\lambda_1 = 100$ and $\lambda_2 = 200$.

The desired trajectory $x_d(t)$ to be tracked is chosen as $x_d(t) = 0$, i.e the VTOL system will have to position itself to the horizontal plane. The control signal is applied to the VTOL lab module through QNET's interfacing hardware board. The experimental results obtained are shown in Fig.s 4.15 - 4.19. In Fig. 4.15, the tracking performance is presented from where it can be observed that the VTOL tracks the reference accurately.

The angular velocity (x_2), sliding surface (s), and control input (u) are shown in Fig.s 4.16 - 4.18. From Fig 4.18 it is clearly observed that the proposed control law is smooth and chattering free. The

convergence of the adaptive gain is confirmed in Fig. 4.19.

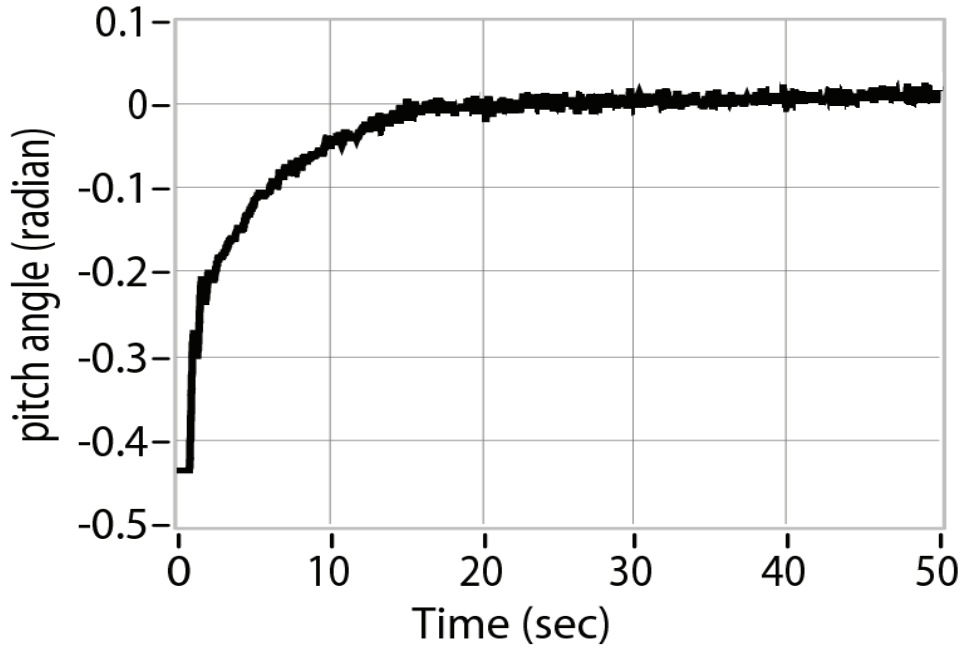

Figure 4.15: Angular position (x_1) obtained by using the proposed adaptive sliding mode controller

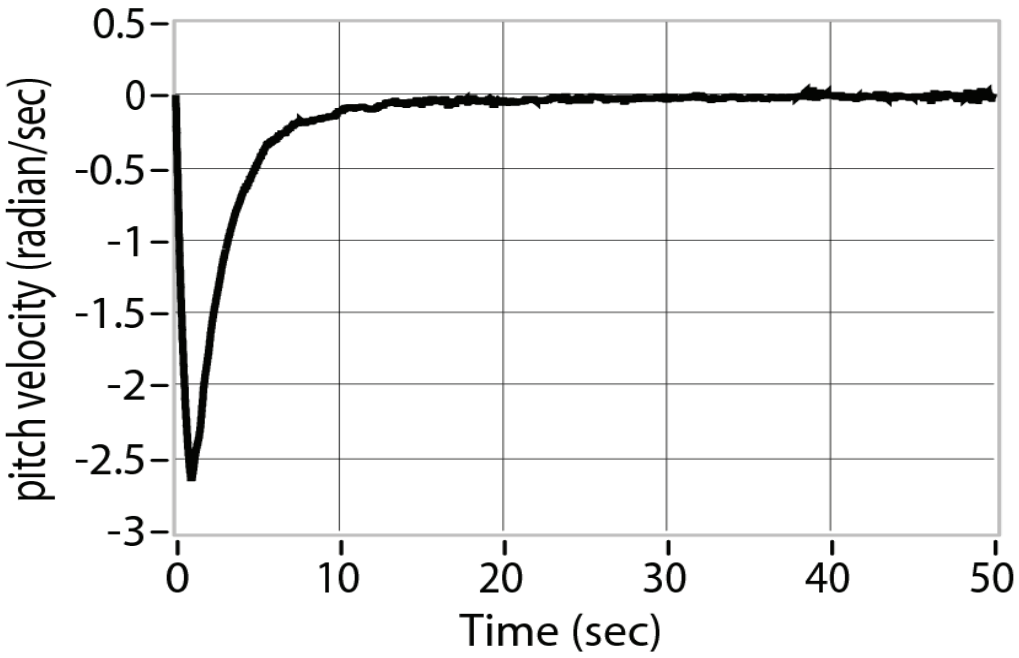

Figure 4.16: Angular velocity (x_2) obtained by using the proposed adaptive sliding mode controller

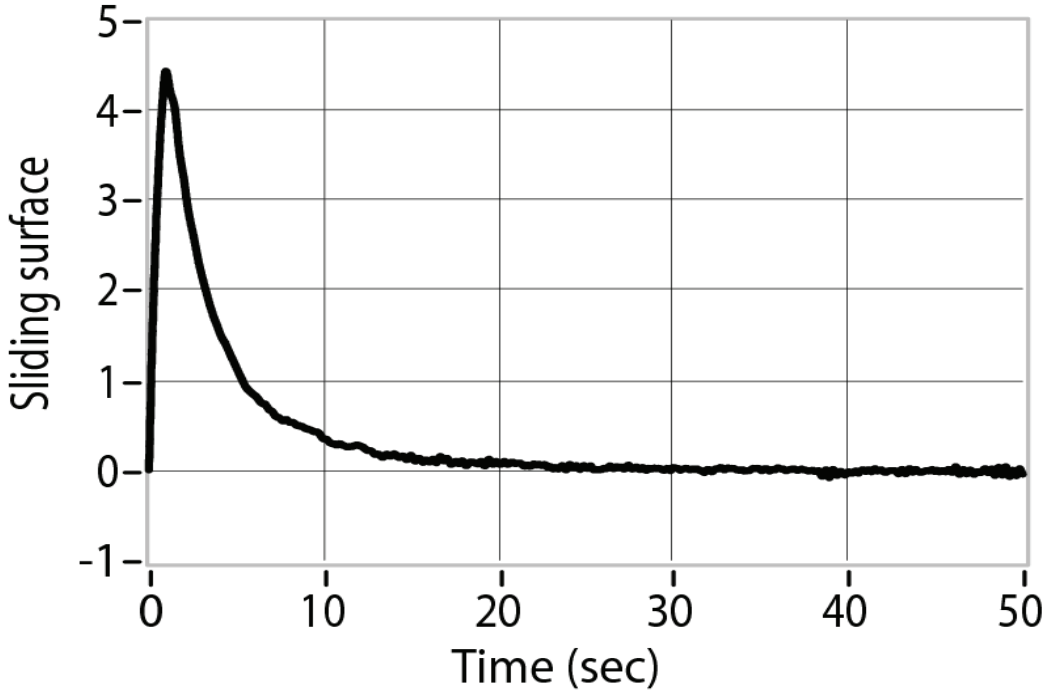

Figure 4.17: Sliding surface s obtained by using the proposed adaptive sliding mode controller

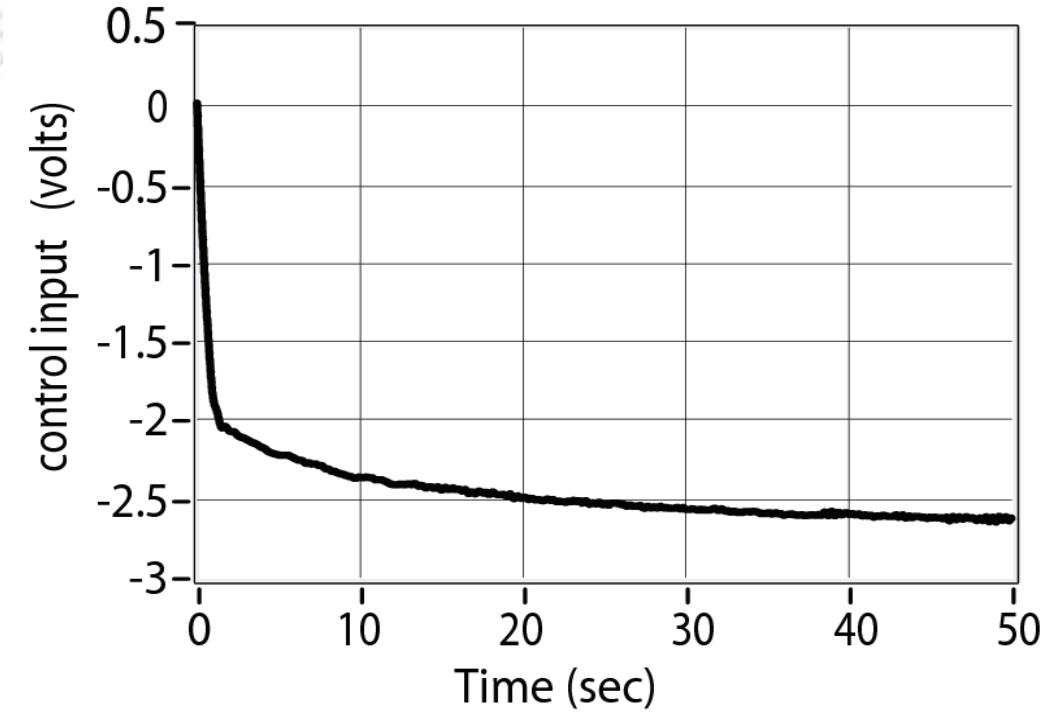

Figure 4.18: Control input u obtained by using the proposed adaptive sliding mode controller

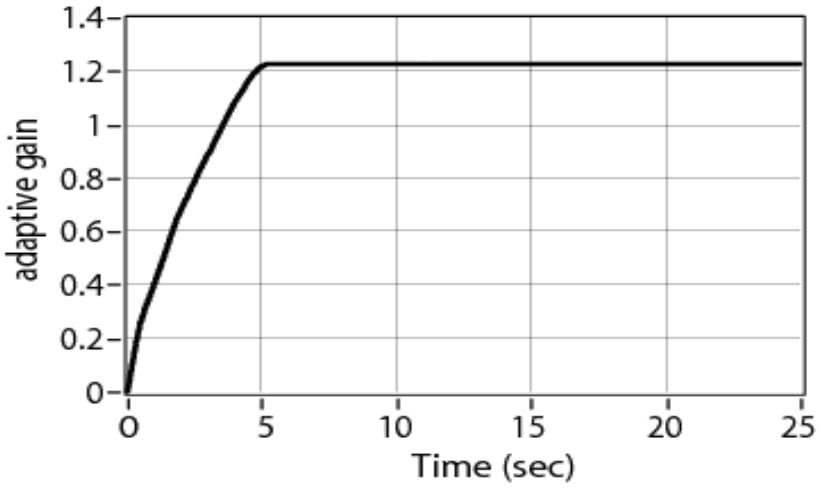

Figure 4.19: Adaptive gain ($\hat{T}$) obtained by using the proposed adaptive sliding mode controller

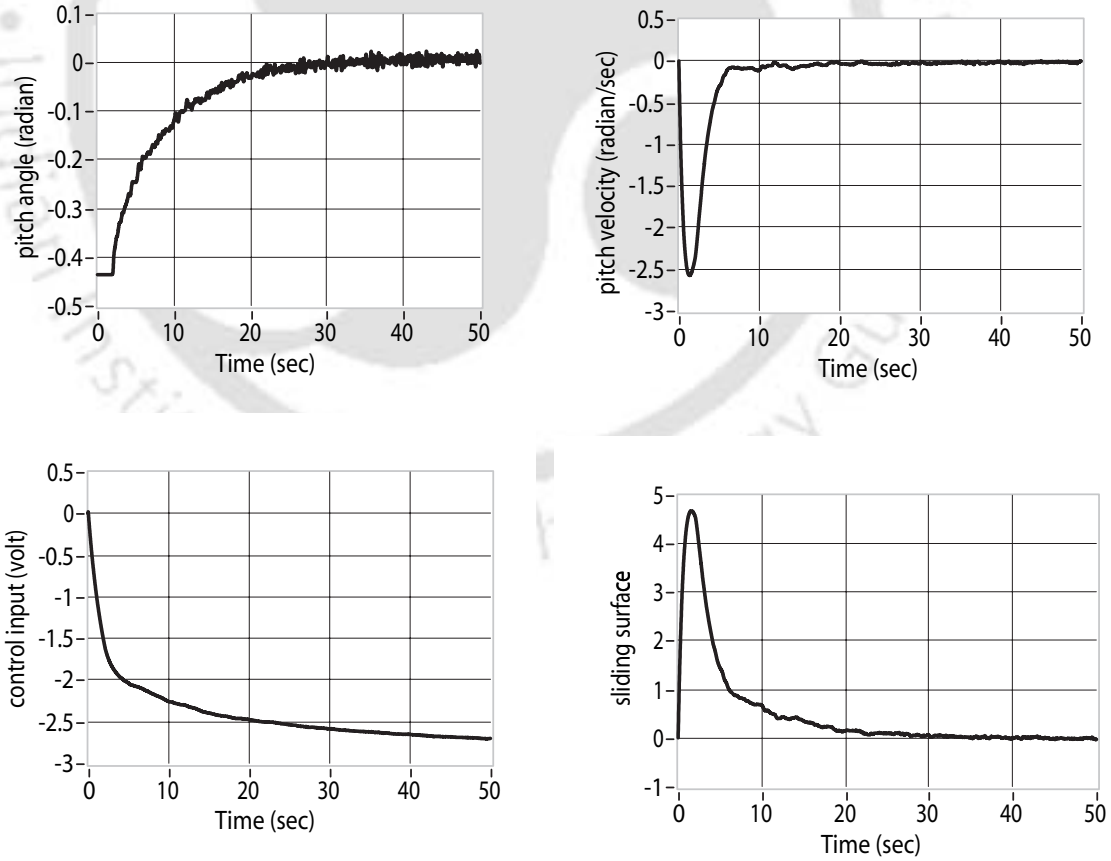

Figure 4.20: Experimental results using the proposed method when parameters are changed by 25%

In order to check the robustness of the proposed adaptive sliding mode controller, the plant param-

eter matrices are perturbed by 25%. In Fig. 4.20, the experimental results are shown with $\hat{A} = 1.25A$ and $\hat{B} = 1.25B$. It is observed from Fig. 4.20 that the proposed adaptive sliding mode controller integrated with LESO observer still works reliably demonstrating the robustness of the proposed controller - observer pair.

4.6 Summary

This chapter proposes an adaptive sliding mode (SM) controller for multi-input multi-output (MIMO) systems. The proposed controller is applied to the twin rotor MIMO system (TRMS) which is an example of a highly coupled nonlinear system perturbed by mismatched uncertainty. The cross-coupling between the main and the tail rotor of the TRMS is considered as an uncertainty. An adaptive tuning rule is designed to deal with the unknown but bounded uncertainty. However, the upper bound of the system uncertainty is not required to be known apriori as is the case with most sliding mode controllers. A proportional plus integral sliding surface is used to eliminate the offset present in the pitch angle. Simulation results show that the proposed adaptive sliding mode controller demonstrates satisfactory tracking performance and is robust to cross-coupling effect and external disturbances. Moreover, the proposed adaptive sliding mode controller shows, in general, lesser error with lower control effort than the PID controllers [84] reported in the literature for the TRMS.
Next, the proposed controller is applied for stabilizing a vertical take-off and landing (VTOL) aircraft system affected by both matched and mismatched kind of uncertainties. The proposed sliding mode controller uses a proportional plus integral sliding surface and an adaptive gain tuning law. Prior knowledge about the upper bound of the system uncertainty, which is the design prerequisite of most sliding mode controllers, is eliminated by using this adaptive method. Moreover, the adaptive gain tuning mechanism also ensures that the gain is not overestimated with respect to the actual unknown value of the uncertainty. Simulation is performed by applying the adaptive sliding mode controller to the linearized model of the VTOL aircraft. From simulation results, the proposed controller is found to be superior in chattering mitigation than some already existing similar kind of adaptive sliding mode controller. Also, the states show faster convergence in the case of the proposed adaptive sliding mode controller. For application to uncertain systems affected by severe matched and mismatched uncertainties like the VTOL aircraft, the proposed adaptive sliding mode control strategy promises

to be a suitable method. Real time experiments conducted on a 1 DOF VTOL system using its laboratory prototype QNET VTOL are described. The proposed adaptive sliding mode controller is applied to the 1 DOF VTOL system for tracking a desired reference trajectory and experimental performance is studied. In the experimental set-up, pitch velocity of the VTOL is the unavailable state which is required for designing the controller. So a linear extended state observer (LESO) is combined with the adaptive sliding mode controller to estimate pitch velocity. Experimental results obtained confirm that the proposed controller is successful in achieving faithful trajectory tracking for the 1 DOF VTOL. Moreover, chattering in the control input is found to be reduced substantially corroborating the fact observed earlier in theoretical simulation studies.

5

Adaptive Terminal Sliding Mode Controller

Contents

5.1 Introduction

It is well recognized that, conventional switching manifolds are usually linear hyper planes which guarantee asymptotic stability. However, for nonlinear systems, nonlinear sliding surface can also be selected [12]. In linear sliding mode (LSM), error dynamics cannot converge to zero in finite time although the parameters can be adjusted to make the convergence arbitrarily fast. However, this will, in turn, increase the control gain, which may cause severe chattering on the sliding surface and, therefore, deteriorate the system performance. To tackle the problems of globally asymptotic stabilization, terminal sliding mode (TSM) control scheme has been developed [5, 93–97] to achieve finite time stabilization. Unfortunately, the terminal sliding mode control features the same drawback of chattering [30] as in the case of conventional sliding mode control. In [98] a second order sliding mode controller was developed for multivariable linear systems using the nonsingular terminal sliding manifold. The major disadvantage of this method is that the application is restricted to linear uncertain systems only and the upper bound of the system uncertainty must be known in advance. In [5, 94] a continuous finite time control scheme for rigid robotic manipulators affected by uncertainty and external disturbance was proposed using a new form of terminal sliding mode. In both these methods, the bound of the uncertainty must be known in advance. Moreover, in these methods a boundary layer technique is used to replace the discontinuous control action by a saturating continuous approximation to reduce the chattering. However, its consequence is that invariance property of the SMC is lost.

In this chapter, a chattering free adaptive terminal sliding mode (TSM) controller is proposed to achieve fast and finite time convergence. In the proposed controller, a nonsingular terminal sliding manifold is used to design the control law. The time derivative of the control signal is used as the control input instead of the actual control. The derivative control law is a discontinuous signal because of the presence of the sign function. However, its integral which is the actual control, is continuous and hence the chattering is eliminated. An adaptive tuning law is used here to estimate the unknown uncertainties. This adaptive tuning method does not require prior knowledge about the upper bound of the system uncertainty for designing the terminal sliding mode controller as was the case with the terminal sliding mode controllers developed so far [5, 64, 93, 94, 97–99].

The outline of this chapter is as follows. In Section 5.2, the proposed chattering free adaptive terminal sliding mode (TSM) control strategy is derived. In Section 5.3 the proposed adaptive TSM controller is applied to stabilize a triple integrator system and the performance is studied. Trajectory tracking

problem of a robotic manipulator is considered in Section 5.4 to investigate the efficacy of the proposed adaptive TSM controller. Summary is drawn in Section 5.5.

5.2 Design of chattering free adaptive terminal sliding mode controller

Let us consider a class of nonlinear system

$$\dot{x} = f(x) + \Delta f(x) + d(t) + Bu \tag{5.1}$$

where $x = [x_1 \;\; x_2 \;\; x_3 ....x_n]^T \in R^n$ is the state vector. Furthermore, $\Delta f(x) \in R^n$ is an uncertain term representing the unmodelled dynamics or structural variation of the system (5.1) and $d(t) \in R^n$ is an external disturbance. Moreover, $u \in R^m$ is the input and B is a known matrix of order $n \times m$. The uncertainties of the system (5.1) are assumed to be bounded and matched such that $\Delta f(x)$ and $d(t)$ $\in$ span B. The control objective is to track a given reference signal x_d in finite time from any initial state.

Let the desired state vector be $x_d = [x_{1d} \;\; x_{2d} \;\; x_{3d} ....x_{nd}]^T$. The tracking error is defined as,

$$\begin{aligned} e = x - x_d &= [(x_1 - x_{1d}) \;\; (x_2 - x_{2d}) \;\; .....(x_n - x_{nd})]^T \\ &= [e_1, e_2, ...e_n]^T. \end{aligned} \tag{5.2}$$

The goal is to design a chattering free adaptive terminal sliding mode controller for a given target x_d such that the resulting tracking error satisfies

$$\lim_{t\to\infty} ||e|| = \lim_{t\to\infty} ||x - x_d|| \to 0 \tag{5.3}$$

where $||\cdot||$ denotes the Euclidean norm of a vector.

The controller is designed in two steps. At first, a linear sliding surface is defined and then using the sliding surface, a terminal sliding manifold is obtained so that the derivative of the control input occurs at the first derivative of the terminal sliding manifold. The actual control input is obtained by integrating the derivative of the control signal which contains the discontinuous function and thus eliminates the chattering [27, 65, 66]. The uncertainty is estimated by using an adaptive tuning law.

A set of sliding surfaces is defined in the error space passing through the origin to represent a sliding

manifold as fo1lows:

$$\begin{aligned} s &= [s_1, s_2, ..., s_m]^T = c^T e = [c_1\ c_2\ ...c_i...c_m]^T e \\ &= \begin{bmatrix} c_{1n}e_n + c_{1(n-1)}e_{n-1} + ... + c_{11}e_1 \\ c_{2n}e_n + c_{2(n-1)}e_{n-1} + ... + c_{21}e_1 \\ . \\ c_{in}e_n + c_{i(n-1)}e_{n-1} + ... + c_{i1}e_1 \\ . \\ c_{mn}e_n + c_{m(n-1)}e_{n-1} + ... + c_{m1}e_1 \end{bmatrix} \end{aligned} \tag{5.4}$$

and $c_i = [c_{in}\ c_{i(n-1)}....c_{i1}]$ be such that all roots of the polynomial

$$\phi(\lambda(e_i)) = c_{in}\lambda^{n-1} + c_{i(n-1)}\lambda^{n-2} + ... + c_{i1}\lambda \tag{5.5}$$

are in the open left half-plane [100], $i = 1, 2, .., m$. The choice of c determines the convergence rate to the sliding surface. Let us consider (5.4), where $e = x - x_d$. The first time derivative of (5.4) yields

$$\begin{aligned} \dot{s} &= c^T \dot{e} \\ &= c^T(\dot{x} - \dot{x}_d) \end{aligned} \tag{5.6}$$

Using (5.1) and (5.6) yields,

$$\dot{s} = c^T(f(x) + \Delta f(x) + d(t) + Bu - \dot{x}_d) \tag{5.7}$$

Taking the derivative of (5.7) gives rise to

$$\begin{aligned} \ddot{s} &= c^T(\frac{d}{dt}f(x) + \frac{d}{dt}\Delta f(x) + \dot{d}(t) + B\dot{u} - \ddot{x}_d) \\ &= c^T(\dot{f}(x) + \Delta\dot{f}(x) + \dot{d}(t) + B\dot{u} - \ddot{x}_d) \end{aligned} \tag{5.8}$$

A nonsingular terminal sliding mode manifold is first designed as

$$\sigma = s + \beta\dot{s}^{\frac{p}{q}} \tag{5.9}$$

Here $\beta = \text{diag}(\beta_1, \beta_2, ..., \beta_n)$ is a positive constant and p/q (p and q are positive odd integers) is chosen in such a way that the condition $1 < \frac{p}{q} < 2$ holds [94]. The linear sliding surface s is combined with the nonsingular terminal sliding manifold σ to realize the terminal sliding mode control. As σ reaches

zero in finite time, both s and $\dot{s}$ are bound to reach zero. Then, the tracking error e asymptotically converges to zero.

Taking the time derivative of (5.9) yields,

$$\begin{aligned}\dot{\sigma} &= \dot{s} + \beta(\frac{p}{q})\dot{s}^{\frac{p}{q}-1}\ddot{s} \\ &= \beta(\frac{p}{q})\dot{s}^{\frac{p}{q}-1}(\ddot{s} + \beta^{-1}(\frac{p}{q})^{-1}\dot{s}^{2-(\frac{p}{q})}) \end{aligned} \tag{5.10}$$

***Assumption* 5.1.** *The first time derivative of the uncertain term, $\Delta\dot{f}(x)$ and the first time derivative of the disturbance, $\dot{d}(t)$ are assumed to be bounded and satisfy the following condition:*

$$||c^T(\Delta\dot{f}(x) + \dot{d}(t))|| \leq \sum_{i=0}^{r} \bar{B}_i||x||^i \qquad r = 0, 1, ..n \tag{5.11}$$

where $\bar{B}_i$ are unknown positive constants, which are not easily obtained due to the complicated structure of the uncertainties in practical control systems. The number of adaptive rules r is determined by the designer in accordance with the knowledge of the relative order of perturbation that the system might encounter. For designing the traditional sliding mode controller, one usually assumes that the upper bound of lumped perturbations satisfies certain conditions. For example, if $r = 0$, then the nature of the disturbance is periodic and it is well represented by a known constant value. If we choose $r = 1$, it covers more area in the range space rather than when $r = 0$ is considered. Thus rest of the control law is designed by considering $r = 1$.

It will be proven in Theorem 5.1 that since the derivative of the control input contains the discontinuous term, the actual control signal which will be obtained after the integration operation will not contain any high frequency switching component. Thus the proposed terminal sliding mode controller will be free from the chattering phenomenon. Moreover, the controller does not need prior knowledge about the upper bound of the disturbance. Instead, the upper bound is obtained by designing an adaptive tuning law.

***Theorem* 5.1.** *Considering the uncertain system (5.1), the tracking error dynamics (5.6) can asymptotically converge to zero if the nonsingular terminal sliding manifold is chosen as (5.9) and the control law is obtained as follows:*

$$\dot{u} = -(c^T B)^{-1}[c^T\dot{f}(x) + \beta^{-1}(\frac{p}{q})^{-1}\dot{s}^{2-(\frac{p}{q})} + (\bar{B}_0 + \bar{B}_1||x||)sign(\sigma) + K^{\dagger}\sigma - c^T\ddot{x}_d] \tag{5.12}$$

where $(c^TB)^{-1}$ *is nonsingular,* $\bar{B}_0$, $\bar{B}_1$ *and* $K^\dagger = diag(K_1^\dagger....K_m^\dagger) > 0$ *are the designed parameters.* In practice the bounds of the uncertain term $(\bar{B}_0 + \bar{B}_1||x||)$ in (5.12) is often difficult to know. Hence an adaptive tuning law is designed to determine $\bar{B}_0$ and $\bar{B}_1$. So the control law is represented as,

$$u = -(c^TB)^{-1}\int_0^t [c^T\dot{f}(x)d\tau + \beta^{-1}(\frac{p}{q})^{-1}\dot{s}^{2-(\frac{p}{q})} + (\hat{\bar{B}}_0 + \hat{\bar{B}}_1||x||)sign(\sigma) + K^\dagger\sigma - c^T\ddot{x}_d]d\tau \quad (5.13)$$

where $\hat{\bar{B}}_0$ and $\hat{\bar{B}}_1$ estimate the bounds of uncertainty, i.e. $c^T(||\Delta\dot{f}(x)+\dot{d}(t)||) \leq \bar{B}_0+\bar{B}_1||x||$. Defining the adaptation error as $\tilde{\bar{B}}_0 = \hat{\bar{B}}_0 - \bar{B}_0$ and $\tilde{\bar{B}}_1 = \hat{\bar{B}}_1 - \bar{B}_1$, the parameter $\hat{\bar{B}}_0$ and $\hat{\bar{B}}_1$ are to be estimated by using the adaptation law

$$\dot{\hat{\bar{B}}}_0 = \frac{1}{\nu_0}(\frac{p}{q})||\beta||\ ||\dot{s}^{(\frac{p}{q})-1}\sigma|| \quad (5.14)$$

and

$$\dot{\hat{\bar{B}}}_1 = \frac{1}{\nu_1}(\frac{p}{q})||\beta||\ ||\dot{s}^{(\frac{p}{q})-1}\sigma||\ ||x|| \quad (5.15)$$

where ν_0 and ν_1 are the positive tuning parameters.

Proof : Let us consider the following Lyapunov function

$$V(t) = \frac{1}{2}\sigma^T\sigma + \frac{1}{2}\nu_0\tilde{\bar{B}}_0^2 + \frac{1}{2}\nu_1\tilde{\bar{B}}_1^2 \quad (5.16)$$

Using (5.8 - 5.15), the time derivative of the Lyapunov function $V(t)$ is obtained as,

$$\begin{aligned}
\dot{V}(t) &= \sigma^T\dot{\sigma} + \nu_0\tilde{\bar{B}}_0\dot{\hat{\bar{B}}}_0 + \nu_1\tilde{\bar{B}}_1\dot{\hat{\bar{B}}}_1 \\
&= \beta(\frac{p}{q})\dot{s}^{(\frac{p}{q})-1}\sigma^T(\ddot{s} + \beta^{-1}(\frac{p}{q})^{-1}\dot{s}^{2-(\frac{p}{q})}) + \nu_0(\hat{\bar{B}}_0 - \bar{B}_0)\dot{\hat{\bar{B}}}_0 + \nu_1(\hat{\bar{B}}_1 - \bar{B}_1)\dot{\hat{\bar{B}}}_1 \\
&= \beta(\frac{p}{q})\dot{s}^{(\frac{p}{q})-1}\sigma^T[c^T(\frac{d}{dt}f(x) + \frac{d}{dt}\Delta f(x) + \dot{d}(t) + B\dot{u} - \ddot{x}_d) + \beta^{-1}(\frac{p}{q})^{-1}\dot{s}^{2-(\frac{p}{q})}] \\
&\quad +(\hat{\bar{B}}_0 - \bar{B}_0)(\frac{p}{q})||\beta||\ ||\dot{s}^{(\frac{p}{q})-1}\sigma|| + (\hat{\bar{B}}_1 - \bar{B}_1)(\frac{p}{q})||\beta||\ ||\dot{s}^{(\frac{p}{q})-1}\sigma||\ ||x|| \\
&\leq ||\beta||(\frac{p}{q})||\dot{s}^{(\frac{p}{q})-1}\sigma^T||\ [\bar{B}_0 + \bar{B}_1||x|| - K^\dagger||\sigma|| - (\hat{\bar{B}}_0 + \hat{\bar{B}}_1||x||)sign(\sigma)] \\
&\quad +(\hat{\bar{B}}_0 - \bar{B}_0)(\frac{p}{q})||\beta||\ ||\dot{s}^{(\frac{p}{q})-1}\sigma|| + (\hat{\bar{B}}_1 - \bar{B}_1)(\frac{p}{q})||\beta||\ ||\dot{s}^{(\frac{p}{q})-1}\sigma||\ ||x|| \\
&\leq -K^\dagger||\sigma|| \quad (5.17)
\end{aligned}$$

The above inequality holds if $\dot{\hat{\bar{B}}}_0 = \frac{1}{\nu_0}(\frac{p}{q})||\beta||\ ||\dot{s}^{(\frac{p}{q})-1}\sigma||$ and $\dot{\hat{\bar{B}}}_1 = \frac{1}{\nu_1}(\frac{p}{q})||\beta||\ ||\dot{s}^{(\frac{p}{q})-1}\sigma||\ ||x||$. Moreover, $||\dot{s}^{(\frac{p}{q})-1}|| > 0$ for any $\dot{s} \neq 0$ and $\dot{s}^{(\frac{p}{q})-1} = 0$ only when $\dot{s} = 0$. Therefore, the convergence to a domain $\sigma = 0$ is guaranteed from any initial condition [30].

Suppose that t_r is the time when σ reaches zero from $\sigma(0) \neq 0$, i.e. $\sigma = 0$ for all $t \geq t_r$. Once σ reaches zero, it will stay at zero using the control law (5.12). Thus the sliding surface s will converge to zero in finite time t_f. The total time from $\sigma(0) \neq 0$ to s_{tf} can be calculated by using the equation $s + \beta \dot{s}^{(\frac{p}{q})} = 0$ (5.9) from which the time taken from s_{tr} to s_{tf} [94] is obtained as,

$$t_f = t_r + \frac{(\frac{p}{q})}{(\frac{p}{q}) - 1} \beta^{-(\frac{p}{q})} ||s_{tr}||^{(\frac{p}{q})-1} \tag{5.18}$$

Hence the error (5.2) asymptotically converges to zero and the system reaches the equilibrium. This completes the proof.

***Remark* 5.1.** *Practically, $||\sigma||$ cannot become exactly zero in finite time and thus the adaptive parameter $\dot{\hat{B}}_i$ may increase boundlessly. A simple way of overcoming this disadvantage is to use the dead zone technique [30] and modify the adaptive tuning law (5.14 - 5.15) as,*

$$\dot{\hat{B}}_0 = \begin{cases} \frac{1}{\nu_0}(\frac{p}{q})||\beta||\ ||\dot{s}^{(\frac{p}{q})-1}\sigma||, & ||\sigma|| \geq \varepsilon \\ 0, & ||\sigma|| < \varepsilon \end{cases} \tag{5.19}$$

and

$$\dot{\hat{B}}_1 = \begin{cases} \frac{1}{\nu_1}(\frac{p}{q})||\beta||\ \dot{s}^{(\frac{p}{q})-1}\sigma||\ ||x||, & ||\sigma|| \geq \varepsilon \\ 0, & ||\sigma|| < \varepsilon \end{cases} \tag{5.20}$$

where ε is a small positive constant.

***Remark* 5.2.** *The parameter ϵ in controller (5.13) is very important and it is one of the parameters determining the convergence rate of the sliding surface. It is clear that a large ϵ will force the system states to converge to the origin with a high speed. However, a very large value of ϵ will require a very high control input but in reality it is always bounded. Thus the parameter ϵ cannot be selected to be too large. In practice, a compromise has to be made between the response speed and the control input.*

***Remark* 5.3.** *The parameters ν_0 and ν_1 in (5.14 - 5.15) determine the convergence rate of the estimated bounds $\hat{\hat{B}}_0$ and $\hat{\hat{B}}_1$. Large values of ν_0 and ν_1 can be chosen to force the estimated bounds $\hat{\hat{B}}_0$ and $\hat{\hat{B}}_1$ to rapidly converge to the actual bounds.*

***Remark* 5.4.** *An exact robust differentiator is available for accurately measuring or estimating the derivative of variables.*

5.3 Stabilization of a triple integrator system

The adaptive terminal sliding mode controller proposed above is applied to a triple integrator system with uncertainty as described below [62],

$$\begin{aligned} \dot{x}_1 &= x_2 \\ \dot{x}_2 &= x_3 \\ \dot{x}_3 &= u + p(x) \\ y &= x_1 \end{aligned} \tag{5.21}$$

where $p(x) = 7sin(10x_1)$ is the bounded uncertainty, y is the output and the initial condition of the system is assumed as $x(0) = [1 \quad 0 \quad -1]^T$ [61]. The desired state is $x_d = [0 \quad 0 \quad 0]^T$ as it is a stabilization problem. Hence in this case the error and state are equivalent i.e, $e = x - x_d = x$.
The third order sliding mode controller presented by Defoort et al. [4] using twisting sliding modes to achieve finite time control is compared with the proposed adaptive TSM controller. As explained in [61] and [62], the control for the system given by (5.21) can be obtained as [4],

$$u = u_{nom} + u_{disk} \tag{5.22}$$

Let $k_1, k_2, ..., k_n > 0$ be such that the polynomial $\lambda^n + k_n\lambda^{n-1} + ... + k_2\lambda + k_1$ is Hurwitz. The system (5.21) can be stabilized to the origin using the feedback control law given in [4, 61, 62] as

$$u_{nom} = -k_1 sign(x_1)|x_1|^{\alpha_1} - k_2 sign(x_2)|x_2|^{\alpha_2} ... - k_n sign(x_n)|x_n|^{\alpha_n} \tag{5.23}$$

$$\text{where} \quad \alpha_1, ..., \alpha_n \quad \text{satisfy} \quad \alpha_{i-1} = \frac{\alpha_i \alpha_{i+1}}{2\alpha_{i+1} - \alpha_i} \quad \text{for} \quad i = 2, ..., n \quad \text{with} \quad \alpha_{n+1} = 1 \tag{5.24}$$

With $n = 3$, $k_1 = 1, k_2 = k_3 = 1.5$ and $\alpha_3 = 3/4$, the control law (5.22) can be expressed as [4],

$$\begin{aligned} u_{nom} &= -sign(x_1)|x_1|^{\frac{1}{2}} - 1.5sign(x_2)|x_2|^{\frac{3}{5}} - 1.5sign(x_3)|x_3|^{\frac{3}{4}} \\ u_{disk} &= u_{disk,1} + u_{disk,2} \end{aligned} \tag{5.25}$$

where the sliding surface $\sigma = x_3 - \int_0^t u_{nom} d\tau$ and u_{disk} is given by [4],

$$\begin{aligned} u_{disk,1} &= -\zeta \int_0^t sign(\sigma)\tau \\ u_{disk,2} &= -\vartheta|\sigma|^{\frac{1}{2}} sign(\sigma) \end{aligned} \tag{5.26}$$

where ζ and ϑ are chosen as 100 and 5 respectively.

Fig. 5.1 shows the system trajectories and the control input obtained by using the third order sliding mode controller proposed by Defoort et al. [4]. Though the twisting control law reduces the chattering, still the control signal is not smooth as is observed in Fig. 5.1.

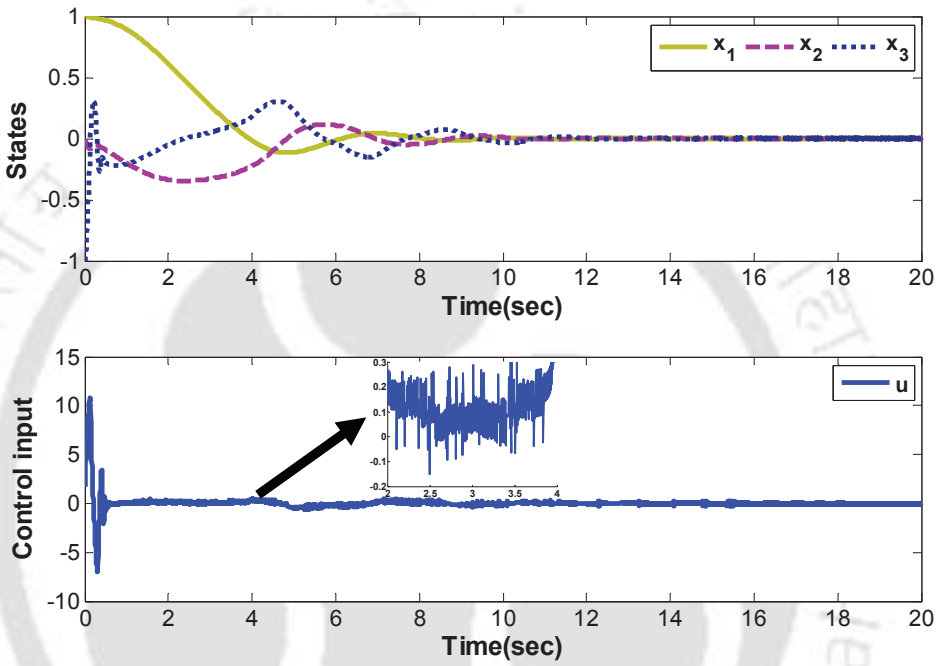

Figure 5.1: State response and control input with the controller proposed in [4]

In the proposed adaptive TSM controller (5.13), the parameters are selected as $c^T = [3\ 2\ 1]$, $\beta = 1$, $\frac{p}{q} = 5/3$, and $\mathrm{K}^{\dagger} = 15$. Hence the adaptive tuning laws for the triple integrator system are found as,

$$\dot{\hat{\bar{B}}}_0 = 1.51||\dot{s}^{p/q-1}\ \sigma||$$
$$\dot{\hat{\bar{B}}}_1 = 1.71||\dot{s}^{p/q-1}\ \sigma||\ ||x||$$

The initial conditions of $\hat{\bar{B}}_0$ and $\hat{\bar{B}}_1$ are chosen as 0, 0 respectively.

The state trajectory and the control input obtained by using the proposed adaptive TSM controller are shown in Fig. 5.2. From Fig. 5.2 it is clear that the system states converge quickly to the origin in spite of the uncertainty and disturbance and the undesired chattering in the control input is eliminated effectively. The corresponding estimated parameters are shown in Fig. 5.3.

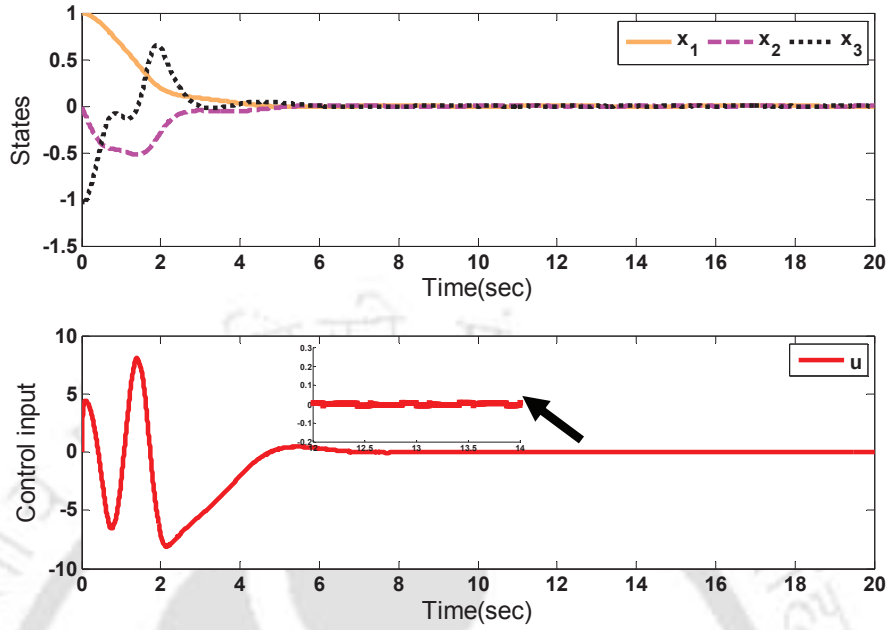

Figure 5.2: State response and control input with the proposed adaptive TSM controller

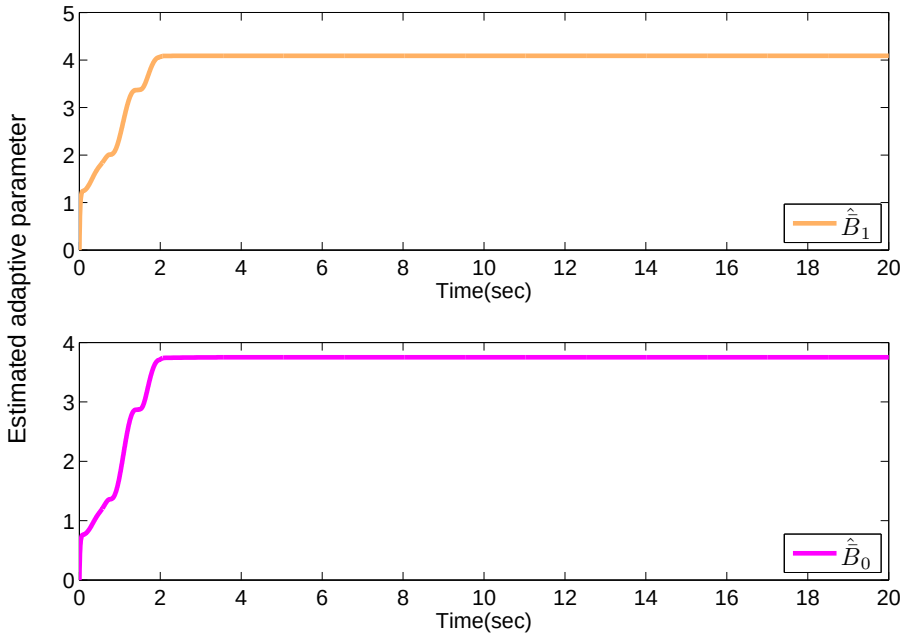

Figure 5.3: Estimated parameters $\hat{B}_0, \hat{B}_1$ with the proposed adaptive TSM controller

5.4 Tracking control of a robotic manipulator

The dynamics of an n-link robotic manipulator can be expressed as [5],

$$M(q)\ddot{q} + C(q,\dot{q})\dot{q} + G(q) = \tau + \tau_d \tag{5.27}$$

where $q, \dot{q}, \ddot{q} \in R^n$ represent the position, velocity and acceleration of the joints respectively, $M(q) = M_0(q) + \Delta M(q) \in R^{n\times n}$ stands for the inertia matrix, $C(q,\dot{q}) = C_0(q,\dot{q}) + \Delta C(q,\dot{q}) \in R^{n\times n}$ is the centripetal Coriolis matrix, $G(q) = G_0(q) + \Delta G(q) \in R^n$ is the gravitational vector, $\tau \in R^n$ is the joint torque vector and $\tau_d \in R^n$ is the disturbance torque vector. Here $M_0(q)$, $C_0(q,\dot{q})$, $G_0(q)$ are the nominal terms and $\Delta M(q)$, $\Delta C(q,\dot{q})$, $\Delta G(q)$ represent the perturbations in the system matrices. Then the dynamic model of the robotic manipulator can be written as,

$$M_0(q)\ddot{q} + C_0(q,\dot{q})\dot{q} + G_0(q) = \boldsymbol{\tau} + \tau_d + F(q,\dot{q},\ddot{q}) \tag{5.28}$$

where $F(q,\dot{q},\ddot{q}) = -\Delta M(q) - \Delta C(q,\dot{q}) - \Delta G(q) \in R^n$ is the lumped system uncertainty which is bounded by the following function

$$||F(q,\dot{q},\ddot{q})|| \leq \rho_0 + \rho_1||q|| + \rho_2||\dot{q}||^2 \tag{5.29}$$

where ρ_0, ρ_1 and ρ_2 are positive constants.

Suppose the control objective is to make the robotic manipulator track a reference trajectory. Let q_d and q be the desired and actual position vectors. The tracking error and its derivatives are defined as $e = q - q_d$, $\dot{e} = \dot{q} - \dot{q}_d$ and $\ddot{e} = \ddot{q} - \ddot{q}_d$. Using (5.28),

$$\ddot{e} = M_0^{-1}(q)[\tau + \tau_d + F(q,\dot{q},\ddot{q}) - C_0(q,\dot{q})\dot{q} - G_0(q)] - \ddot{q}_d \tag{5.30}$$

The time derivative of (5.30) yields,

$$\begin{aligned}
\frac{d}{dt}\ddot{e} &= M_0^{-1}(q)[\dot{\tau} + \dot{\tau}_d + \dot{F}(q,\dot{q},\ddot{q}) - \frac{d}{dt}(C_0(q,\dot{q})\dot{q} + G_0(q))] \\
&\quad + \dot{M}_0^{-1}(q)[\tau + \tau_d + F(q,\dot{q},\ddot{q}) - C_0(q,\dot{q})\dot{q} - G_0(q)] - \frac{d}{dt}\ddot{q}_d \\
&= M_0^{-1}(q)[\dot{\tau} - \frac{d}{dt}(C_0(q,\dot{q})\dot{q} + G_0(q))] + \dot{M}_0^{-1}(q)[\tau - C_0(q,\dot{q})\dot{q} - G_0(q)] - \frac{d}{dt}\ddot{q}_d \\
&\quad + M_0^{-1}(q)\dot{\tau}_d + M_0^{-1}(q)\dot{F}(q,\dot{q},\ddot{q}) + \dot{M}_0^{-1}(q)\tau_d + \dot{M}_0^{-1}(q)F(q,\dot{q},\ddot{q})
\end{aligned}$$

$$
\begin{aligned}
= \; & M_0^{-1}(q)[\dot{\tau} - \frac{d}{dt}(C_0(q,\dot{q})\dot{q} + G_0(q))] \\
& + \dot{M}_0^{-1}(q)[\tau - C_0(q,\dot{q})\dot{q} - G_0(q)] - \frac{d}{dt}\ddot{q}_d + \bar{F}(q,\dot{q},\ddot{q})
\end{aligned} \tag{5.31}
$$

where $\bar{F}(q,\dot{q},\ddot{q}) = M_0^{-1}(q)\dot{\tau}_d + M_0^{-1}(q)\dot{F}(q,\dot{q},\ddot{q}) + \dot{M}_0^{-1}(q)\tau_d + \dot{M}_0^{-1}(q)F(q,\dot{q},\ddot{q})$

such that,

$$
\bar{F}(q,\dot{q},\ddot{q}) \leq \bar{B}_0 + \bar{B}_1||q|| + \bar{B}_2||\dot{q}||^2 \tag{5.32}
$$

Here $\bar{B}_0$, $\bar{B}_1$ and $\bar{B}_2$ are positive constants.

***Remark* 5.5.** *The assumptions in the above inequalities are valid as the input disturbance τ_d is assumed to be bounded, i.e. $||\tau_d|| < \chi$ where χ is a positive constant. Furthermore, the modeling uncertainty $F(q,\dot{q},\ddot{q})$ is also bounded by the assumption $||F(q,\dot{q},\ddot{q})|| \leq \rho_0 + \rho_1||q|| + \rho_2||\dot{q}||^2$.*

Let us consider the linear sliding surface as,

$$
s = \dot{e} + ce \tag{5.33}
$$

where $c = \mathrm{diag}(\mathrm{c}_1, ..., \mathrm{c}_\mathrm{n})$ is a design matrix. The first and second derivative of (5.33) can be obtained as,

$$
\begin{aligned}
\dot{s} &= \ddot{e} + c\dot{e} \\
\ddot{s} &= \frac{d}{dt}\ddot{e} + c\ddot{e} = \frac{d}{dt}(\ddot{q} - \ddot{q}_d) + c\ddot{e}
\end{aligned} \tag{5.34}
$$

The nonsingular terminal sliding manifold (NTSM) for an n-link robotic manipulator is chosen as

$$
\sigma = s + \beta \dot{s}^{p/q} \tag{5.35}
$$

where Here $\beta = \mathrm{diag}(\beta_1, \beta_2, ..., \beta_\mathrm{n})$ is a design matrix.

Taking the derivative of (5.35) yields

$$
\begin{aligned}
\dot{\sigma} &= \dot{s} + \beta(p/q)\dot{s}^{(p/q)-1}\ddot{s} \\
&= \beta(p/q)\dot{s}^{(p/q)-1}(\ddot{s} + (q/p)\beta^{-1}\dot{s}^{2-(p/q)})
\end{aligned} \tag{5.36}
$$

For an n-link robotic manipulator (5.27), if the NTSM manifold is chosen as (5.35), then the tracking error e will converge to zero if the time derivative of the control input is selected as,

$$
\dot{\tau} = \dot{u}_0 + \dot{u}_1 \tag{5.37}
$$

where

$$\begin{aligned}\dot{u}_0 &= M_0(q)\frac{d}{dt}\ddot{q}_d + \frac{d}{dt}[C_0(q,\dot{\boldsymbol{q}})\dot{q} + G_0(q)] - ((q/p)\beta^{-1}M_0\dot{s}^{2-(p/q)}) - cM_0\ddot{e} \\ &\quad -M_0\dot{M_0}^{-1}(\tau - C_0(q,\dot{q})\dot{q} - G_0(q)) \end{aligned} \tag{5.38}$$

$$\dot{u}_1 = -K^{\dagger}M_0(q)\sigma - M_0(q)(\bar{B}_0 + \bar{B}_1||q|| + \bar{B}_2||\dot{q}||^2)sign(\sigma) \tag{5.39}$$

Here $K^{\dagger} = \text{diag}(\text{k}_1^{\dagger}..\text{k}_\text{n}^{\dagger})$ is a positive matrix.

Defining the adaptation error as $\tilde{\bar{B}}_0 = \hat{\bar{B}}_0 - \bar{B}_0$, $\tilde{\bar{B}}_1 = \hat{\bar{B}}_1 - \bar{B}_1$ and $\tilde{\bar{B}}_2 = \hat{\bar{B}}_2 - \bar{B}_2$, the parameters $\hat{\bar{B}}_0$, $\hat{\bar{B}}_1$ and $\hat{\bar{B}}_2$ are to be estimated by using the adaptation law

$$\dot{\hat{\bar{B}}}_0 = \frac{1}{\nu_0}(\frac{p}{q})||\beta||\ ||\dot{s}^{(\frac{p}{q})-1}\sigma|| \tag{5.40}$$

$$\dot{\hat{\bar{B}}}_1 = \frac{1}{\nu_1}(\frac{p}{q})\ ||\beta||\ ||\dot{s}^{(\frac{p}{q})-1}\sigma||\ ||q|| \tag{5.41}$$

$$\dot{\hat{\bar{B}}}_2 = \frac{1}{\nu_2}(\frac{p}{q})\ ||\beta||\ ||\dot{s}^{(\frac{p}{q})-1}\sigma||\ ||\dot{q}||^2 \tag{5.42}$$

where ν_0, ν_1 and ν_2 are the positive tuning parameters.

The dead zone technique [30] is used to modify the adaptive tuning law as

$$\begin{aligned}\dot{\hat{\bar{B}}}_0 &= \begin{cases} \frac{1}{\nu_0}(\frac{p}{q})||\beta||\ ||\dot{s}^{(\frac{p}{q})-1}\sigma||, & ||\sigma|| \geq \varepsilon \\ 0, & ||\sigma|| < \varepsilon \end{cases} \\ \dot{\hat{\bar{B}}}_1 &= \begin{cases} \frac{1}{\nu_1}(\frac{p}{q})||\beta||\ ||\dot{s}^{(\frac{p}{q})-1}\sigma||\ ||q||, & ||\sigma|| \geq \varepsilon \\ 0, & ||\sigma|| < \varepsilon \end{cases} \\ \dot{\hat{\bar{B}}}_2 &= \begin{cases} \frac{1}{\nu_2}(\frac{p}{q})||\beta||\ ||\dot{s}^{(\frac{p}{q})-1}\sigma||\ ||\dot{q}||^2, & ||\sigma|| \geq \varepsilon \\ 0, & ||\sigma|| < \varepsilon \end{cases} \end{aligned} \tag{5.43}$$

where ε is a small positive constant.

Now the adaptive terminal sliding mode control law for the robotic manipulator is obtained as,

$$\dot{u}_1 = -K^{\dagger}M_0(q)\sigma - M_0(q)(\hat{\bar{B}}_0 + \hat{\bar{B}}_1||q|| + \hat{\bar{B}}_2||\dot{q}||^2)sign(\sigma) \tag{5.44}$$

Using Lyapunov stability criterion as discussed earlier in Section 5.2, the NTSM manifold σ in (5.35) can be shown to possess finite time reachability to zero which ensures that the tracking error of the robotic manipulator $e = q - q_d$ converges to zero in finite time.

5.4.1 Effectiveness

Let us compare the proposed adaptive terminal sliding mode (TSM) controller with the NTSM controller designed by Feng et al. [5] described by:

$$\tau = C_0(q,\dot{q})\dot{q} + G_0(q) + M_0(q)\ddot{q}_d + u_a + u_b \tag{5.45}$$

where

$$\begin{aligned} u_a &= -\frac{q}{p}M_0(q)\beta^{-1}\dot{e}^{2-p/q} \\ u_b &= -\frac{p}{q}\frac{[s^T\beta\ diag(\dot{e}^{p/q-1}{M_0}^{-1}(q))]^T}{||s^T\beta\ diag(\dot{e}^{p/q-1}{M_0}^{-1}(q))||} \\ &\quad \times[||s||\ ||\beta\ diag(\dot{s}^{p/q-1}){M_0}^{-1}(q)\ ||(\rho_0+\rho_1||\dot{q}||+\rho_2||\dot{q}||^2)] \end{aligned} \tag{5.46}$$

Here ρ_0, ρ_1 and ρ_2 are supposed to be known parameters, that means $||F(q,\dot{q},\ddot{q})||$ (5.29) must be known. It is obvious that implementation of the NTSM controller (5.45 - 5.46) is highly complicated as it involves computation of the nominal model of the robotic manipulator accompanied by the difficult compulsion of knowing $||F(q,\dot{q},\ddot{q})||$ apriori. Both these requirements are difficult enough to discourage practical implementation of the NTSM controller. Moreover, if the switching control u_b is not approximated by the saturation function, the NTSM controller exhibits high chattering in the control signal. On the other hand, the proposed adaptive TSM controller has the major advantage that prior knowledge about the bounds $||\bar{F}(q,\dot{q},\ddot{q})||$ (5.32) are not required as these are adaptively estimated. Again, since the actual control is obtained by integrating the discontinuous switching function, the control signal is smoother and chatterless as compared to the NTSM controller proposed in [5].

5.4.2 Simulation Studies

The proposed chattering free adaptive terminal sliding mode (TSM) controller is applied for trajectory tracking of a two-link rigid robotic manipulator shown in Fig.5.4.

For the above two-link manipulator, the dynamic equation (5.27) has the following parameters,

$$M(q) = \begin{bmatrix} (m_1+m_2)l_1^2 + m_2l_2^2 + 2m_2l_1l_2cos(q_2) + J_1 & m_2l_2^2 + m_2l_1l_2cos(q_2) \\ m_2l_2^2 + m_2l_1l_2cos(q_2) & m_2l_2^2 + J_2 \end{bmatrix}$$

$$C(q,\dot{q})\dot{q} = \begin{bmatrix} -m_2 l_1 l_2 sin(q_2)\dot{q}_2^2 - 2m_2 l_1 l_2 sin(q_2)\dot{q}_1\dot{q}_2 \\ m_2 l_1 l_2 sin(q_2)\dot{q}_2^2 \end{bmatrix},$$
$$G(q) = \begin{bmatrix} (m_1+m_2) l_1 g cos(q_1) + m_2 l_2 g cos(q_1+q_2) \\ m_2 l_2 g cos(q_1+q_2) \end{bmatrix} \quad (5.47)$$

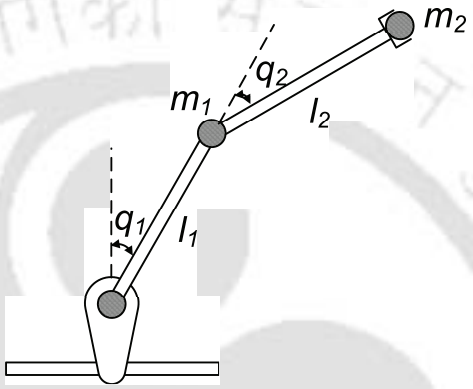

Figure 5.4: Configuration of a two-link robotic manipulator

Here $q(t) = [q_1(t), q_2(t)]^T$ is the angular position vector where $q_1(t)$ and $q_2(t)$ are the angular positions of joints 1 and 2, $M(q)$ is the inertia matrix, $C(q,\dot{q})$ is the centripetal Coriolis matrix, $G(q)$ is the gravity vector and $\tau = [\tau_1, \tau_2]^T$ is the applied torque. The two-link robotic manipulator has four inner states $x_1(t) = q_1(t)$, $x_2(t) = \dot{q}_1(t)$, $x_3(t) = q_2(t)$, $x_4(t) = \dot{q}_2(t)$, two output states $y_1(t) = q_1(t)$ and $y_2(t) = q_2(t)$ and two inputs $u_1(t) = \tau_1$ and $u_2(t) = \tau_2$. Friction terms are ignored. Table 5.1 lists the physical parameters of the two-link robotic manipulator considered in the simulation study [5]. The

Table 5.1: Physical parameters of the two-link robotic manipulator [5]

Symbol	Definition	value
l_1	Length of the first link	$1m$
l_2	Length of the second link	$0.85m$
J_1	Moment of inertia of the D.C. motor 1	$5kg-m$
J_2	Moment of inertia of the D.C. motor 2	$5kg-m$
m_1	Mass of the link 1	$0.5kg$
m_2	Mass of link 2	$1.5kg$
$\hat{m}_1$	Nominal Mass of link 1	$0.4kg$
$\hat{m}_2$	Nominal Mass of link 2	$1.2kg$
g	Gravitational constant	$9.81m/s^2$

reference signals are $q_{d1} = 1.25 - (7/5)e^{-t} + (7/20)e^{-4t}$ and $q_{d2} = 1.25 + e^{-t} - (1/4)e^{-4t}$. The initial states are selected as $q_1(0) = 0$, $q_2(0) = 2.5$, $\dot{q}_1(0) = 0$ and $\dot{q}_2(0) = 0$. The external disturbances

considered are $\tau_{d1} = 2sint + 0.5sin200\pi t$ and $\tau_{d2} = cos2t + 0.5sin200\pi t$ [94]. The parameters of the proposed controller are selected as $p = 5,\ q = 3,\ \beta = diag(0.023, 0.023), c = diag(45, 45)$ and $K^{\dagger} = diag(60, 60)$.

The choice of the design parameters ν_0, ν_1 and ν_2 is influenced by the convergence rate of the estimated bounded parameters $\hat{\bar{B}}_0$, $\hat{\bar{B}}_1$ and $\hat{\bar{B}}_2$ and the adaptation update laws used are given by

$$\begin{aligned}
\dot{\hat{\bar{B}}}_0 &= 1.74||\beta||\ ||\dot{s}^{(\frac{p}{q})-1}\sigma|| \\
\dot{\hat{\bar{B}}}_1 &= 1.45||\beta||\ ||\dot{s}^{(\frac{p}{q})-1}\sigma||\ ||q|| \\
\dot{\hat{\bar{B}}}_2 &= 3.30||\beta||\ ||\dot{s}^{(\frac{p}{q})-1}\sigma||\ ||\dot{q}||^2
\end{aligned}$$

respectively with initial conditions $\hat{\bar{B}}_0(0) = 1$, $\hat{\bar{B}}_1(0) = 1$ and $\hat{\bar{B}}_2(0) = 1$.

The simulations are carried out in the MATLAB - Simulink platform by using ODE 4 solver with a fixed step size of 0.005 sec.

The tracking response and the control input obtained by using the NTSM controller (5.45 - 5.46)

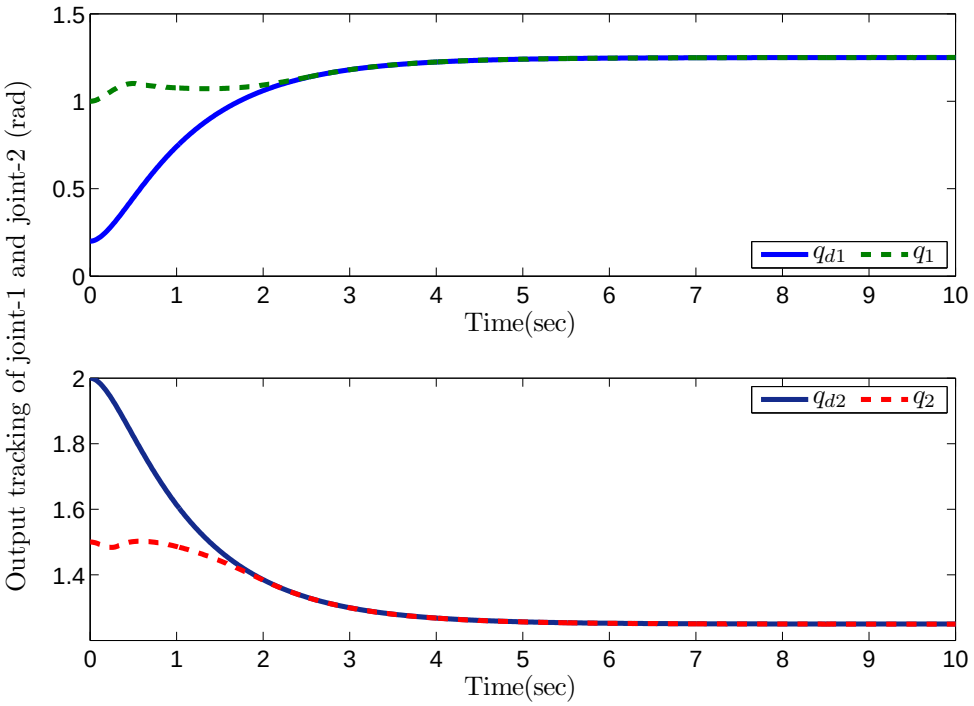

Figure 5.5: Output tracking response of joint 1 and joint 2 with the controller proposed in [5]

proposed by Feng et al. [5] are shown in Fig. 5.5 and Fig. 5.6 respectively. It is observed from these figures that although the tracking performance is satisfactory, the major drawback of the NTSM

controller is the high frequency chattering present in the control input. Moreover, another design constraint the NTSM controller suffers from is that the parameters ρ_0, ρ_1 and ρ_2, i.e. $||F(q, \dot{q}, \ddot{q})||$ (5.29) are needed to be known apriori.

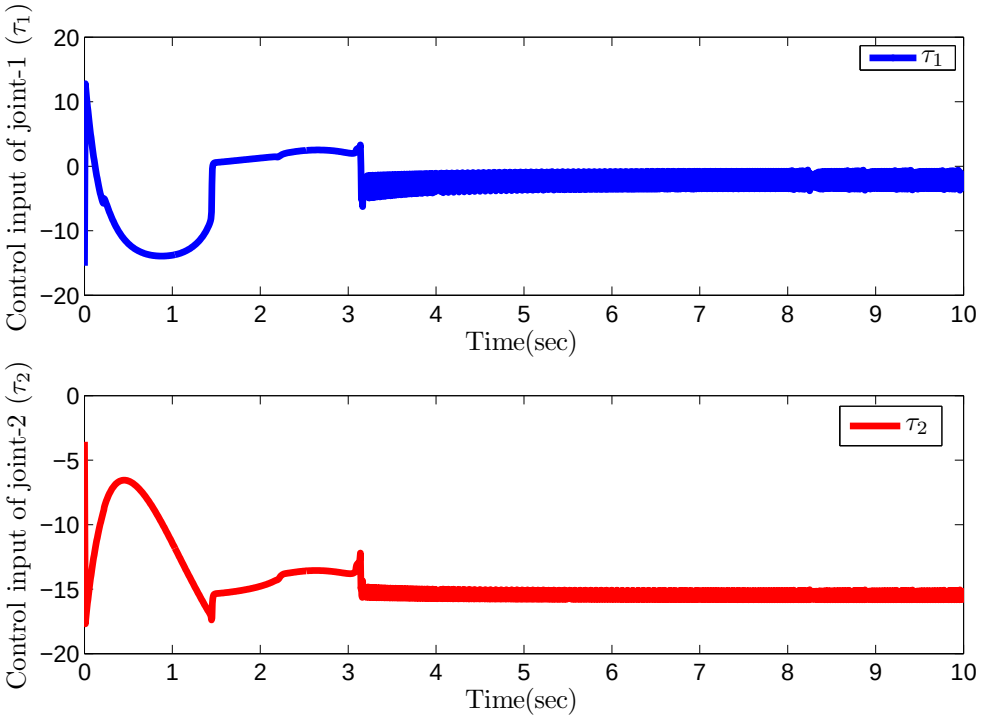

Figure 5.6: Control input of joint 1 and joint 2 with the controller proposed in [5]

Simulation results obtained by applying the proposed adaptive TSM control laws (5.38) and (5.44) are shown in Fig. 5.7 - Fig. 5.10. It is observed from Fig. 5.7 that both the joints 1 and 2 track the reference trajectory faithfully. The control inputs applied to both the joints show no chattering as is evident in Fig. 5.8. The convergence plots of the estimated parameters $\hat{\bar{B}}_0$, $\hat{\bar{B}}_1$ and $\hat{\bar{B}}_2$ are shown in Fig. 5.9. The sliding surfaces and the sliding manifolds are plotted in Fig. 5.10 which confirms that these converge to zero quickly.

For comparison purpose, another class of sliding mode controller is considered in the simulation study. The third order sliding mode controller developed by Defoort et al. [4] is now applied to the

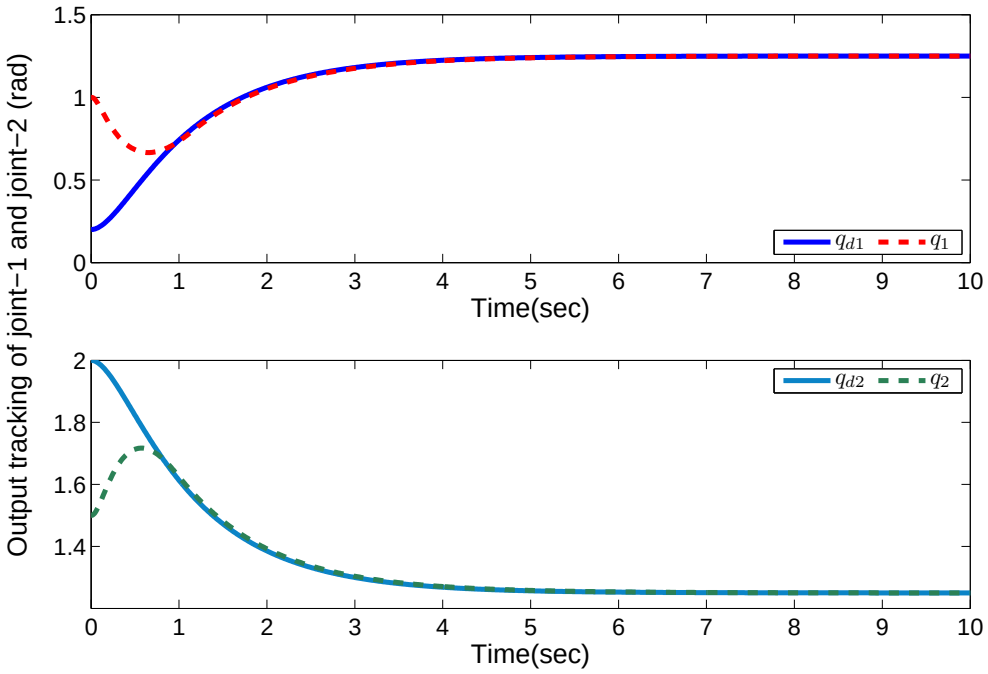

Figure 5.7: Output tracking response of joint 1 and joint 2 using the proposed controller

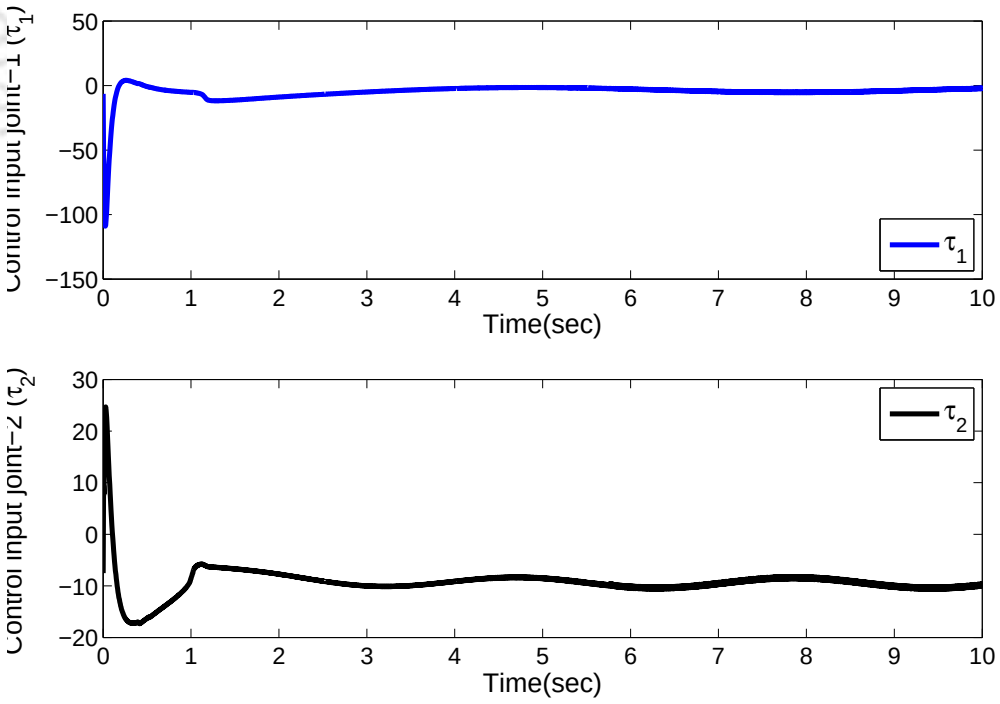

Figure 5.8: Control input of joint 1 and joint 2 using the proposed controller

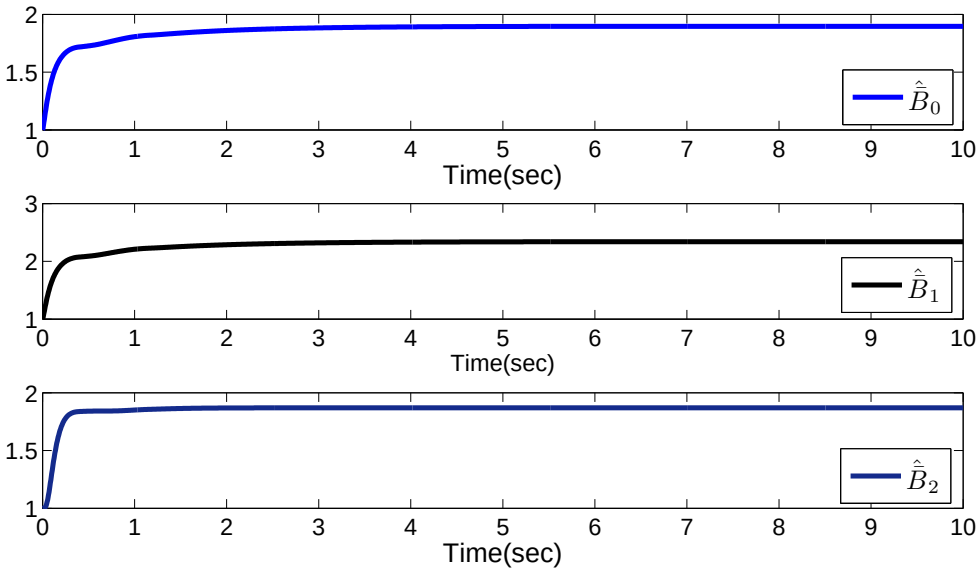

Figure 5.9: Estimated parameters $\hat{\bar{B}}_0$, $\hat{\bar{B}}_1$ and $\hat{\bar{B}}_2$ using the proposed adaptive tuning method

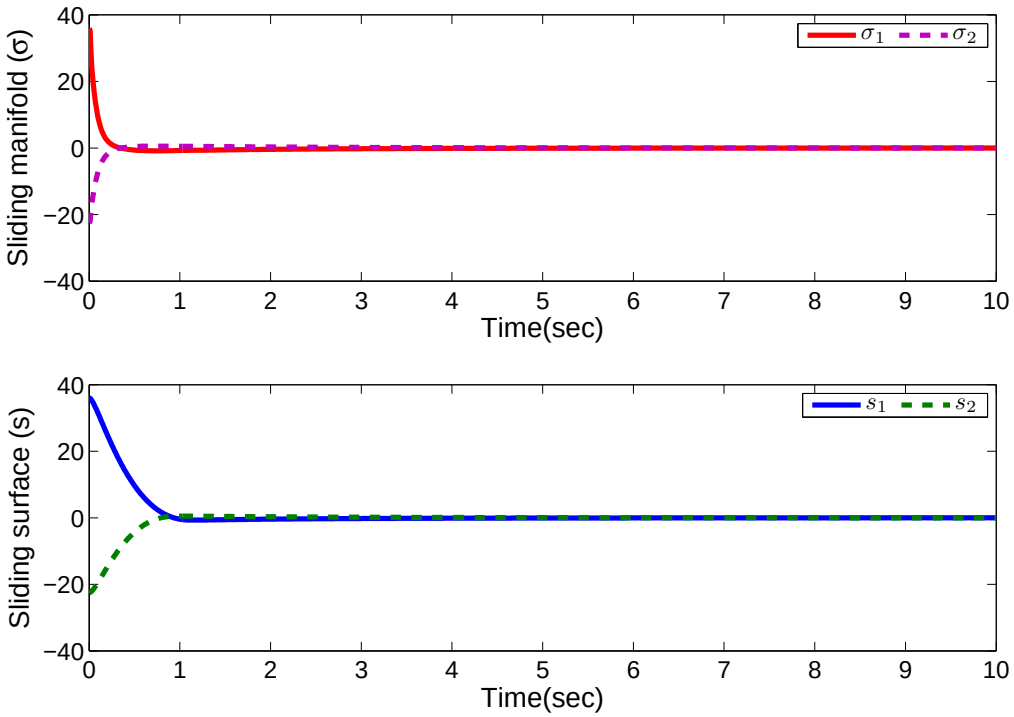

Figure 5.10: Sliding surfaces and sliding manifolds using the proposed controller

robotic manipulator example. The sliding mode function is chosen as [4]

$$s = \dot{e} - \int_0^t u_{nom} d\tau$$

$$u_{nom} = -k_1 |e|^{\alpha_1} sign(e) - k_2 |\dot{e}|^{\alpha_2} sign(\dot{e})$$

with control parameters $k_1 = 40I, k_2 = 17I$ and $\alpha_1 = 3/5, \alpha_2 = 3/4$. The control law proposed by Defoort et al. [4] is given by $\tau = M_0(q,\dot{q})\ddot{q}_d + C_0\dot{q} + G_0 + M_0(q,\dot{q})u_{nom} + M_0(q,\dot{q})u_{disk}$ where u_{disk} is obtained by using the twisting algorithm given by $u_{disk} = -\zeta \int_0^t sign(s)d\tau - \vartheta|s|^{1/2}sign(s)$. The design parameters ζ and ϑ are are chosen as $15I$ and $1I$ respectively.

The tracking performance and the control inputs with the same initial conditions as in the previous

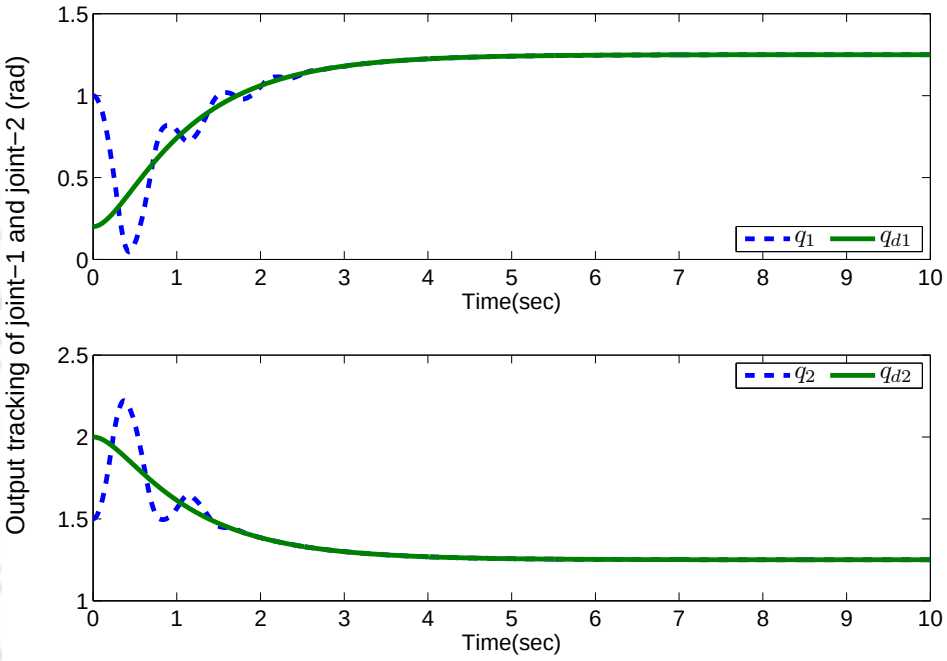

Figure 5.11: Output tracking response of joint 1 and joint 2 with the controller proposed by Defoort et al. [4]

examples are plotted in Fig. 5.11 and Fig. 5.12. It is observed from these figures that although the control law proposed by Defoort et al. [4] assures fast convergence of the states to the reference, the transient response is highly oscillatory at start. In addition, the controller proposed by Defoort et al. [4] is affected by the chattering phenomenon. Moreover, the variation seen in the control input in [4] is quite high which is undesirable as a high input variation can damage the actuator or it may get saturated. In contrast the proposed adaptive TSM controller input is smooth and chattering free.

Output Performance: To evaluate the output performance, the integrated absolute error (IAE) of the output is computed. The IAE is defined as the sum of the absolute values, i.e., IAE of joint-1 $=\sum_{k=1}^{n}|q_1(k) - q_{d1}(k)|$ and IAE of joint-2 $= \sum_{k=1}^{n}|q_2(k) - q_{d2}(k)|$ where n is the number of sampling instants and $q_{d1}(k)$ and $q_{d2}(k)$ are the desired positions of joint-1 and joint-2 respectively at the k-th

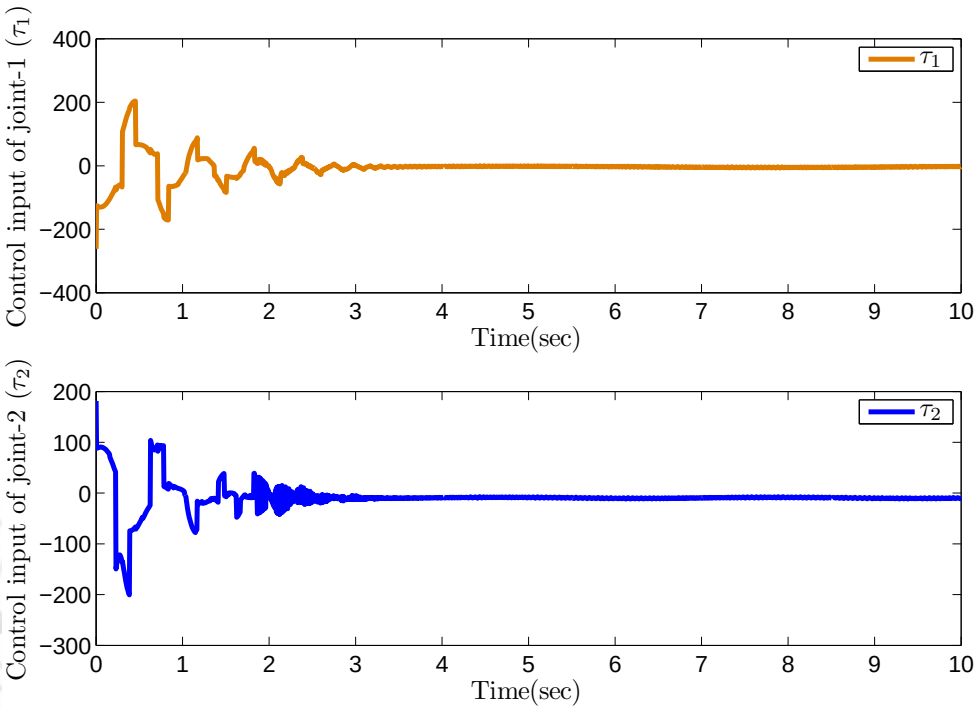

Figure 5.12: Control input of joint 1 and joint 2 with the controller proposed by Defoort et al. [4]

sampling instant.

Input Performance : To evaluate the manipulated input usage, the total variation (TV) [101] of the input $u(t)$, which is sum of all its moves up and down is computed. It is is difficult to define TV compactly for a continuous signal, but if the input signal is discretized as a sequence, i.e $u_1, u_2, u_3, ..., u_i, ...u_n$, then TV can be defined as

$$TV = \sum_{i=1}^{n} |u_{i+1} - u_i| \tag{5.48}$$

The total variation is a good measure of the smoothness of a signal. TV is desired to have a small value because a large value of TV means more excessive input usage or a more complicated controller [101]. Energy of the input is calculated by using the 2-norm method. The control energy is expected to be as small as possible. The output and input performances are calculated for the period from 0 to 10s with a sampling time of 0.05s.

The output and input performances of the proposed adaptive TSM controller as well as the controllers designed by Feng et al. [5] and Defoort et al. [4] for the two-link robotic manipulator are tabulated in Table 5.2. It is noted that the proposed adaptive TSM controller offers comparable

Table 5.2: Comparison of controller performance

Controller performance				
Types of controller		IAE	Total variation (TV)	2-norm of input
Feng et al. [5]	Joint-1	14.85	205.01	72.22
	joint-2	7.22	127.92	207.79
Defoort et al. [4]	Joint-1	7.03	523.10	581.98
	joint-2	5.01	563.44	446.85
Proposed adaptive TSM controller	joint-1	7.01	114.29	114.61
	joint-2	4.05	74.02	140.03

tracking performance by applying a smoother control input having minimal total variation as compared to the controllers designed by Feng et al. [5] and Defoort et al. [4]. Moreover, the overall control energy spent in the case of the proposed adaptive TSM controller is not more than those in the other two methods.

5.5 Summary

A chattering free adaptive terminal sliding mode controller for uncertain systems is proposed in this chapter. The nonsingular terminal sliding manifold guarantees fast and finite time convergence. The controller acts on the first derivative of the control input which contains the switching term involving the sign function. The actual control law is obtained by integrating the discontinuous derivative control signal and hence it is continuous. The requirement of prior knowledge about the uncertainty bounds for designing terminal sliding mode controllers is not a necessary requirement in the proposed controller. The proposed adaptive TSM controller is successfully applied for stabilization of a triple integrator system affected by uncertainty. Trajectory tracking of a two-link robotic manipulator which is a nonlinear system with mismatched uncertainty is also considered in our simulation study. Simulation results demonstrate that the proposed control strategy is successful in eliminating the undesired chattering in the control input while ensuring satisfactory stabilization as well as tracking performances. Hence the proposed controller is suitable for practical applications.

6

Nonlinear Sliding Surface based Adaptive Sliding Mode Controller

Contents

6.1 Introduction

In the previous chapters, stabilization and tracking problems of linear as well as nonlinear uncertain systems were considered and attempts were made for their improvement using chattering free adaptive sliding mode control which employed a linear sliding surface. In general, fast settling time and small overshoot are the two important requirements in most of the design problems. However, it is well known that quick response produces a large overshoot which is not at all desirable in many practical electromechanical applications [102]. On the other hand, a low overshoot can be achieved at the cost of a high settling time. However, a short settling time is also necessary for a quick response, but it increases the overshoot. Thus the user has to choose between fast response and low overshoot and most of the design problems make a trade-off between these two transient indices keeping the damping ratio fixed.

This particular problem can be solved by using the composite nonlinear feedback (CNF) technique [103–105]. CNF method uses a variable damping ratio to achieve high transient performance. Initially, the damping ratio is chosen as a very low value to ensure quick response and as the output approaches the reference, the damping ratio is increased to reduce the overshoot.In [6, 67, 106, 107], the CNF method was used to design a nonlinear sliding surface which increased the damping ratio from its initial low value as the output approached the set point. This resulted in a fast response at the beginning and gradually as the output approached the set point, the effect was to reduce the settling time and overshoot.

This chapter focuses to improve the transient performance of an uncertain system by developing a chattering free sliding mode controller which uses a nonlinear sliding surface. Here a proportional plus constant reaching law based chattering free sliding mode controller is proposed using nonlinear sliding surface to improve the transient performance. An adaptive tuning law is used to deal with unknown but bounded system uncertainties. Further, a discrete integral sliding mode controller based on nonlinear sliding surface is designed to investigate the performance in the discrete domain.

This chapter is organized as follows:

The proposed adaptive sliding mode (SM) controller using nonlinear sliding surface is discussed in Section 6.2. Section 6.3 discusses about nonlinear sliding surface based discrete integral sliding mode controller for uncertain systems. A brief summary is presented in Section 6.4.

6.2 Adaptive chattering free sliding mode (SM) controller using nonlinear sliding surface

A class of dynamic system is considered as follows,

$$\begin{aligned} \dot{x} &= f(x) + g(x)u \\ y &= \sigma(x) \end{aligned} \tag{6.1}$$

where $x \in R^n$ is the state variable, $u \in R^m$ is the control input, $y \in R$ is the output and $\sigma(x) \in R$ is the measured output function known as the sliding variable. Moreover, $f(x)$ and $g(x)$ are smooth functions.

Using appropriate transformation, the above nonlinear system (6.1) can be transformed into the following Brunowsky canonical form [106],

$$\begin{aligned} \dot{x}_i &= x_{i+1} \quad i = 1, ..., (n-1) \\ \dot{x}_n &= a_{n1}x_1 + a_{n2}x_2 + ... + a_{nn}x_n + B_n u + B_n f_m(x,t) \end{aligned} \tag{6.2}$$

The above system can be expressed as,

$$\begin{aligned} \dot{x} &= Ax + B(u + f_m(x,t)) \\ y_1 &= C_1 x \end{aligned} \tag{6.3}$$

where $x \in R^n$ is the state vector, $u \in R^m$ is the control input, y_1 is the output and $f_m(x,t) \in R^m$ represents parametric perturbation and external disturbances and is assumed to be matched. Here A, B and C_1 are known matrices with proper dimensions and n, m are also known. The system (6.3) can be transformed into regular form by using a transformation matrix T_r [106], such that $z = T_r x = [z_1 \;\; z_2]^T$. Then the following transformed system is obtained,

$$\begin{aligned} \dot{z}_1 &= a_{11}z_1 + a_{12}z_2 \\ \dot{z}_2 &= a_{21}z_1 + a_{22}z_2 + B_2 u + B_2 f_m(z,t) \\ y_1 &= Cz_1 \end{aligned} \tag{6.4}$$

Here, $z_1 \in R^{n-1}$, $z_2 \in R$ and $C = C_1(T_r)^{-1}$.

From (6.4) the following can be written,

$$\dot{z} = A_{reg}z + Bu + Bf_m(z,t) \tag{6.5}$$

where $f_m(z,t)$ contains all the uncertain terms along with disturbances and A_{reg} can be expressed as,

$$\begin{aligned} A_{reg} &= \begin{bmatrix} a_{11} & a_{12} \\ a_{21} & a_{22} \end{bmatrix} \\ B &= [0 \quad B_2]^T \end{aligned} \tag{6.6}$$

The nonlinear sliding surface is selected as [106],

$$c^T(t) = [F - \Upsilon(r,y)a_{12}^T P \quad 1] \tag{6.7}$$

where $\Upsilon(r,y)$ is a negative nonlinear function and F is a real matrix. Then

$$\begin{aligned} s &= c^T(t)e \\ &= [F - \Upsilon(r,y)a_{12}^T P \quad 1]e \end{aligned} \tag{6.8}$$

where $e = [e_1 \quad e_2]^T = [z_1 - z_{1d} \quad z_2 - z_{2d}]^T$ and $z_d = [z_{1d} \quad z_{2d}]^T$ is the desired state. Here F is chosen such that $(a_{11} - a_{12}F)$ has stable poles and the dominant poles have low damping ratio. Furthermore, $\Upsilon(r,y)$ is a negative nonlinear function which raises its value starting with zero such that the damping ratio for the overall system increases from an initial low value to higher ones [67, 106]. Moreover, P is a positive definite matrix which can be found by solving the Lyapunov criterion given by,

$$(a_{11} - a_{12}F)^T P + P(a_{11} - a_{12}F) = -R \tag{6.9}$$

where R is also a positive definite matrix.

6.2.1 Stability in sliding mode

During the sliding mode, $s = 0$ and hence from (6.8)

$$e_2 = -Fe_1 + \Upsilon(r,y)a_{12}^T P e_1 \tag{6.10}$$

Using (6.5) and (6.10) yields

$$\dot{e}_1 = (a_{11} - a_{12}F + a_{12}\Upsilon(r,y)a_{12}^T P)e_1 + h \tag{6.11}$$

where $h = a_{11}z_{1d} + a_{12}z_{2d} - \dot{z}_{1d}$. Suppose that the desired trajectory z_d is consistently generated by using the system model. Then there exists some control u such that

$$\begin{aligned} \dot{z}_{1d} &= a_{11}z_{1d} + a_{12}z_{2d} \\ \dot{z}_{2d} &= a_{21}z_{1d} + a_{22}z_{2d} + B_2 u \end{aligned} \tag{6.12}$$

Using (6.11) and (6.12) yields,

$$\dot{e}_1 = (a_{11} - a_{12}F + a_{12}\Upsilon(r,y)a_{12}^T P)e_1 \tag{6.13}$$

To prove the stability in the sliding mode, let us consider the following Lyapunov function,

$$\begin{aligned} V_1 &= e_1^T P e_1 \\ &\text{Taking its derivative and using (6.13) yields} \\ \dot{V}_1 &= \dot{e}_1^T P e_1 + e_1^T P \dot{e}_1 \\ &= e_1^T (a_{11} - a_{12}F)^T P e_1 + e_1^T P (a_{11} - a_{12}F) e_1 + 2e_1^T P a_{12}\Upsilon(r,y)a_{12}^T P e_1 \\ &= e_1^T [(a_{11} - a_{12}F)^T P + P(a_{11} - a_{12}F)] e_1 + 2e_1^T P a_{12}\Upsilon(r,y)a_{12}^T P e_1 \\ &= e_1^T [(a_{11} - a_{12}F)^T P + P(a_{11} - a_{12}F) + 2P a_{12}\Upsilon(r,y)a_{12}^T P] e_1 \\ &= e_1^T [-R + 2P a_{12}\Upsilon(r,y)a_{12}^T P] e_1 \\ &\text{Let there exist a matrix } Q = e_1^T P a_{12}. \text{ Thus } \dot{V}_1 \text{ can be simplified as,} \\ \dot{V}_1 &= -e_1^T R e_1 + 2Q\Upsilon(r,y)Q^T \\ &\text{Since } R > 0 \text{ and } \Upsilon(r,y) < 0, \\ \dot{V}_1 &< 0 \end{aligned} \tag{6.14}$$

Thus stability in sliding mode is proved. Taking first derivative of s and using (6.8) and (6.5), the following is obtained:

$$\dot{s} = \dot{c}^T(t)z - \dot{c}^T(t)z_d - c^T(t)\dot{z}_d + c^T(t)(A_{reg}z + Bu + Bf_m(z,t)) \tag{6.15}$$

Taking the second derivative of s yields

$$\begin{aligned}\ddot{s} &= \dot{c}^T(t)\dot{z} + \ddot{c}^T(t)z + c^T(t)A_{reg}\dot{z} + \dot{c}^T(t)A_{reg}z + c^T(t)B\dot{u} + \dot{c}^T(t)Bu \\ &\quad + c^T(t)B\dot{f}_m(z,t) + \dot{c}^T(t)Bf_m(z,t) - \frac{d}{dt}(\dot{c}^T(t)z_d + c^T(t)\dot{z}_d)\end{aligned}$$

$$\begin{aligned}&= c^T(t)A_{reg}^2 z + 2\dot{c}^T(t)A_{reg}z + \ddot{c}^T(t)z + c^T(t)A_{reg}Bu \\ &\quad + 2\dot{c}^T(t)Bu + c^T(t)B_2\dot{u} - \ddot{c}^T(t)z_d - \dot{c}^T(t)\dot{z}_d - c^T(t)\ddot{z}_d \\ &\quad - \dot{c}^T(t)\dot{z}_d + c^T(t)A_{reg}Bf_m(z,t) + 2\dot{c}^T(t)Bf_m(z,t) + c^T(t)B\dot{f}_m(z,t) \qquad (6.16)\end{aligned}$$

Let all the uncertainties be norm bounded and
$(c^T(t)A_{reg}Bf_m(z,t) + 2\dot{c}^T(t)Bf_m(z,t) + c^T(t)B\dot{f}_m(z,t)) = \Delta F(z,t)$.
Assuming $y_1(z) = s$ and $y_2(z) = \dot{s}$, the system dynamics can be written as,

$$\begin{aligned}\dot{y}_1(z) &= y_2(z) \\ \dot{y}_2(z) &= \Phi(z,u) + \Psi(z)v \qquad (6.17)\end{aligned}$$

where $v = \dot{u}$ and $\Phi(z,u)$ collects all the uncertain terms not involving $\dot{u}$. Thus the systems (6.15) and (6.16) are now controlled by the input v. A sliding mode controller can be designed for the above system using the control input v to keep the system trajectories in the sliding manifold.
Let the sliding manifold be considered as,

$$\sigma = y_2(z) + \kappa y_1(z) \qquad (6.18)$$

where κ is a positive constant.
Taking the derivative of (6.18) yields,

$$\dot{\sigma} = \dot{y}_2(z) + \kappa\dot{y}_1(z) \qquad (6.19)$$

Using (6.15) and (6.16), the following is obtained,

$$\begin{aligned}\dot{\sigma} &= c^T(t)A_{reg}^2 z + 2\dot{c}^T(t)A_{reg}z + \ddot{c}^T(t)z + c^T(t)A_{reg}Bu \\ &+ 2\dot{c}^T(t)Bu + c^T(t)B\dot{u} - \ddot{c}^T(t)z_d - \dot{c}^T(t)\dot{z}_d - c^T(t)\ddot{z}_d \\ &- \dot{c}^T(t)\dot{z}_d + \kappa\dot{s} + \Delta F(z,t) \qquad (6.20)\end{aligned}$$

Using the constant plus proportional reaching law yields,

$$\dot{\sigma} = -k_1\sigma - k_2 sign(\sigma) \tag{6.21}$$

Using (6.20) and (6.21), the control law is obtained as,

$$\begin{aligned} \dot{u} &= -(c^T(t)B)^{-1}[c^T(t)A_{reg}^2 z + 2\dot{c}^T(t)A_{reg}z + \ddot{c}^T(t)z \\ &+ c^T(t)A_{reg}Bu + 2\dot{c}^T(t)Bu - \ddot{c}^T(t)z_d - \dot{c}^T(t)\dot{z}_d - c^T(t)\ddot{z}_d \\ &- \dot{c}^T(t)\dot{z}_d + k_1\sigma + k_2 sign(\sigma) + \kappa\dot{s}] \end{aligned} \tag{6.22}$$

where $k_1 \geq 0$ and $k_2 > \{|(c^T(t)A_{reg}Bf_m(z,t) + 2\dot{c}^T(t)Bf_m(z,t) + c^T(t)B\dot{f}_m(z,t))| = |\Delta F(z,t)|\}$ to satisfy the reaching law condition $\sigma\dot{\sigma} \leq -\eta|\sigma|$ for some $\eta > 0$.

In practice, the upper bound of the system uncertainty is often unknown in advance and hence the error term $|\Delta F(z,t)|$ is difficult to find. An adaptive tuning law is proposed to estimate k_2 using which the control law (6.22) can be written as

$$\begin{aligned} \dot{u} &= -(c^T(t)B)^{-1}[c^T(t)A_{reg}^2 z + 2\dot{c}^T(t)A_{reg}Bz + \ddot{c}^T(t)z \\ &+ c^T(t)A_{reg}Bu + 2\dot{c}^T(t)Bu - \ddot{c}^T(t)z_d - \dot{c}^T(t)\dot{z}_d - c^T(t)\ddot{z}_d \\ &- \dot{c}^T(t)\dot{z}_d + k_1\sigma + \hat{T}sign(\sigma) + \kappa\dot{s}] \end{aligned} \tag{6.23}$$

where $\hat{T}$ estimates the value of k_2. Defining the adaptation error as $\tilde{T} = \hat{T} - T$, the parameter $\hat{T}$ is estimated by using the adaptation law as in (4.57) [40, 69, 70, 108] and given below,

$$\dot{\hat{T}} = \nu|\sigma| \tag{6.24}$$

where ν is a positive constant. A Lyapunov function V_2 is selected as $V_2 = \frac{1}{2}\sigma^2 + \frac{1}{2}\gamma\tilde{T}^2$ whose time derivative is as follows,

$$\begin{aligned} \dot{V}_2 &= \sigma\dot{\sigma} + \gamma\tilde{T}\dot{\tilde{T}} \\ &\text{Using (6.20) yields,} \\ \dot{V}_2 &= \sigma[c^T(t)A_{reg}^2 z + 2\dot{c}^T(t)A_{reg}z + \ddot{c}^T(t)z + c^T(t)A_{reg}Bu \end{aligned}$$

$$
\begin{aligned}
&+ \quad 2\dot{c}^T(t)Bu + c^T(t)B\dot{u} - \ddot{c}^T(t)z_d - \dot{c}^T(t)\dot{z}_d - c^T(t)\ddot{z}_d - \dot{c}^T(t)\dot{z}_d \\
&+ \quad \kappa\dot{s} + \Delta F(z,t)] + \gamma(\hat{T} - T)\dot{\hat{T}} \\
&\quad \text{Using (6.23) and (6.24) yields,} \\
\dot{V}_2 &= \sigma[\Delta F(z,t) - \hat{T}sign(\sigma) - k_1\sigma] + \gamma(\hat{T} - T)\nu|\sigma| \\
&\quad \text{Since } k_1 \geq 0, \text{ the above equation can be written as} \\
\dot{V}_2 &\leq \mid \Delta F(z,t) \mid |\sigma| - \hat{T}|\sigma| + T|\sigma| - T|\sigma| + \gamma(\hat{T} - T)\nu|\sigma| \\
&\leq (|\Delta F(z,t)| - T)|\sigma| - (\hat{T} - T)|\sigma| + \gamma(\hat{T} - T)\nu|\sigma| \\
&\leq -(-|\Delta F(z,t)| + T)|\sigma| - (\hat{T} - T)(-\gamma\nu|\sigma| + |\sigma|) \\
&\leq -\beta_\sigma\sqrt{2}|\sigma/\sqrt{2}| - \beta_\nu\sqrt{\gamma/2}(\hat{T} - T)/\sqrt{\gamma/2} \\
&\quad \text{where } \beta_\sigma = (T - |\Delta F(z,t)|) \text{ and } \beta_\nu = (|\sigma| - \gamma\nu|\sigma|) \\
&\quad \text{So, } \dot{V}_2 \leq -min\{\beta_\sigma\sqrt{2}, \beta_\nu\sqrt{2/\gamma}\}(|\sigma/\sqrt{2}| + \tilde{T}\sqrt{\gamma/2}) \\
&\leq -\beta V_2^{1/2}
\end{aligned} \tag{6.25}
$$

where $\beta = min\{\beta_\sigma\sqrt{2}, \beta_\nu\sqrt{2/\gamma}\}$ with $\beta > 0$. The above inequality holds if $\dot{\hat{T}} = \nu|\sigma|$, $\beta_\sigma > 0, \beta_\nu > 0$, $T > |\Delta F(z,t)|$ and $\gamma < \frac{1}{\nu}$. Therefore, finite time convergence to a domain $\sigma = 0$ is guaranteed from any initial condition [40, 62]. The adaptive tuning law (6.24) is modified by using the dead zone technique.

It is evident from (6.23) that $\dot{u}$ is discontinuous but integration of $\dot{u}$ yields a continuous control law u. Hence the undesired high frequency chattering of the control signal is eliminated. Thus the above adaptive SM control with nonlinear sliding surface offers following advantages. Firstly, an improved transient performance can be obtained without the knowledge about the upper bound of the system uncertainties. Secondly, the chattering in the control input is eliminated.

Assumption 6.1. *An exact robust differentiator is available for exactly measuring or estimating the derivative of variables.*

6.2.2 Choice of nonlinear function $\Upsilon(r, y)$

The nonlinear function $\Upsilon(r, y)$ is used to change the system's damping ratio as the output y approaches the reference position r [104] [67]. It possesses the properties mentioned below:

- When the output is far from the reference value, $\Upsilon(r, y)$ equals to zero (or a very small value).
- As the output approaches its final desired value, $\Upsilon(r, y)$ value gradually becomes highly negative.
- The nonlinear function $\Upsilon(r, y)$ should be continuous, differentiable and its higher derivatives must exist.

The choice of $\Upsilon(r, y)$ is not unique. Some examples of $\Upsilon(r, y)$ used in literature are discussed below [102].

$$\Upsilon(r, y) = -\varrho e^{-\psi(y-r)^2} \tag{6.26}$$

where r and y are the reference input and the system output respectively. Here $\varrho > 0$, $\psi > 0$ are the tuning parameters. It is observed that the nonlinear function decreases its value from 0 to $-\varrho$ as the value of error $(y - r)$ decreases from infinity (very high value) to zero. Another type of nonlinear function $\Upsilon(r, y)$ used is given by,

$$\Upsilon(r, y) = -\varrho e^{-\psi|y-r|} \tag{6.27}$$

The value of $\Upsilon(r, y)$ changes from 0 to $-\varrho$ as the error $(y-r)$ approaches zero [109] from a high value. $\Upsilon(r, y)$ can assume the following form also,

$$\Upsilon(r, y) = -\frac{\varrho}{1 - e^{-1}}(e^{-(1-(y-y_0)/(r-y_0))^2} - e^{-1}) \tag{6.28}$$

where r is the reference input, $y_0 = y(0)$ is the initial state and ϱ is the tuning parameter. The function $\Upsilon(r, y)$ changes its value from 0 to $-\varrho$ as the error $(y-r)$ approaches zero from a high value.

6.2.3 Simulation Results

The proposed controller is simulated in MATLAB-Simulink by using ODE 8 solver with a fixed step size of 0.005 sec.

6.2.3.1 Time response of second order process with time delay

The proposed adaptive SM controller is applied to a second order uncertain system with time delay. The performance of the proposed adaptive SM controller using nonlinear sliding surface is compared with that obtained by using adaptive SM controller with different linear sliding surfaces. The second order process with time delay is given by [9]

$$G(s) = \frac{0.05e^{-0.5s}}{(1 + 0.1s)(1 + s)} \tag{6.29}$$

which can be simplified to the following form using Padé approximation,

$$G(s) = \frac{0.05}{(1 + 0.5s)(1 + 0.1s)(1 + s)} \tag{6.30}$$

The state space model given by Eq.(6.3) is obtained with

$$A = \begin{bmatrix} 0 & 1 & 0 \\ 0 & 0 & 1 \\ -20 & -32 & -13 \end{bmatrix}, B = \begin{bmatrix} 0 \\ 0 \\ 1 \end{bmatrix}, C_1 = \begin{bmatrix} 1 & 0 & 0 \end{bmatrix} \tag{6.31}$$

The matched uncertainty considered here is $f_m(x,t) = 0.5sin(10t)$.

Since the system is already in the regular form, the following submatrices can be written, $z_1 = [x_1 \;\; x_2]^T$, $z_2 = x_3$ and coefficient matrices

$$a_{11} = \begin{bmatrix} 0 & 1 \\ 0 & 0 \end{bmatrix}, a_{12} = \begin{bmatrix} 0 \\ 1 \end{bmatrix}$$
$$a_{21} = \begin{bmatrix} -20 & -32 \end{bmatrix}, a_{22} = -13, \; B_2 = 1, \; C = C_1 \tag{6.32}$$

- Design of nonlinear sliding surface:

The nonlinear sliding surface consists of a linear and a nonlinear term. Initially, the nonlinear term has a very low value and as the system gradually approaches its desired position, the nonlinear term decreases its value to a high negative value and thereby changes the value of the damping ratio. As a result, the system response has low overshoot and small settling time. Let us recall,

$$c^T(t) = [F - \Upsilon(r,y)a_{12}^T P \quad 1] \tag{6.33}$$

Here the gain matrix F is designed for low damping ratio and high setting time. Moreover, F can be designed by using pole placement technique. Let initially the system have damping ratio ξ_1 and settling time t_{s1}. The closed loop poles are located at $(-\xi_1\omega_n + \sqrt{(}\xi_1^2 - 1)\omega_n)$ and $(-\xi_1\omega_n - \sqrt{(}\xi_1^2 - 1)\omega_n)$. The natural frequency of oscillations ω_n is given by,

$$\omega_n = \frac{4}{\xi_1 t_{s1}} \tag{6.34}$$

Let us choose the initial damping ratio $\xi_1 = 0.4$ and settling time $t_{s1} = 3.5$. Using (6.34), the poles can be found to be located at $-1.1429 + 2.6186i, -1.1429 - 2.6186i$. Thus F can be calculated using pole placement technique as $F = [8.1633 \;\; 2.2857]$. Solution of the Lyapunov equation (6.9) yields,

$$P = \begin{bmatrix} 0.2144 & 0.0061 \\ 0.0061 & 0.0246 \end{bmatrix} \text{ using } \mathrm{R} = \begin{bmatrix} 0.1 & 0 \\ 0 & 0.1 \end{bmatrix} \tag{6.35}$$

The nonlinear function $\Upsilon(r, y)$ is designed as,

$$\Upsilon(r, y) = -215.04e^{-\psi(y-r)^2} \tag{6.36}$$

where $\psi = 10$,$r = 1$.

- Design of control law

Using nonlinear sliding surface, the overall SM control law is obtained from (6.22) choosing $\kappa = 15$, $k_1 = 10$. The adaptive tuning law is designed as $\dot{\hat{T}} = 0.015|\sigma|$ with $T_0 = 0$. Here A_{reg}, B are obtained by using the equations (6.6) and (6.32). The nonlinear sliding surface $c^T(t)$ is designed as explained earlier.

6.2.3.2 Comparison with adaptive SM controller using linear sliding surface

Transient Performance of the nonlinear sliding surface based adaptive SM controller is compared against the adaptive SM controller using linear sliding surface. Following three different linear sliding surfaces are chosen for our comparison:

1. Linear sliding surface 1 with $\xi = 0.4$, $t_s = 3.5sec$
2. Linear sliding surface 2 with $\xi = 0.5$, $t_s = 3.0sec$
3. Linear sliding surface 3 with $\xi = 0.7$, $t_s = 2.5sec$

The adaptive SM control law with linear sliding surface is obtained from (6.22), given by

$$\begin{aligned} \dot{u} &= -(c^T(t)B)^{-1}[c^T(t)A_{reg}^2 z + c^T(t)Bu + \kappa\dot{s} + k_1\sigma + \hat{T}sign(\sigma) \\ &\quad -c^T(t)\ddot{z}_d] \end{aligned} \tag{6.37}$$

The output which is the angular position is plotted in Fig. 6.1 for the nonlinear sliding surface based as well as linear sliding surface based adaptive SM controllers. From Fig. 6.1 it is clearly observed that the peak overshoot and settling time both improve significantly in the case of the nonlinear sliding surface based adaptive SM controller. A detailed comparison of transient performances between these two types of adaptive SM controllers is presented in Table 6.1.

The convergence of adaptive gains $\hat{T}$ for different sliding surfaces are confirmed in Fig. 6.2. Notably, the knowledge of the upper bounds on the uncertainties is not a required prerequisite for designing the SM controller.

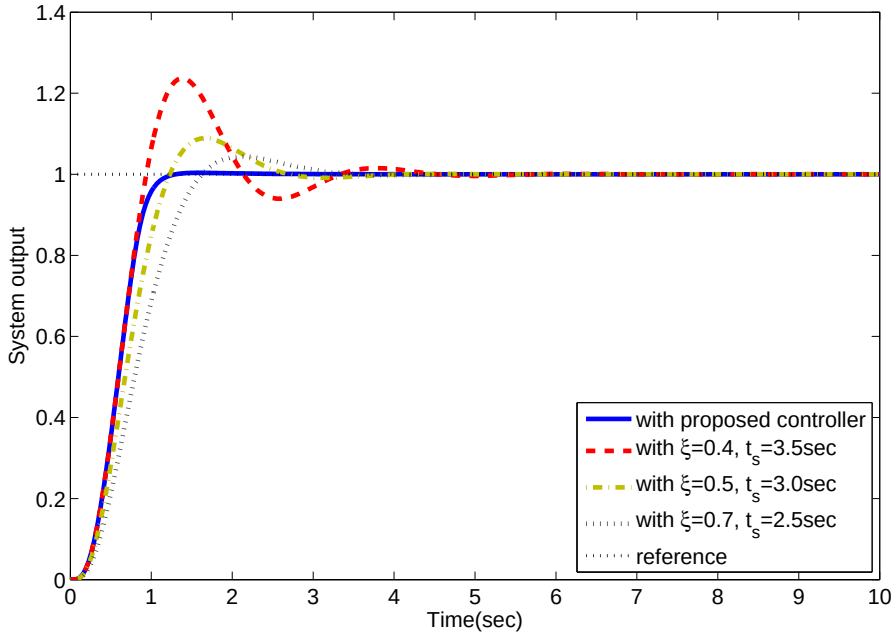

Figure 6.1: Output response of adaptive SM controller with different sliding surfaces

Table 6.1: Transient response indices for different values of ξ and t_s

Type of sliding surface	Peak (%) overshoot	Settling time (sec)
Linear sliding surface with $\xi = 0.4$, t_s=3.5 sec	24	3.5
Linear sliding surface with $\xi = 0.5$, t_s=3.0 sec	8	3.0
Linear sliding surface with $\xi = 0.7$, t_s=2.5 sec	5	2.5
Proposed controller with nonlinear sliding surface	0	1.1

6.2.4 Stabilization of an uncertain system

The problem of ship roll stabilization is taken up now and the performance of the proposed controller is compared with that of Fulwani et al. [6]. The state space representation of the ship roll model is given by Equation (6.3) with [6],

$$A = \begin{bmatrix} 0 & 1 & 0 \\ 0 & 0 & 1 \\ -2 & -2.7 & -1.7 \end{bmatrix}, B = \begin{bmatrix} 0 \\ 0 \\ 1 \end{bmatrix} \quad (6.38)$$

$$C_1 = \begin{bmatrix} 1 & 0 & 0 \end{bmatrix} \quad (6.39)$$

The uncertainty is considered as $f_m(x,t) = sin(10t)$.

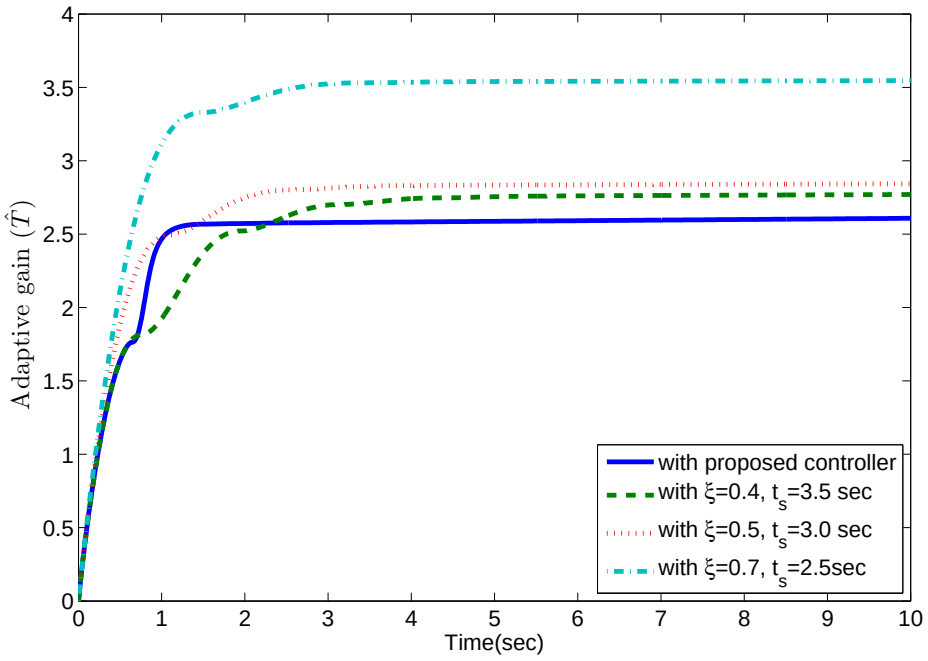

Figure 6.2: Adaptive gains of SM controller with different sliding surfaces

The objective is to stabilize the output quickly to the equlibrium. The parameters for designing the controller are chosen as $F = [25 \quad 4]$, $\kappa = 30$, $k_1 = 20$ and the initial condition is assumed as $x(0) = [0.1\ 0\ 0]^T$ [6]. By solving the Lyapunov equation (6.9), P is obtained as,

$$P = \begin{bmatrix} 0.0071 & -0.0170 \\ -0.0170 & 0.1105 \end{bmatrix} \quad \text{where} \quad \mathrm{R} = 0.34 \begin{bmatrix} 1 & 0 \\ 0 & 1 \end{bmatrix} \tag{6.40}$$

The nonlinear function $\Upsilon(r, y)$ is selected as [6],

$$\Upsilon(y) = -50e^{-100y^2} \tag{6.41}$$

The adaptive tuning law is designed as $\dot{\hat{T}} = 4|\sigma|$ with $T_0 = 0$.

Fig. 6.3 shows the system output and the control input using the control law proposed by Fulwani et al. [6]. From Fig. 6.3 it is observed that the output converges fast to the reference without any overshoot. However, it is clear that the control input is not smooth and contains excessive chattering. Moreover, the start-up control input is also very high.

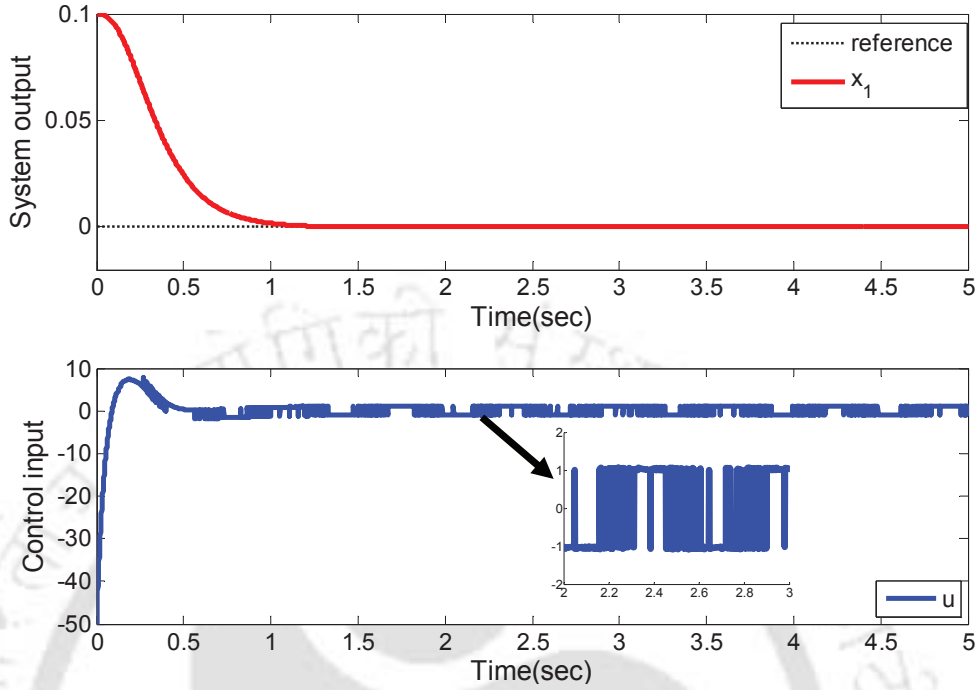

Figure 6.3: System output and control input using the control law [6]

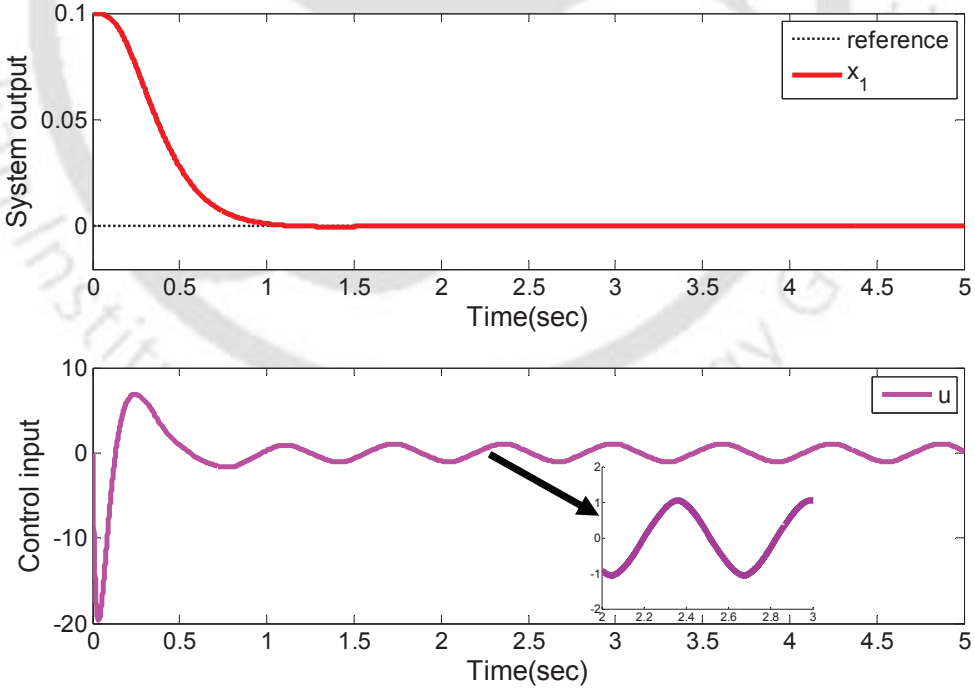

Figure 6.4: System output and control input using the proposed controller

The simulation results obtained by using the proposed adaptive SM controller are plotted in Fig. 6.4. It is noticed that the system output has no overshoot and reaches the origin in the same time as in the

method of Fulwani et al. [6]. Furthermore, the proposed controller produces a chattering free control input. Also, the proposed method reduces the start-up control input considerably. Convergence of the sliding surface, the sliding manifold and the adaptive gain obtained by using the proposed method are shown in Fig. 6.5.

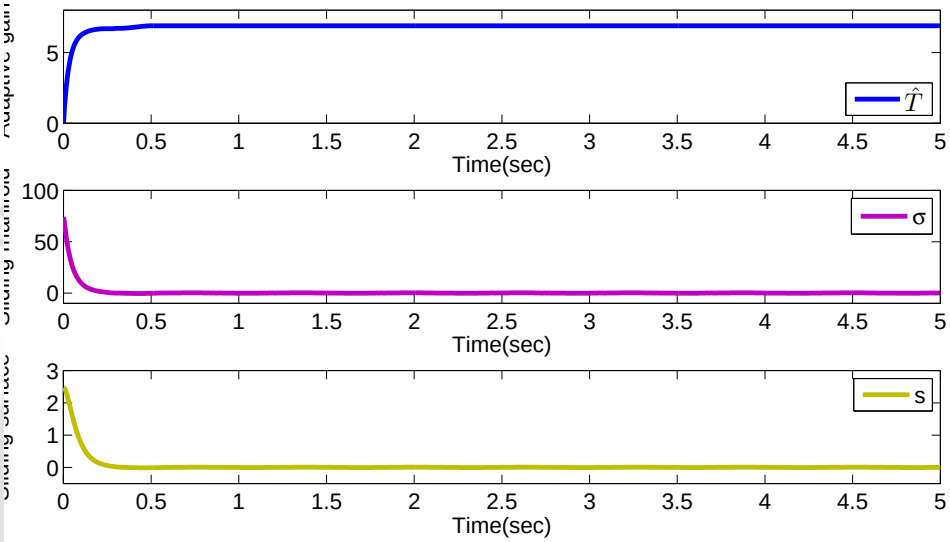

Figure 6.5: Adaptive gain, sliding manifold and sliding surface using the proposed controller

Input Performance **:** Although good transient performance is the primary aim of the controller, large variation in the control input to achieve the same is undesirable. For rating the controller performance, an index to measure the total variation (TV) in the control input u has been proposed in literature [101] as

$$TV = \sum_{i=1}^{n} |u_{i+1} - u_i| \tag{6.42}$$

which is desired to have a small value. The total variation is a good measure of the smoothness of a signal. A large value of TV means more input usage or a more complicated controller [101]. Also, input energy is another important index for the controller and is calculated by using the 2-norm method. The control energy is expected to be as small as possible. The input performance of the proposed controller is computed in terms of TV and 2-norm energy for the period from 0 to 5s with a sampling time of 0.01s. The input performance of the proposed controller and that of Fulwani et al. [6] are tabulated in Table 6.2.

Table 6.2: Input performance comparison

Type of Controller	Total Variation (TV)	Control Energy
Fulwani et al.'s method [6]	137.31	86.72
Proposed controller	8.35	52.18

It is noted from Table 6.2 that the proposed controller offers comparable output performance by applying a smoother control input having minimal total variation as compared to the controller designed by Fulwani et al. [6]. Furthermore, the control effort spent is much lower in the case of the proposed controller than in [6].

6.2.5 Performance comparison with third order sliding mode controller

The performance of the proposed adaptive sliding mode (SM) controller is now compared with the third order sliding mode controller developed by Defoort et al. using twisting algorithm [4, 62]. For the sake of comparison, stabilization of the triple integrator system described in [62] and discussed earlier in Section 5.3 is reconsidered as given below,

$$\begin{aligned} \dot{x}_1 &= x_2 \\ \dot{x}_2 &= x_3 \\ \dot{x}_3 &= u + p(x), \quad y = x_1 \end{aligned} \tag{6.43}$$

where $p(x) = sin(10x_1)$ is the bounded uncertainty, y is the output and the initial condition of the system is assumed as $x(0) = [1 \;\; 0 \;\; -1]^T$ [62]. The system trajectory and the control input obtained by using Defoort et al.'s method are shown in Fig. 6.6. It is observed from Fig. 6.6 that the third order sliding mode controller using twisting algorithm is not able to reduce the chattering in the control input completely.

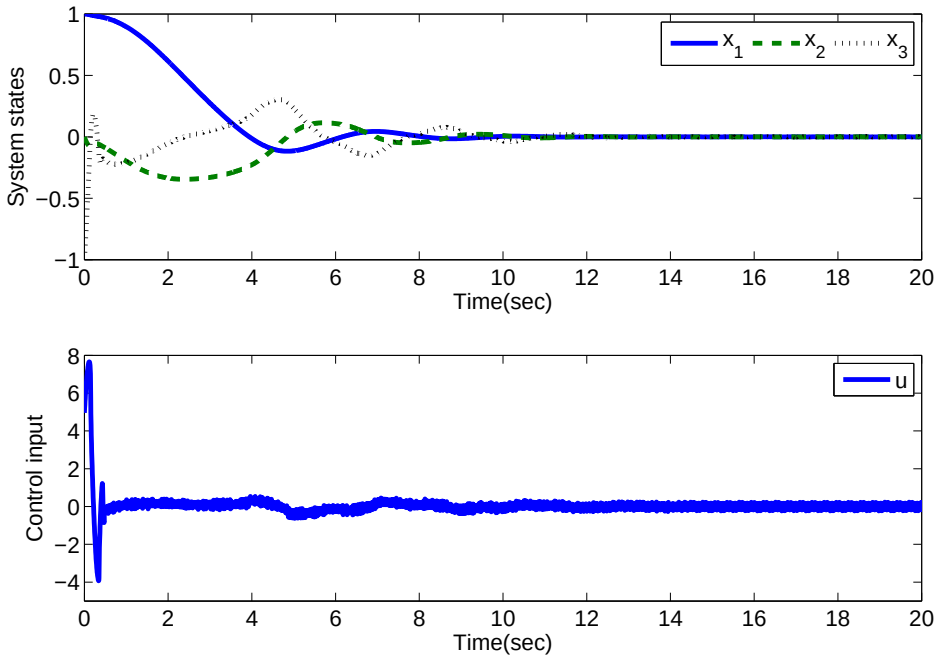

Figure 6.6: System output and control input using the control law [4]

The proposed adaptive SM controller using a nonlinear sliding surface is now applied to the triple integrator system. The parameters in the control law (6.22) are chosen as $\kappa = 3$, $k_1 = 5$ and the nonlinear function is selected as $\Upsilon(y) = -60.07e^{-10y^2}$. The adaptive tuning law is designed as $\dot{\hat{T}} = 0.1|\sigma|$ with $T_0 = 0$. The nonlinear sliding surface is designed by choosing the damping ratio $\xi = 0.3$ and settling time $t_s = 5$ sec [61, 62]. The positive definite matrix P obtained by solving the Lyapunov equation (6.9) is given as,

$$P = \begin{bmatrix} 0.2674 & 0.0070 \\ 0.0070 & 0.0356 \end{bmatrix} \text{ using } \mathrm{R} = \begin{bmatrix} 0.1000 & 0.0000 \\ 0.0000 & 0.1000 \end{bmatrix} \tag{6.44}$$

The system states and the control input for the triple integrator system using the proposed controller are plotted in Fig. 6.7. It is evident from Fig. 6.7 that the proposed adaptive SM controller produces faster convergence of the system states to equilibrium and smoother chattering free control input as compared to the method proposed by [4].

Convergence of the adaptive gain, the sliding manifold and the sliding surface by using the proposed controller is shown in Fig. 6.8.

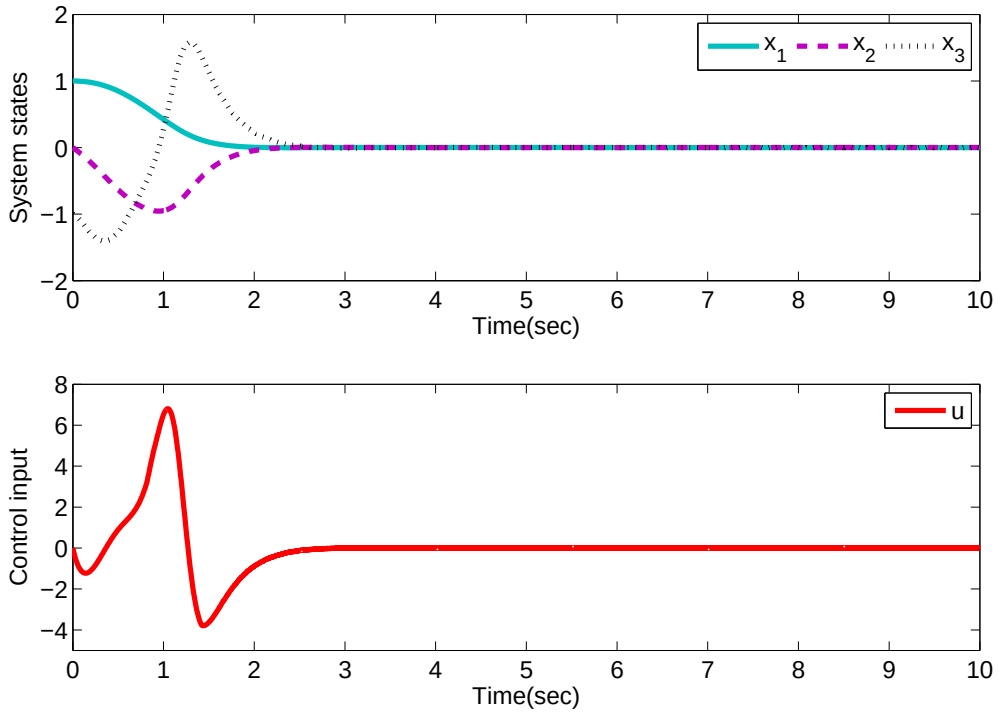

Figure 6.7: System states and control input using the proposed controller

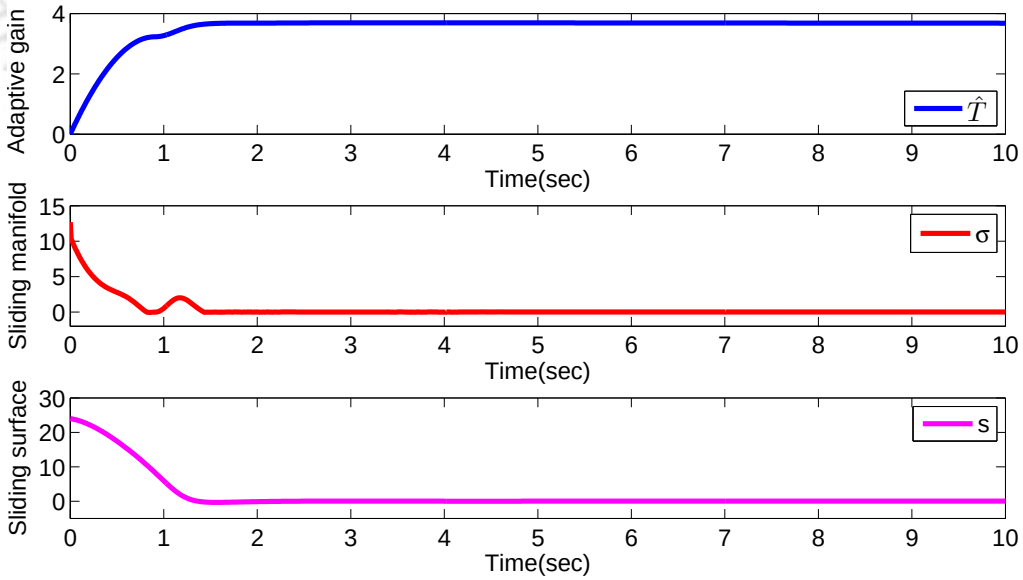

Figure 6.8: Adaptive gain, sliding manifold and sliding surface using the proposed controller

System output obtained by using the proposed adaptive SM controller employing both nonlinear

and linear sliding surfaces is compared with that obtained by using Defoort et al.'s method [4] in Fig. 6.9. From Fig. 6.9 it is clearly observed that the best transient performance is demonstrated by the proposed controller using nonlinear sliding surface. A detailed comparison of the transient as well as input performance between the proposed controller and Defoort et al.'s method [4] is tabulated in Table 6.3. From Table 6.3 it is evident that the proposed controller produces zero overshoot, faster settling time, lesser input variation and lower control action than those obtained by using the controller proposed by Defoort et al. [4]. The input performance is calculated for the period from 0 to 20s with a sampling time of 0.01s.

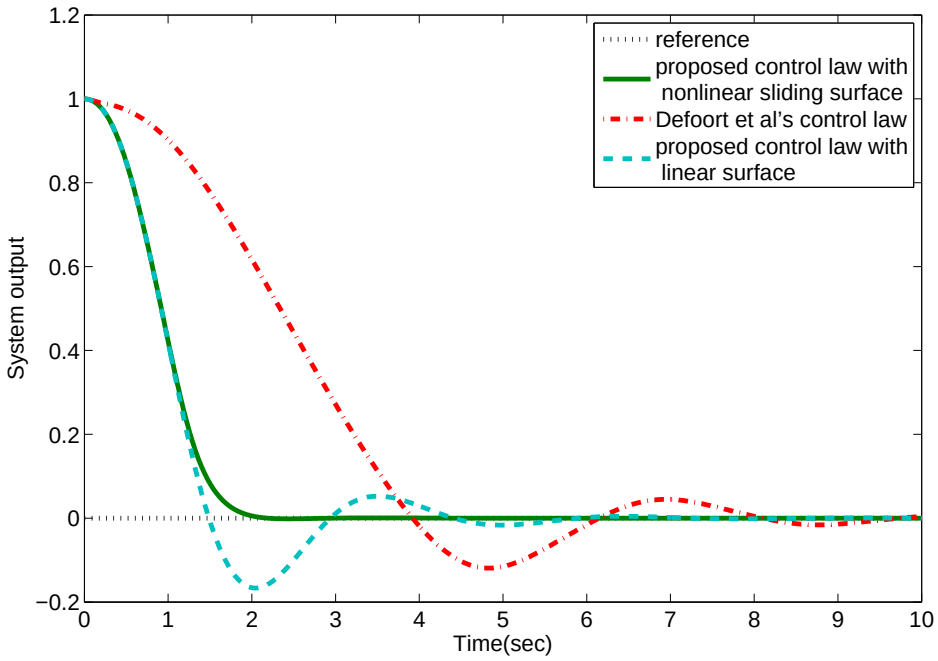

Figure 6.9: System outputs produced by the proposed adaptive SM controller and [4]

Table 6.3: Transient response indices and input performance for the triple integrator system

Type of Controller	Over -shoot (%)	Settling time (sec)	Total variation (TV)	Control energy
Defoort et al.'s method [4]	12	7.5	642.05	41.79
Proposed controller	0	2	35.61	41.07

6.3 Composite nonlinear feedback based discrete integral sliding mode controller

The use of digital computers and samplers in the control circuitry in the recent years has made the use of discrete time system representation more justifiable for controller design than continuous time representation. As such study and research on discrete sliding mode has received wide attention [57] [110] [111] [112] [113] [114]. To analyze the effect of sampling time, discrete time sliding mode control (DSMC) is well studied in the literature [7] [115] [116] [117] [118]. In this section, a nonlinear feedback based discrete integral sliding mode controller is proposed for uncertain systems with matched uncertainty.

The main idea behind the integral sliding mode (ISM) controller is to design the control law as a sum of a nominal control and a discontinuous control. Nominal control takes care of the nominal plant dynamics and the discontinuous ISM control rejects disturbances. Here the composite nonlinear feedback (CNF) controller, which is based on variable damping ratio, is used as the nominal controller to achieve good transient performance and the discrete integral sliding mode (ISM) controller is combined to ensure invariance against disturbances [114].

6.3.1 Discrete ISM controller for linear system with matched uncertainty

Let us consider a continuous time linear uncertain system as given below,

$$\begin{aligned} \dot{x} &= Ax + B(u + f_m(x,t)) \\ y &= Cx \end{aligned} \tag{6.45}$$

where $x \in R^n$ is the state vector, $u \in R^m$ is the control input and $y \in R^p$ is the output vector. The matrices A, B, C and dimensions n, m, p are known apriori. Furthermore, $f_m(x,t)$ is the matched uncertainty caused by unmodeled dynamics and external disturbance.

Let the above continuous system be sampled at τ samples per second, assuming that the disturbance is slowly varying. The discrete equivalent of the above plant (6.45) is then given by [119],

$$\begin{aligned} x(k+1) &= \phi_\tau x(k) + \Gamma_\tau u(k) + \tilde{d}(k) \\ y(k) &= Cx(k) \end{aligned} \tag{6.46}$$

where the matrices ϕ_τ, Γ_τ, C are of appropriate dimensions and $\tilde{d}(k)$ is the matched uncertainty. The above matrices are defined as follows [119],

$$\begin{aligned} \phi_\tau &= e^{A\tau} \\ \Gamma_\tau &= \int_0^\tau e^{At} B dt \\ \tilde{d}(k) &= \int_0^\tau e^{At} B f_m((k+1)\tau - t) dt \end{aligned} \tag{6.47}$$

For a smooth bounded disturbance $f_m(t)$ [7],

$$\begin{aligned} \tilde{d}(k) &= \int_0^\tau e^{At} B f_m((k+1)\tau - t) dt \\ &= \Gamma_\tau f_m(k) + \frac{1}{2}\Gamma_\tau v_m(k)\tau + O(\tau^3) \\ &= \Gamma_\tau d(k) \end{aligned} \tag{6.48}$$

where $d(k) = f_m(k) + \frac{1}{2}v_m(k)\tau$ and $O(\tau^3)$ is the error. Here $v_m(t) = \frac{d}{dt}f_m(t)$, $v_m(k) = v_m(k\tau)$. To see the details of the above expressions [7] can be referred to. It should be noted that the disturbance $d(k)$ is bounded and slowly varying, thus $0 \leq |d(k)| \leq d_m(k)$, where $d_m(k)$ is the maximum value of the bounded disturbance [7].

Using (6.48), (6.46) can be written as,

$$\begin{aligned} x(k+1) &= \phi_\tau x(k) + \Gamma_\tau u(k) + \Gamma_\tau d(k) \\ y(k) &= Cx(k) \end{aligned} \tag{6.49}$$

A discrete integral sliding surface $\sigma(k)$ is defined as follows [119]:

$$\sigma(k) = Gx(k) - Gx(0) + h(k) \tag{6.50}$$

where $\sigma(k) \in R^n$, $h(k) \in R^m$ and $x(0)$ is the initial condition of the system. The value of $G \in R^{m\times n}$ is to be chosen later [20].

Then $h(k)$ is calculated as,

$$h(k) = h(k-1) - (G\Gamma_\tau u_c(k-1) + G\phi_\tau x(k-1)) \tag{6.51}$$

where $\phi_\tau \in R^{n\times n}$, $\Gamma_\tau \in R^{n\times m}$ and $u_c(k)$ is the control signal. In the case of discrete ISM controller $u_c(k) = Kx(k)$, where K is the state feedback matrix designed by using pole placement technique. For discrete CNF-ISM controller, $u_c(k)$ will be designed by using CNF method to be explained in Subsection 6.3.2.

From (6.49), (6.50) and(6.51), the following is obtained,

$$\begin{aligned}\sigma(k+1) &= Gx(k+1) - Gx(0) + h(k+1) \\ &= G\phi_\tau x(k) + G\Gamma_\tau(u(k) + d(k)) - Gx(0) + h(k) - G\Gamma_\tau u_c(k) - G\phi_\tau x(k) \end{aligned} \tag{6.52}$$

where $u(k)$ is given by [119, 120],

$$u(k) = u_c(k) + u_{eq}(k) \tag{6.53}$$

Here $u_{eq}(k)$ is the equivalent control [119]. For designing $u_c(k)$, the procedure explained in Section 6.3 will be followed. Using the above relation (6.53) in (6.52) yields

$$\sigma(k+1) = G\Gamma_\tau u_{eq}(k) + G\Gamma_\tau d(k) + h(k) - Gx(0) \tag{6.54}$$

The equivalent control $u_{eq}(k)$ is found by solving $\sigma(k+1) = 0$ and is given by,

$$u_{eq}(k) = (G\Gamma_\tau)^{-1}(Gx(0) - G\Gamma_\tau d(k) - h(k)) \tag{6.55}$$

The above control law (6.55) is realizable if and only if $G\Gamma_\tau$ is a nonsingular square matrix so that its inverse $(G\Gamma_\tau)^{-1}$ exists.

The actual disturbance signal $d(k)$ can be estimated as the previous instant's disturbance signal ($\hat{d}(k) = d(k-1)$) if the disturbance is bounded and slowly varying [7]. Hence the estimated equivalent control $u_{eq}(k)$ law can be expressed as,

$$u_{eq}(k) = (G\Gamma_\tau)^{-1}(Gx(0) - G\Gamma_\tau \hat{d}(k) - h(k)) \tag{6.56}$$

Using (6.53) the discrete ISM controller is obtained as,

$$u(k) = u_c(k) + (G\Gamma_\tau)^{-1}(Gx(0) - G\Gamma_\tau \hat{d}(k) - h(k)) \tag{6.57}$$

Let us consider the sliding dynamics given by (6.52),

$$\sigma(k+1) = G\phi_\tau x(k) + G\Gamma_\tau(u(k) + d(k)) - Gx(0) + h(k) - G\Gamma_\tau u_c(k) - G\phi_\tau x(k) \tag{6.58}$$

Using $u(k) = u_c(k) + u_{eq}(k)$ in equation (6.58) yields

$$\sigma(k+1) = G\Gamma_\tau(u_{eq}(k) + d(k)) - Gx(0) + h(k) \tag{6.59}$$

Using (6.56) in (6.59) yields

$$\sigma(k+1) = G\Gamma_\tau d(k) - G\Gamma_\tau \hat{d}(k) = G\Gamma_\tau(d(k) - d(k-1)) = O(\tau^2) \tag{6.60}$$

The above equation (6.60) is based on [7,121] which establishes that the sliding surface is bounded by the rate of change of disturbance. Taking into account the availability of high speed Digital Signal Processing (DSP) tools and microcontrollers, the sampling time can be chosen to be suitably small which leads to very small boundary layer thickness [107]. The above equation (6.60) also describes the stability of the sliding surface as discrete ISM control keeps the sliding surface within the limit of $O(\tau^2)$ as mentioned in [7].

6.3.2 Composite nonlinear feedback (CNF) based controller design

Fig. 6.10 shows the block diagram of the proposed composite nonlinear feedback (CNF) based discrete integral sliding mode controller (ISM). The CNF controller is based upon the method proposed in [103,104,109,122]. The purpose of using the CNF controller is to track the reference input quickly without producing large overshoot. This has been made possible by combining a discrete linear feedback controller with small damping ratio and a nonlinear feedback controller. The nonlinear feedback law initially has zero gain and the gain increases when the system reaches closer to the reference input, thereby enhancing the damping of the system. Hence the controller guarantees low overshoot and faster rise. The overall CNF control law $u_c(k)$ can be expressed as,

$$u_c(k) = u_L(k) + u_N(k) \tag{6.61}$$

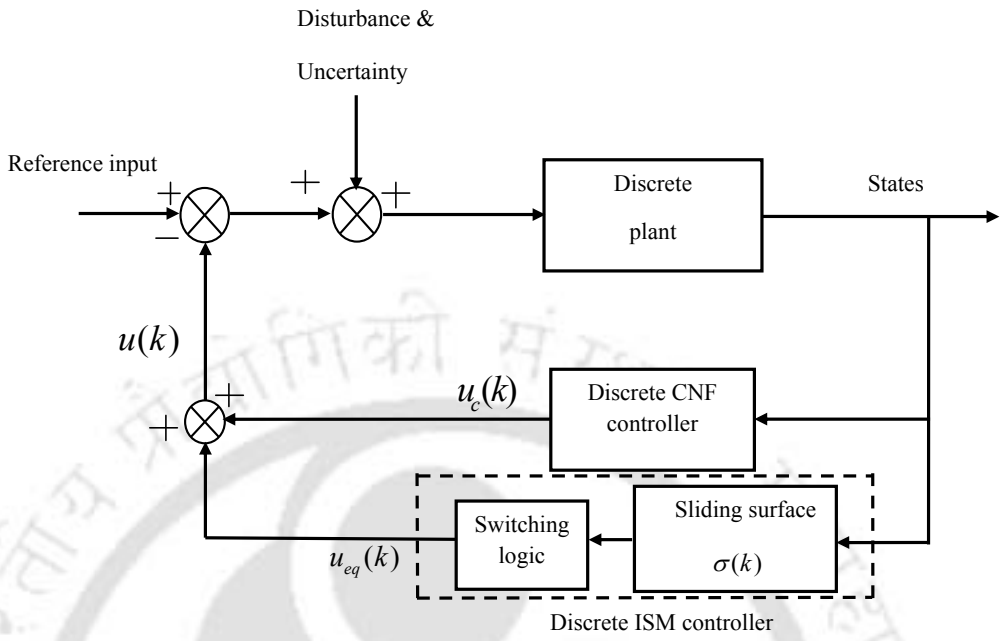

Figure 6.10: Block diagram of CNF based Discrete ISM controller

where $u_L(k)$ symbolizes the linear state feedback control and $u_N(k)$ is the nonlinear feedback law. The followings are the steps involved in the design of the composite controller:

- A linear state feedback control law is given by,

$$u_L(k) = Kx(k) + Lr \tag{6.62}$$

where r is the reference input and L is a matrix of an appropriate dimension [102]. The value of K is so chosen such that the overall closed loop system meets the specific design criterion. The damping ratio ξ and the settling time t_s define the specific location of the poles. Pole placement technique is used to find the state feedback gain matrix K [106,122]. In designing the CNF based ISM controller, $r = 0$ is assumed since the output is to be regulated at zero. Hence $u_L(k) = Kx(k)$.

- The nonlinear feedback law can be expressed as,

$$u_N(k) = \Upsilon(r, y)\Gamma_\tau^T P(\phi + \Gamma_\tau K)x(k) \tag{6.63}$$

where $\phi = \phi_\tau + \Gamma_\tau(G\Gamma_\tau)^{-1}G$ is obtained from the closed loop behavior of the overall system, to be explained in Subsection 6.3.3. Here, $\Upsilon(r, y)$ is a locally Lipschitz function in y having values

from zero to negative. Furthermore, $\Upsilon(r, y)$ is used to change the damping ratio of the closed loop system as the output approaches the reference input. Then $P > 0$ is the solution of the following Lyapunov equation,

$$P = (\phi + \Gamma_\tau K)^T P(\phi + \Gamma_\tau K) + R \tag{6.64}$$

where R is a positive definite matrix.

- The linear and nonlinear feedback control laws expressed in (6.62) and (6.63) can be combined to get the overall expression for the CNF controller as

$$u_c(k) = Kx(k) + \Upsilon(r, y)\Gamma_\tau^T P(\phi + \Gamma_\tau K)x(k) \tag{6.65}$$

Using (6.53), (6.56) and (6.65), the overall discrete CNF-ISM control law can be expressed as

$$u(k) = Kx(k) + \Upsilon(r, y)\Gamma_\tau^T P(\phi + \Gamma_\tau K)x(k) + (G\Gamma_\tau)^{-1}(Gx(0) - G\Gamma_\tau \hat{d}(k) - h(k)) \tag{6.66}$$

6.3.3 Closed loop behavior and stability of the overall system

Using (6.49), the discrete state equation can be written as,

$$x(k+1) = \phi_\tau x(k) + \Gamma_\tau u(k) + \Gamma_\tau d(k) \tag{6.67}$$

where $u(k) = u_c(k) + u_{eq}(k)$ is the overall control input.

Using (6.53) and (6.67) yields,

$$x(k+1) = \phi_\tau x(k) + \Gamma_\tau(u_c(k) + u_{eq}(k)) + \Gamma_\tau d(k) \tag{6.68}$$

Using (6.56), (6.68) can be expressed as,

$$\begin{aligned} x(k+1) &= \phi_\tau x(k) + \Gamma_\tau u_c(k) + \Gamma_\tau(d(k) - \hat{d}(k)) \\ &\quad + \Gamma_\tau(G\Gamma_\tau)^{-1}Gx(0) - \Gamma_\tau(G\Gamma_\tau)^{-1}h(k) \end{aligned} \tag{6.69}$$

Using (6.50) and (6.65), (6.69) can be expressed as,

$$\begin{aligned} x(k+1) &= \phi_\tau x(k) + \Gamma_\tau(Kx(k) + \Upsilon(r,y)\Gamma_\tau^T P(\phi + \Gamma_\tau K)x(k)) \\ &\quad +\Gamma_\tau(d(k) - \hat{d}(k)) - \Gamma_\tau(G\Gamma_\tau)^{-1}(\sigma(k) - Gx(k)) \end{aligned} \tag{6.70}$$

Using (6.60), $\sigma(k)$ is obtained as,

$$\sigma(k) = G\Gamma_\tau(d(k-1) - d(k-2)) \tag{6.71}$$

Using (6.71), (6.70) can be obtained as,

$$\begin{aligned} x(k+1) &= \phi_\tau x(k) + \Gamma_\tau(Kx(k) + \Upsilon(r,y)\Gamma_\tau^T P(\phi + \Gamma_\tau K)x(k)) \\ &\quad +\Gamma_\tau(d(k) - 2d(k-1) + d(k-2)) + \Gamma_\tau(G\Gamma_\tau)^{-1}Gx(k) \end{aligned} \tag{6.72}$$

Remark 6.2. *The proposed method uses the bound of the variation/difference of the disturbance, $d(k-1)-d(k-2)$ where $k = 0, 1, 2, , , ,$. It is clear that disturbance decreases as the sampling frequency increases. The magnitude of the ultimate bound of the state $x(k)$ can be made very small if the disturbance $d(k)$ varies slowly or the sampling period is set very short and hence more accurate results can be obtained.*

Remark 6.3. *Here $\Upsilon(r,y)$ is a nonlinear function which has values varying from zero to a high negative value. Initially it is assumed that $\Upsilon(r,y) = 0$, which later assumes a high negative value.*

When $\Upsilon(r,y) = 0$ is considered, (6.72) becomes,

$$x(k+1) = (\phi_\tau + \Gamma_\tau(G\Gamma_\tau)^{-1}G + \Gamma_\tau K)x(k) + \Gamma_\tau[d(k) - 2d(k-1) + d(k-2)] \tag{6.73}$$

Thus the boundary layer thickness is given by [7],

$$O(\tau^3) = \Gamma_\tau[d(k) - 2d(k-1) + d(k-2)] \tag{6.74}$$

From (6.73 - 6.74) it can be observed that $x(k)$ will stay in the neighborhood of the reference state within a boundary of $O(\tau^3)$ [7]. It is noteworthy that by using the discrete integral sliding mode controller, disturbance can be better compensated with smaller steady state boundary and higher accuracy.

Let us assume that $d(k)$ is bounded as given by $-M \leq \Gamma_\tau[d(k) - 2d(k-1) + d(k-2)] = w(k) \leq M$

with $0 < M < \infty$.

Then the closed loop dynamics (6.73) can be expressed as,

$$x(k+1) = (\phi_\tau + \Gamma_\tau(G\Gamma_\tau)^{-1}G + \Gamma_\tau K)x(k) + w(k) \tag{6.75}$$

Accordingly

$$\begin{aligned} x^T(k)[x(k+1) - x(k)] &= x^T(k)(\phi_\tau + \Gamma_\tau(G\Gamma_\tau)^{-1}G + \Gamma_\tau K - I)x(k) + x^T(k)w(k) \\ &\leq \rho_{max}x^T(k)x(k) + ||x^T(k)w(k)|| \\ &\leq \rho_{max}||x(k)||^2 + ||x^T(k)M|| \end{aligned} \tag{6.76}$$

where ρ_{max} represents the largest negative eigenvalue of the square matrix $(\phi_\tau + \Gamma_\tau(G\Gamma_\tau)^{-1}G + \Gamma_\tau K - I)$. In order to achieve better stability of the closed loop system, larger the M value, more negative ρ_{max} must be and the condition to be satisfied by M and ρ_{max} is $||M|| \leq ||\rho_{max}||$ [119].

6.3.4 Simulation Results

In this section, two examples are illustrated to show the effectiveness of the proposed discrete CNF-ISM controller. At first, a linear single input single output (SISO) sytem with matched uncertainty [119] is considered. Then, a linear multi-input multi-output (MIMO) system with matched uncertainty is illustrated [7]. Both these examples are simulated on the MATLAB-Simulink platform by using the fixed step discrete solver.

6.3.4.1 Single input single output (SISO) system

Let us consider a SISO system with matched uncertainty as given in [119],

$$\begin{aligned} \dot{x} &= Ax + Bu + Bf_m(x,t) \\ y &= Cx \end{aligned} \tag{6.77}$$

where

$$A = \begin{bmatrix} 10 & 15 & 13 \\ -20 & -10 & 17 \\ 0 & 15 & 15 \end{bmatrix}, B = \begin{bmatrix} 0 \\ -3 \\ 5 \end{bmatrix}, C = \begin{bmatrix} 1 & 0 & 0 \end{bmatrix} \tag{6.78}$$

The matched uncertainty is considered as $f_m(x,t) = 0.3sin(2\pi t)$ [119]. It is assumed that the

initial state is $x(0) = [-1 \quad 1 \quad 1]^T$. The system is sampled with a sampling time $\tau = 0.01$ sec. The discretized model (6.49) of the above plant can then be expressed as [119],

$$\begin{aligned} x(k+1) &= \phi_\tau x(k) + \Gamma_\tau u(k) + \Gamma_\tau d(k) \\ y(k) &= Cx(k) \end{aligned} \tag{6.79}$$

where

$$\phi_\tau = \begin{bmatrix} 1.0890 & 0.1604 & 0.1606 \\ -0.2002 & -0.9022 & 0.1609 \\ -0.0158 & 0.1541 & 1.1748 \end{bmatrix}, \Gamma_\tau = \begin{bmatrix} 0.0014 \\ -0.0244 \\ 0.0519 \end{bmatrix} \tag{6.80}$$

The discretized disturbance $d(k)$ has the following expression,

$$d(k) = 0.3sin(0.02\pi k) + 0.009cos(0.02\pi k) \tag{6.81}$$

The objective is to design a discrete CNF-ISM controller for the system (6.79 - 6.80) to stabilize the system at zero quickly without any overshoot.

The design procedure is described below:

The damping ratio ξ should be so chosen such that the overshoot lies within 20% acceptable norm [106]. For the above example, the value of ξ is chosen as 0.57 and accordingly the settling time t_s is obtained as 0.42 sec as the natural frequency of the system ω_n is known apriori as 16.8rad/sec. Correspondingly the discrete dominant poles of the system are placed at $0.9000 - 0.1250i, 0.9000 + 0.1250i$ and the other pole exists far from the dominant poles, at 0.1. Using pole placement technique, the value of the state feedback gain matrix K is obtained as,

$$K = -[9.9668 \quad 11.5170 \quad 48.8051] \tag{6.82}$$

For designing the nonlinear part for the CNF controller, the nonlinear function is chosen as,

$$\Upsilon(r, y) = -\varrho e^{-\psi y^2} \tag{6.83}$$

Here $\Upsilon(r, y)$ is not a function of r because the reference input r is assumed as zero, since the output is to be regulated at zero. For the above example, $\varrho = 20.50$ and $\psi = 9$ are chosen. Lyapunov equation (6.64) is solved to obtain

$$P = \begin{bmatrix} 426.0891 & 116.4046 & 93.5674 \\ 116.4046 & 129.6438 & 90.8654 \\ 93.5674 & 90.8654 & 79.2154 \end{bmatrix} \text{ using } \mathrm{R} = \begin{bmatrix} 10.00 & 0.000 & 0.000 \\ 0.000 & 10.00 & 0.000 \\ 0.000 & 0.000 & 10.00 \end{bmatrix} \quad (6.84)$$

So, the composite nonlinear feedback (CNF) controller (6.65) designed for the above system yields the following control law,

$$u_c(k) = -[9.9668 \quad 11.5170 \quad 48.8051]x(k) + \Upsilon(r,y)[1.8311 \quad 1.0123 \quad 0.8646]x(k) \quad (6.85)$$

For designing the equivalent control of the integral sliding mode controller (i.e.$u_{eq}(k)$), G is chosen as [20],

$$G = (\Gamma_\tau^T \Gamma_\tau)^{-1} \Gamma_\tau^T \quad (6.86)$$

Using (6.80) and (6.86) yields,

$$G = [0.4254 \quad -7.4143 \quad 15.7706] \quad (6.87)$$

Using (6.80) and (6.87), the equivalent control law (6.56) is found as,

$$u_{eq}(k) = -\hat{d}(k) - h(k) + [0.4254 \quad -7.4143 \quad 15.7706]x(0) \quad (6.88)$$

The overall control law of the proposed discrete CNF-ISM controller (6.66) can be expressed as,

$$\begin{aligned} u(k) = & -[9.9668 \quad 11.5170 \quad 48.8051]x(k) + \Upsilon(r,y)[1.8311 \quad 1.0123 \quad 0.8646]x(k) \\ & -\hat{d}(k) - h(k) + [0.4254 \quad -7.4143 \quad 15.7706]x(0) \end{aligned} \quad (6.89)$$

Fig. 6.11 shows the state x_1 obtained by using the proposed discrete CNF-ISM control scheme for the SISO system given by (6.79 - 6.80) and is compared with the results obtained by using the discrete ISM controller (6.57). It is noticed that the proposed discrete CNF-ISM control scheme achieves superior performance having zero overshoot and lower settling time. However, the rise time is almost the same in both the cases.

Figs. 6.12 - 6.13 show the states x_2 and x_3 obtained by using the proposed discrete CNF-ISM controller as well as the discrete ISM controller (6.57). It is observed that with the proposed discrete CNF-ISM controller, the closed loop system settles more quickly with no overshoot as compared against the discrete ISM controller.

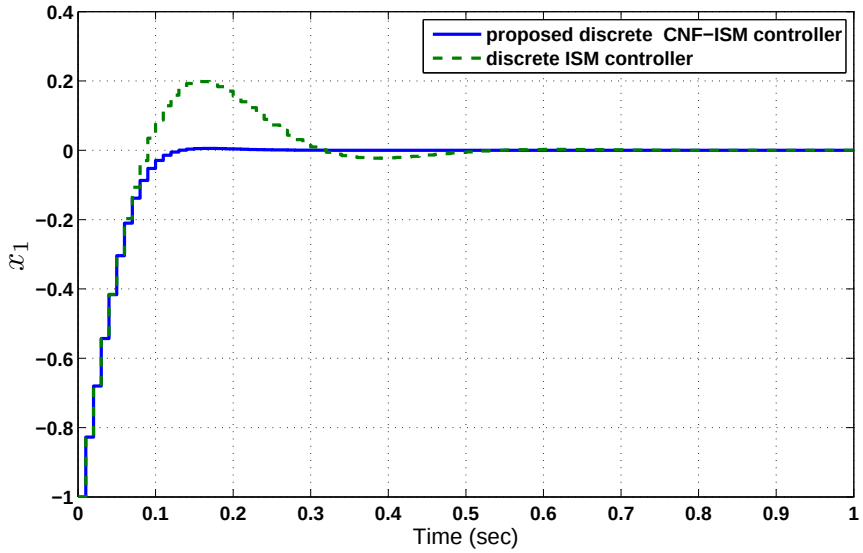

Figure 6.11: System state x_1 ; solid line with proposed discrete CNF-ISM controller and broken line with discrete ISM controller

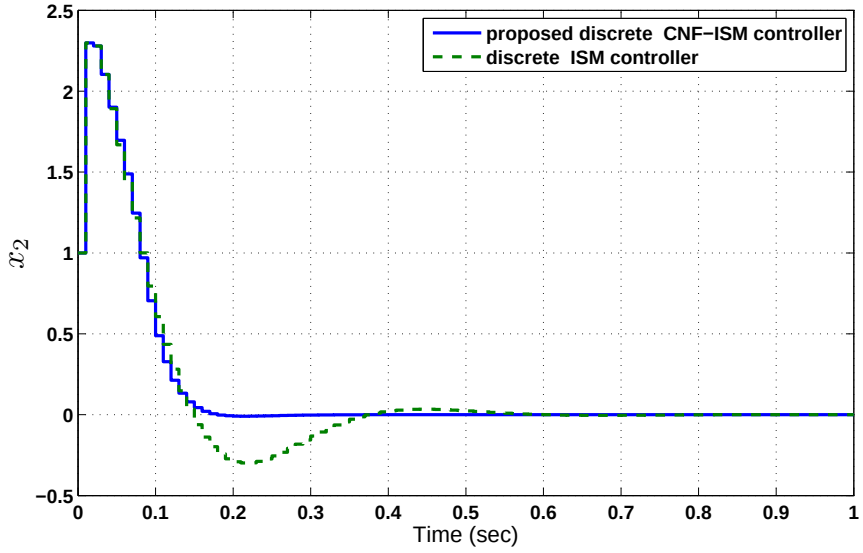

Figure 6.12: System state x_2 ; solid line with proposed discrete CNF-ISM controller and broken line with discrete ISM Controller

Fig. 6.14 compares the the control inputs obtained for the proposed discrete CNF-ISM controller against the discrete ISM controller (6.57). The energy norm of the input for the proposed discrete CNF-ISM controller is 43.65 and that of the discrete ISM controller is 43.44. The proposed discrete CNF-ISM controller uses 0.5% more energy in comparison to the discrete ISM controller.

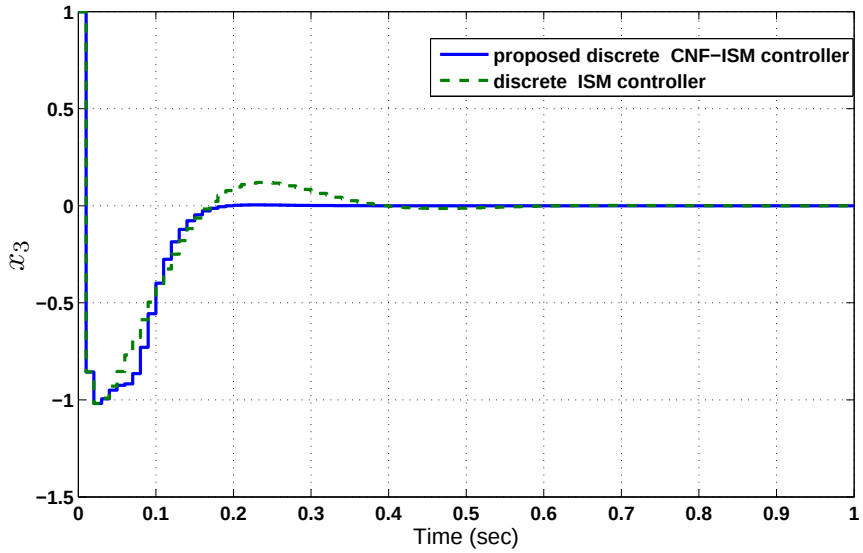

Figure 6.13: System state x_3 ; solid line with proposed discrete CNF-ISM controller and broken line with discrete ISM Controller

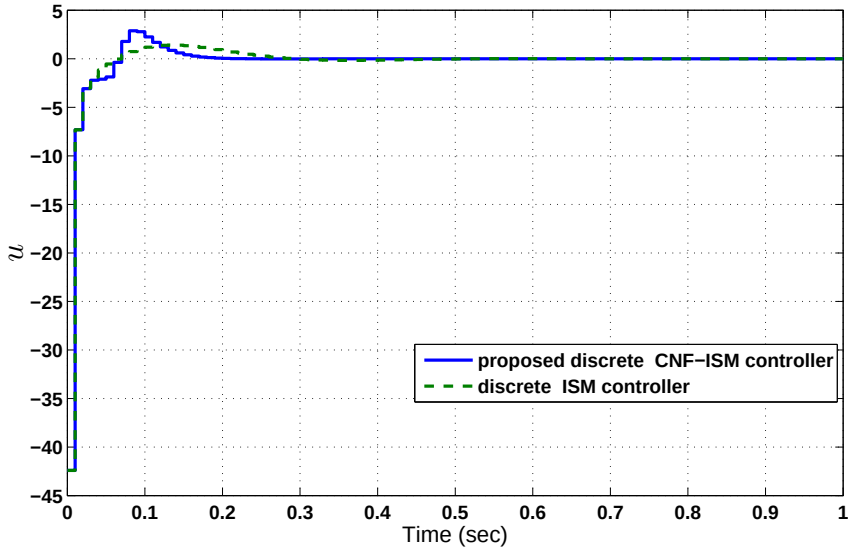

Figure 6.14: Control input for the closed loop system; solid line with proposed discrete CNF-ISM controller and broken line with discrete ISM controller

6.3.4.2 Comparison of the proposed discrete CNF-ISM controller with different discrete ISM controllers

The output responses obtained by using the proposed discrete CNF-ISM controller as well as different discrete ISM controllers designed by varying the damping ratio ξ and the settling time t_s are shown in Fig. 6.15. The proposed discrete CNF-ISM controller shows superior performance with zero

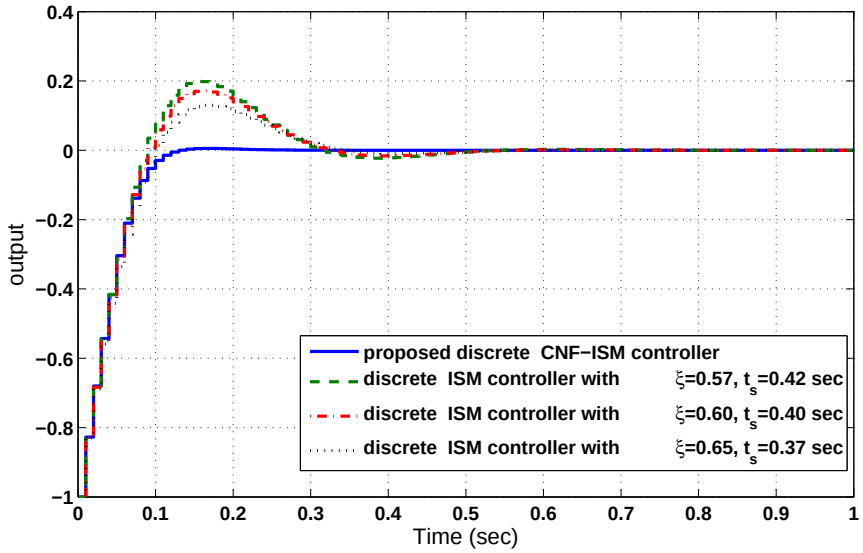

Figure 6.15: System output for the closed loop system for different values of ξ and t_s , solid line with proposed discrete CNF-ISM controller and broken line with discrete ISM controller

overshoot and lower settling time as compared to the discrete ISM controllers. Detailed comparison of these controllers as regards the transient performance is summarized in Table 6.4. It is noticed from Table 6.4 that the proposed discrete CNF-ISM controller produces significant reduction in the peak overshoot and settling time over those in the case of the discrete ISM controllers. As noticed in Fig.6.14, the control effort in the proposed discrete CNF-ISM controller is slightly higher than that in the discrete ISM controller. Hence, a trade-off between the level of transient performance and amount of control effort will have to be chosen in practical design considerations.

Table 6.4: Transient response indices for different values of ξ and t_s

Damping Ratio(ξ) **and Settling Time** ($t_s(sec)$)	**Peak Overshoot** (%)	**Settling Time (sec)**
Discrete ISM controller with $\xi = 0.57$, t_s=0.42	20	0.42
Discrete ISM controller with $\xi = 0.60$, t_s=0.40	17	0.37
Discrete ISM controller with $\xi = 0.65$, t_s=0.37	13	0.34
Proposed discrete CNF-ISM controller	1	0.12

6.3.4.3 Multiple-input multiple-output (MIMO) system

Let us consider a MIMO system with matched uncertainty given in [7] described below,

$$\dot{x} = Ax + B(u + f_m(x,t)) \tag{6.90}$$

where

$$A = \begin{bmatrix} 1 & -2 & 3 \\ -4 & 5 & -6 \\ 7 & -8 & 9 \end{bmatrix}, B = \begin{bmatrix} 1 & -2 \\ -3 & 4 \\ 5 & 6 \end{bmatrix}, f_m(x,t) = \begin{bmatrix} 0.3sin(4\pi t) \\ 0.3cos(4\pi t) \end{bmatrix} \tag{6.91}$$

The initial state is at $x(0) = [1 \quad 1 \quad -1]^T$. The system is sampled at a time interval of $\tau = 0.001$ sec. A suitable nonlinear function $\Upsilon(r, y)$ is used that has a very low value at the initial stage and has a relatively higher value when the system approaches its final state [109]. Here the chosen nonlinear function is,

$$\Upsilon(r, y) = -57.3871e^{-8y^2} \tag{6.92}$$

For a system, overshoot less than 20% is acceptable [102, 106] and hence the poles are selected by choosing the damping ratio $\xi = 0.7$ and accordingly the settling time t_s is 0.5 sec. Accordingly, the dominant poles are found as 0.9510+0.1520i and 0.9510-0.1520i while the other pole is placed far away at 0.1 [123]. Using pole placement technique, the state feedback gain matrix can be calculated as,

$$K = \begin{bmatrix} 769.1649 & 42.8508 & 126.9456 \\ 129.9735 & 312.7895 & 108.7556 \end{bmatrix} \tag{6.93}$$

In order to find the the CNF control law from (6.65), Lyapunov equation (6.64)is solved to obtain

$$P = \begin{bmatrix} 397.5233 & 167.4345 & 20.2155 \\ 167.4345 & 70.7267 & 8.0097 \\ 20.2155 & 8.0097 & 4.1436 \end{bmatrix} \quad \text{using} \quad \mathrm{R} = \begin{bmatrix} 0.100 & 0.000 & 0.000 \\ 0.000 & 0.100 & 0.000 \\ 0.000 & 0.000 & 0.100 \end{bmatrix} \tag{6.94}$$

The Matrix G is chosen as [7],

$$G = \begin{bmatrix} 0.2621 & -0.3108 & -0.0385 \\ 3.4268 & 2.4432 & 1.1787 \end{bmatrix} \tag{6.95}$$

Fig.6.16 shows the state x_1 obtained by using the proposed discrete CNF-ISM controller and is compared with that obtained by using the discrete ISM control scheme by Abidi et al. [7]. It shows clearly that both the rise time and the settling time can be minimized simultaneously by using the proposed discrete CNF-ISM controller. Transient performance indices evaluated by using both these controllers are compared in Table 6.5. It is noted from Table 6.5 that the proposed controller shows superior transient performance by reducing the rise time and settling time by about 63% from those

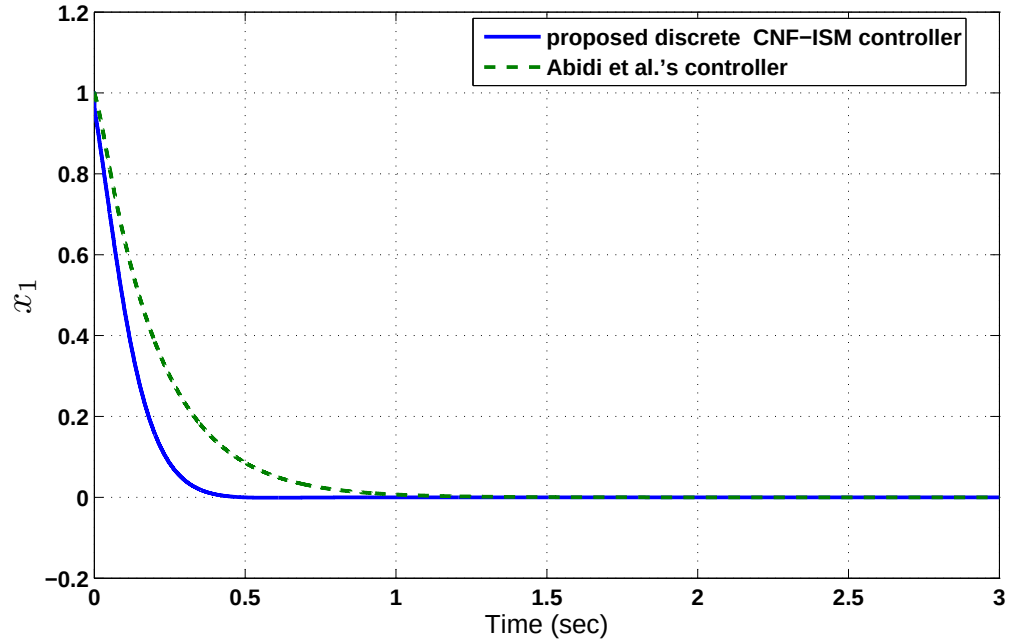

Figure 6.16: System state x_1 ; solid line with proposed discrete CNF-ISM method and broken line with Abidi et al.'s method [7]

obtained by using the discrete ISM controller of Abidi et al. [7].

Table 6.5: Transient performance comparison

Type of Controller	**Rise Time (sec)**	**Peak Overshoot (%)**	**Settling Time (sec)**
Discrete ISM controller (Abidi et al.) [7]	0.48	0.0	0.80
Proposed discrete CNF-ISM controller	0.23	0.0	0.35

Figs. 6.17 - 6.18 show the control inputs u_1, u_2 obtained by using the proposed discrete CNF-ISM controller and those obtained by using the discrete ISM controller proposed by Abidi et al. [7]. The energy norms of the input for the proposed discrete CNF-ISM controller and Abidi et al.'s discrete ISM controller are 205.17 and 203.76 respectively. The proposed discrete CNF-ISM controller uses 0.7% more energy in comparison to the controller proposed by Abidi et al. [7]. However, the proposed discrete CNF-ISM controller driven closed loop system settles at 0.35 sec whereas with Abidi et al.'s controller, the settling time is 0.8 sec.

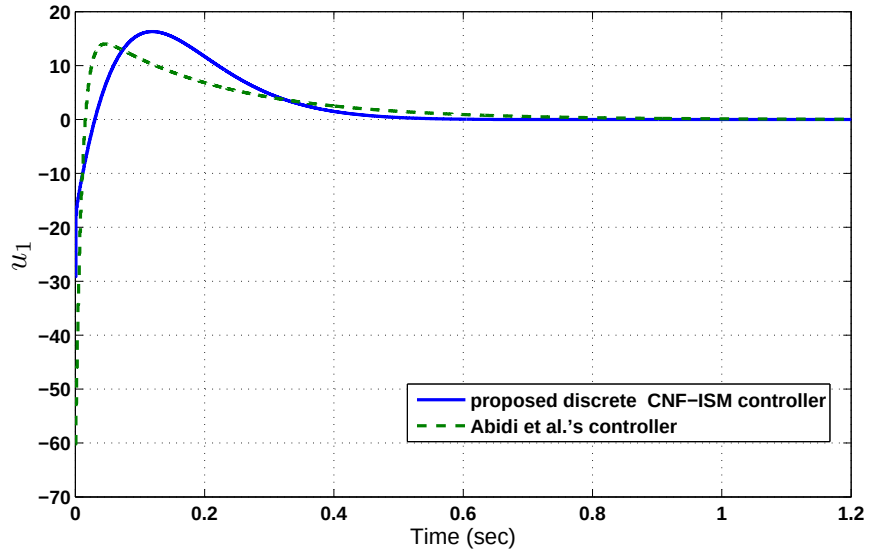

Figure 6.17: Control law u_1 ; solid line with proposed discrete CNF-ISM method and broken line with Abidi et al.'s method [7]

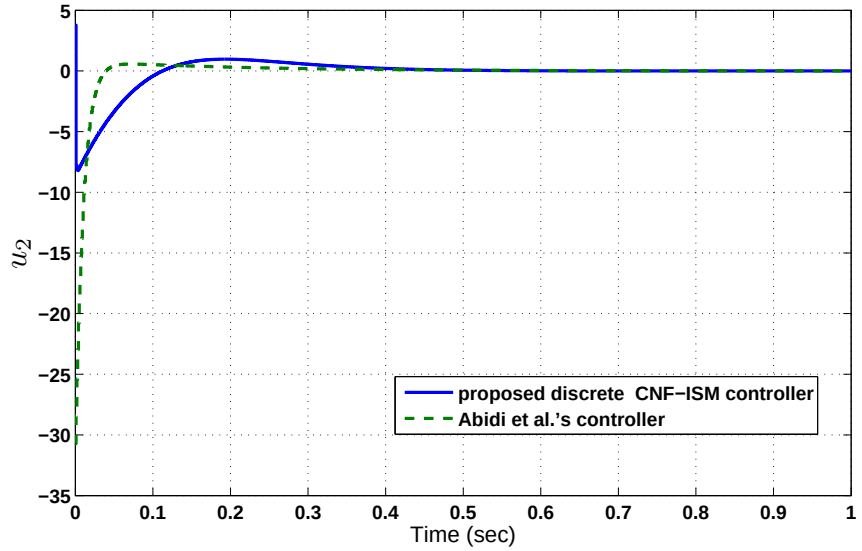

Figure 6.18: Control law u_2 ; solid line with proposed discrete CNF-ISM method and broken line with Abidi et al.'s method [7]

6.4 Summary

In this chapter, an adaptive chattering free sliding mode (SM) controller based on nonlinear sliding surface is proposed to enhance the transient performance of uncertain systems. An adaptive tuning rule is developed to measure the unknown bounded uncertainty. The upper bound of the uncertainty

is required to be known in most of the sliding mode controllers, whereas the proposed method adaptively estimates the uncertainty. The nonlinear sliding surface introduces a variable damping ratio which adapts its value in accordance with the system response to ensure quicker settling time and lesser overshoot. A major benefit offered by the proposed controller is the reduction of chattering in the control input. Simulation results show that the proposed adaptive SM controller provides smooth control action, can converge fast and has low sensitivity to parameter variations. Next, a composite nonlinear feedback (CNF) based integral sliding mode (ISM) controller for uncertain systems is proposed in the discrete domain. The developed controller has the property of integral sliding mode that has invariance against uncertainty in the whole operating range. The proposed controller uses a state feedback law which has a low value of damping ratio initially thereby ensuring a fast response. The nonlinear control law used in the controller enhances the damping ratio as the system response approaches the reference input. The increased damping ratio guarantees faster settling time and lesser overshoot while maintaining the stability of the closed loop system. The illustrative examples demonstrate the effectiveness of the proposed controller for both single input single output (SISO) and multi-input multi-output (MIMO) uncertain systems.

7

Conclusions and Scope for Future Work

Contents

7.1 Conclusions

This thesis attempts to design sliding mode controllers for uncertain systems having both matched and mismatched types of uncertainty. In conventional first order sliding mode controllers, chattering in the control input is the major disadvantage. Of late, second and higher order sliding mode controllers have evolved promising better chattering mitigation. This thesis attempts to design chattering free sliding mode (SM) controllers to overcome the shortcomings of conventional first order sliding mode controllers. The basic philosophy of the proposed control scheme is that instead of the normal control input, its time derivative is used for designing the controller. The discontinuous sign function is contained in the derivative control and the actual control is obtained by integrating the discontinuous sign function and hence it is continuous and smooth. This strategy is the core idea which is followed in this thesis to develop sliding mode controllers of different types. Another limitation of the conventional sliding mode controllers is the design prerequisite of knowing the upper bound of the system uncertainty apriori which is practically difficult to realize. The proposed controller attempts to overcome this difficulty by using an adaptive gain tuning methodology.

An adaptive integral sliding mode controller using chattering free sliding mode technique is proposed in this thesis. Reaching phase is totally eliminated in the integral sliding mode and hence the system becomes invariant towards the matching uncertainty right from the beginning. Application of the proposed controller to both stabilization and tracking problems of single input single output (SISO) system demonstrates the efficacy of the proposed control strategy.

An adaptive chattering free sliding mode control scheme is proposed for a class of dynamic systems with matched and mismatched perturbations. The controller is used to stabilize the twin rotor MIMO system (TRMS) in significant cross-couplings to reach a desired position and accurately track a specified trajectory. The TRMS model is divided into a horizontal and a vertical subsystem. The cross-coupling existing between the two subsystems is considered as the system uncertainty. The major advantage offered by this adaptive sliding mode controller is that advance knowledge about the upper bound of the system uncertainty is not a necessary requirement and the control input is smooth. The problem of controlling of a vertical take-off and landing (VTOL) aircraft system affected by both types of uncertainties, matched and mismatched, is also addressed by applying the proposed control scheme. A proportional plus integral sliding surface is used in the proposed control technique. An adaptive gain tuning mechanism is used to ensure that the switching gain is not overestimated with respect to

the actual unknown value of the uncertainty.

Experimental studies conducted on the laboratory set-up of 1 degree of freedom VTOL system validate the efficacy of the proposed controller.

An adaptive terminal sliding mode (TSM) controller is proposed where the nonsingular terminal sliding manifold guarantees fast and finite time convergence. The proposed adaptive TSM controller is successfully applied for stabilization of a triple integrator system affected by uncertainty. Trajectory tracking of a two-link robotic manipulator which is a nonlinear system with mismatched uncertainty is considered which demonstrates the efficiency of the proposed control strategy.

A nonlinear sliding surface based chattering free adaptive sliding mode controller is proposed to improve the transient performance of an uncertain system. The basic philosophy of the proposed scheme is that using a nonlinear sliding surface, the damping ratio of a system can be changed from its initial low value to a final high value. The initial low value of damping ratio results in a quick response and the later high damping avoids overshoot. To improve the transient performance in discrete time uncertain systems, an integral sliding mode is used with composite nonlinear feedback (CNF).

The control strategies developed in this thesis using the chattering free adaptive sliding mode show robust performance even in presence of matched and mismatched uncertainties. The controllers developed ensure high transient performance while preserving the robustness property of conventional sliding mode controllers but successfully overcoming their inherent chattering disadvantage. As such, the proposed control strategies promise high application potential in many important fields like electric drives, robotics, power electronics, servo applications and aerospace where performance needs to be guaranteed consistently despite being challenged by an uncertain environment.

7.2 Scope for future work

Future possible directions of research based on the design methods developed in this thesis are outlined below:

- A natural extension of this work may be to design discrete sliding mode algorithms with adaptive techniques which will enhance the flexibility in implementation. Now-a-days, a large class of continuous systems are controlled by digital signal processors (DSPs) and high end micro controllers. Hence discrete SM controller will be easier and effective from implementation point of view.

- Another possible extension of this work may be the incorporation of an optimal sliding mode controller to optimize the control effort.
- Nonlinear sliding surface based adaptive sliding mode controller may be extended to improve the transient performance of general references, such as sinusoidal and other periodic signals.
- The proposed design method may be extended by using intelligent controllers based on fuzzy logic and neural network to incorporate flexibility and intelligence.
- The extension of these techniques with constraints on system states is also an avenue worth exploring.
- The high performance requirement of many practical applications like electric drives, electro-pneumatics, power system stabilizers and robotics may be addressed by using the proposed techniques.

A

Appendix

Contents

A.1 Modeling of 1 DOF VTOL Aircraft System

The free body diagram of a 1-DOF VTOL aircraft system that pivots about the pitch axis is shown in Fig. A.1.

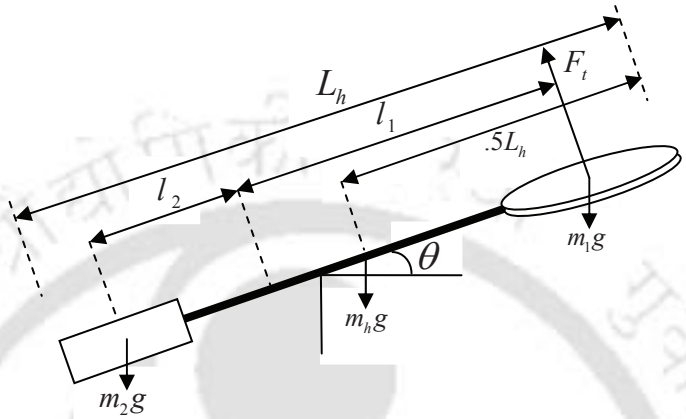

Figure A.1: Free body diagram of 1 DOF VTOL aircraft system

where,

m_1 = propeller mass,
m_2 = counterweight mass,
m_h = VTOL body mass,
l_1 = length from pivot to propeller center,
l_2 = length from pivot to center of counterweight mass,
L_h = total length of VTOL body.
θ = pitch angle

Torque (τ) equation for the VTOL rigid body is given by,

$$\tau + m_2 g \cos(\theta(t)) l_2 - m_1 g \cos(\theta(t)) l_1 - \frac{1}{2} m_h g \cos(\theta(t)) L_h = 0 \tag{A.1.1}$$

Current-torque relationship is given by,

$$\tau = k_t i_m \tag{A.1.2}$$

where k_t is the current-torque constant. So with respect to current, the torque equation can be written as,

$$k_t i_m + m_2 g \cos(\theta(t)) l_2 - m_1 g \cos(\theta(t)) l_1 - \frac{1}{2} m_h g \cos(\theta(t)) L_h = 0 \tag{A.1.3}$$

In equilibrium condition i.e. when $\theta = 0$, i_m becomes i_{eq} and torque equation becomes,

$$k_t i_{eq} + m_2 g l_2 - m_1 g l_1 - \frac{1}{2} m_h g L_h = 0 \tag{A.1.4}$$

Angular (pitch) motion with respect to thrust torque τ is given by,

$$j\ddot{\theta}(t) + b_v\dot{\theta}(t) + k\theta(t) = \tau = k_t i_m \tag{A.1.5}$$

Here b_v is the viscous damping, k is the stiffness and j is the equivalent moment of inertia acting about the pitch axis, which is given by,

$$j = \sum_{i=1}^{n} m_i r_i^2 \tag{A.1.6}$$

where for object i, m_i is its mass and r_i is the perpendicular distance between the axis of rotation and the object. So the transfer function for the VTOL system can be obtained as,

$$G(s) = \frac{\theta(s)}{I_m(s)} = \frac{\frac{k_t}{j}}{s^2 + \frac{b_v s}{j} + \frac{k}{j}} \tag{A.1.7}$$

By comparing the denominator of (A.1.7) with the characteristic equation of a second order system,

$$s^2 + 2\zeta\omega_n s + \omega_n^2 \tag{A.1.8}$$

the damping ratio ζ and natural frequency ω_n can be easily found out.

Voltage-current equation for the VTOL motor is given by,

$$v_m(t) = R_m i_m(t) + L_m \dot{i}_m(t) \tag{A.1.9}$$

where R_m is the motor resistance and L_m is the motor inductance. So the transfer function of the VTOL motor is obtained as,

$$\frac{I_m(s)}{V_m(s)} = \frac{1}{R_m + L_m s} \tag{A.1.10}$$

The output-input relationship of the VTOL needs to be obtained as position-voltage relationship

which is given by,

$$\begin{aligned}\frac{\theta(s)}{V_m(s)} &= \frac{I_m(s)}{V_m(s)} \times \frac{\theta(s)}{I_m(s)} = \frac{1}{R_m + L_m s} \times \frac{\frac{k_t}{j}}{s^2 + \frac{b_v s}{j} + \frac{k}{j}} \\ &= \frac{1}{L_m \times (R_m/L_m + s)} \times \frac{\frac{k_t}{j}}{s^2 + \frac{b_v s}{j} + \frac{k}{j}} \end{aligned} \tag{A.1.11}$$

The value of the VTOL motor inductance (L_m) is very small practically, so the pole contributed by $(R_m/L_m + s)$ is located far away from the dominant poles of the system and can be neglected. Therefore the overall transfer function (A.1.11) can be approximated by,

$$\frac{\theta(s)}{V_m(s)} = \frac{1}{L_m} \times \frac{\frac{k_t}{j}}{s^2 + \frac{b_v s}{j} + \frac{k}{j}} \tag{A.1.12}$$

The state space model of the above system is described by,

$$\begin{bmatrix} \dot{x}_1 \\ \dot{x}_2 \end{bmatrix} = \begin{bmatrix} 0 & 1 \\ -\frac{k}{j} & -\frac{b_v}{j} \end{bmatrix} \begin{bmatrix} x_1 \\ x_2 \end{bmatrix} + \begin{bmatrix} 0 \\ \frac{k_t}{jL_m} \end{bmatrix} u \tag{A.1.13}$$

$$y = \begin{bmatrix} 1 & 0 \end{bmatrix} \begin{bmatrix} x_1 \\ x_2 \end{bmatrix} \tag{A.1.14}$$

where x_1 is the pitch angle and x_2 is the angular velocity.

References

[1] C. W. Tao, J. S. Taur, and Y. C. Chen, "Design of a parallel distributed fuzzy lqrc ontroller for the twin rotor multi-inputmulti-output system," *Fuzzy Sets and Systems*, vol. 161, pp. 2081–2103, 2010.

[2] Y. J. Huang, T. C. Kuo, and H. K. Way, "Robust vertical takeoff and landing aircraft control via integral sliding mode," *IEE Procedings Control Theory Application*, vol. 150, (4), pp. 383–388, 2003.

[3] C. C. Wen and C. C. Cheng, "Design of sliding surface for mismatched uncertain systems to achieve asymptotical stability," *Journal of the Franklin Institute*, vol. 345, pp. 926–941, 2008.

[4] M. Defoort, F. Nollet, T. Floquet, and W. Perruquetti, "A third-order sliding-mode controller for a stepper motor," *IEEE Transactions on Industrial Electronics*, vol. 56, (9), pp. 3337 – 3346, 2009.

[5] Y. Feng, X. Yu, and Z. Man, "Non-singular terminal sliding mode control of rigid manipulators," *Automatica*, vol. 38, pp. 2159 –2167, 2002.

[6] D. Fulwani, B. Bandyopadhyay, and L. Fridman, "Non-linear sliding surface: towards high performance robust control," *IET Control Theory and Applications*, vol. 6(2), pp. 235–242, 2012.

[7] K. Abidi, J.-X. Xu, and Y. Xinghuo, "On the discrete-time integral sliding-mode control," *IEEE Transactions on Automatic Control*, vol. 52, (4), pp. 709–715, 2007.

[8] C. W. Tao, J. S. Taur, Y. H. Chang, and C. W. Chang, "A novel fuzzy-sliding and fuzzy-integral-sliding controller for the twin-rotor multi-input multi-output system," *IEEE Transactions on Fuzzy Systems*, vol. 18, (5), pp. 893–905, 2010.

[9] K. J. Astrom and B. Wittenmark, *Computer-Controlled Systems, Theory and Design*. Prentice-Hall, 1990.

[10] E. F. Camacho and C. Bordons, *Model Predictive Control*. Springer, 2004.

[11] F. Ikhouane and M. Krstic, "Robustness of the tuning functions adaptive backstepping design for linear systems," *IEEE Transactions on Automatic Control*, vol. 43(3), pp. 431–437, 1998.

[12] W. Perruquetti and J. P. Barbot, *Sliding mode control in Engineering, Automation and Control Series*. Marcel Dekker Inc., New York (USA), 2002.

[13] H. K. Khalil, *Nonlinear Systems, Third Edition.* Prentice Hall, 2002.

[14] S. V. Emelyanov, "Variable structure control systems," *Nauka*, vol. 35, pp. 120–125, 1967.

[15] V. I. Utkin, "Variable structure systems with sliding modes," *IEEE Transactions on Automatic Control*, vol. 22 (2), pp. 212–222, 1977.

[16] J. Y. Hang, W. Gao, and J. C. Hung, "Variable structure control: A survey," *IEEE Transactions on Industrial Electronics*, vol. 40, (1), pp. 2 – 22, 1993.

[17] K. K. Young, *Variable Structure Control for Robotics and Aerospace Systems.* Elsevier, Amsterdam, The Netherlands, 1993.

[18] U. Itkis, *Control systems of variable structure.* Wiley, New York, 1976.

[19] V. I. Utkin and J. Shi, "Integral sliding mode in systems operating under uncertainty conditions," in *Proceedings of the 35th IEEE conference on decision and control, pp. 4591-4596*, 1996.

[20] F. Castanos and L. Fridman, "Analysis and design of integral sliding manifolds for systems with unmatched perturbations," *IEEE Transactions on Automatic Control*, vol. 51, (5), pp. 853–858, 2006.

[21] V. I. Utkin, J. Guldner, and J. Shi, *Sliding Mode Control in Electromechanical Systems.* Taylor & Francis, London, UK, 1999.

[22] C. Edwards and S. K. Spurgeon, *Sliding mode control: theory and applications.* Taylor & Francis, London, U.K., 1998.

[23] J.-J. Slotine and W. Li, *Applied nonlinear control.* Prentice Hall, Englewood Cliffs, NJ, USA, 1991.

[24] A. Levant, "Sliding order and sliding accuracy in sliding mode control," *International Journal of Control*, vol. 58, (6), pp. 1247–1263, 1993.

[25] ——, "Higher-order sliding modes, differentiation and output-feedback control," *International Journal of Control*, vol. 76, (9/10), pp. 924–941, 2003.

[26] ——, "Universal single-input single-output (SISO) sliding-mode controllers with finite-time convergence," *IEEE Transactions on Automatic Control*, vol. 46, (1), pp. 1447–1451, 2001.

[27] G. Bartolini, A. Ferrara, and E. Usai, "Chattering avoidance by second-order sliding mode control," *IEEE Transactions on Automatic Control*, vol. 43, (2), pp. 241–246, 1998.

[28] G. Bartolini, A. Ferrara, E. Usai, and V. I. Utkin, "On multi-input chattering-free second-order sliding mode control," *IEEE Transactions on Automatic Control*, vol. 45(8), pp. 1711–1717, 2000.

[29] G. Bartolini, A. Ferrara, and E. Punta, "Multi-input second-order sliding-mode hybrid control of constrained manipulators," *Dynamics and Control*, vol. 10, (3), pp. 277–296, 2000.

[30] V. I. Utkin, *Sliding Modes in Control and Optimization.* Springer, Berlin, 1992.

[31] C. W. Tao, M.-L. Chan, and T.-T. Lee, "Adaptive fuzzy sliding mode controller for linear systems with mismatched time-varying uncertainties," *IEEE Transactions on Systems, Man, and Cybernetics Part B: Cybernetics*, vol. 33, (2), pp. 283–294, 2003.

[32] H. H. Choi, "An explicit formula of linear sliding surfaces for a class of uncertain dynamic systems with mismatched uncertainties," *Automatica*, vol. 34, (8), pp. 1015–1020, 1998.

[33] ——, "An lmi-based switching surface design method for a class of mismatched uncertain systems," *IEEE Transactions on Automatic Control*, vol. 48, (9), pp. 1634–1638, 2003.

[34] Y.-W. Tsai, K.-K. Shyu, and K.-C. Chang, "Decentralized variable structure control for mismatched uncertain large-scale systems: a new approach," *System and Control Letters*, vol. 43, (2), pp. 117–125, 2001.

[35] K.-K. Shyu, Y.-W. Tsai, and C.-K. Lai, "A dynamic output feedback controllers for mismatched uncertain variable structure systems," *Automatica*, vol. 37, (5), pp. 775–779, 2001.

[36] W.-J. Cao and J.-X. Xu, "Nonlinear integral-type sliding surface for both matched and unmatched uncertain systems," *IEEE Transactions on Automatic Control*, vol. 49, (8), pp. 1355–1360, 2004.

[37] C.-H. Chou and C.-C. Cheng, "A decentralized model reference adaptive variable structure controller for largescale time-varying delay systems," *IEEE Transactions on Automatic Control*, vol. 48, (7), pp. 1123–1127, 2003.

[38] C.-C. Cheng and Y. Chang, "Design of decentralised adaptive sliding mode controllers for large-scale systems with mismatched perturbations," *International Journal of Control*, vol. 81, (10), pp. 1507–1518, 2008.

[39] Y.-J. Huang, T.-C. Kuo, and S.-H. Chang, "Adaptive sliding-mode control for nonlinear systems with uncertain parameters," *IEEE Transactions on Systems , Man, and CybernaticsPart B: Cybernatics*, vol. 38, (2), pp. 534–539, 2008.

[40] F. Plestan, Y. Shtessel, V. Bregeault, and A. Poznyak, "New methodologies for adaptive sliding mode control," *International Journal of Control*, vol. 83, (9), pp. 1907–1919, 2010.

[41] O. Hajek, "Discontinuous differential equations i-ii," *Journal of Differential Equations*, vol. 32, (2), pp. 149–170, 1979.

[42] A. F. Filippov, "Differential equations with discontinuous right-hand side," *American Mathematical Society Translations*, vol. 42, pp. 199–231, 1964.

[43] W. Gao and J. C. Hung, "Variable structure control of nonlinear systems: A new approach," *IEEE Transactions on Industrial Electronics*, vol. 40, (1), pp. 45–50, 1993.

[44] A. Isidori, *Nonlinear Control Systems II*. Springer -Verlag, Berlin., 1999.

[45] A. Levant, "Robust exact differentiation via sliding mode technique," *Automatica*, vol. 34, (3), pp. 379–384, 1998.

[46] S. P. Bhat and D. S. Bernstein, "Continuous finite-time stabilization of the translational and rotational double integrators," *IEEE Tansactions on Automatic Control*, vol. 43 (5), pp. 678–682, 1998.

[47] ——, "Finite-time stability of continuous autonomous systems," *SIAM journal and control optimization*, vol. 38 (3), pp. 751–766, 2000.

[48] Y. Hong, "Finite-time stabilization and stabilizability of a class of controllable systems," *System and control letters*, vol. 46, pp. 231–236, 2002.

[49] E. Moulay and W. Perruquetti, "Finite time stability of non linear systems," in *IEEE Conference on Decision and Control, Hawaii, USA, pp. 3641-3646*, 2003.

[50] ——, "Finite time stability and stabilization of a class of continuous systems," *Journal of Math Analysis Application*, vol. 323, (2), pp. 1430–1443, 2006 b.

[51] ——, "Finite time stability conditions for non autonomous continuous systems," *International Journal of control*, vol. 81, (5), pp. 797–803, 2008.

[52] ——, *Finite-time stability and stabilization: state of the art, in Advances in Variable Structure and Sliding Mode Control, 334, Lecture Notes in Control and Information Sciences, Springer-Verlag, 2006b.* Springer-Verlag, 2006b.

[53] L. Fridman, "An averaging approach to chattering," *IEEE Transactions on Automatic Control*, vol. 46, (8), pp. 1260–1265, 2001.

[54] I. Boiko, L. Fridman, and M. I. Castellanos, "Analysis of second-order sliding-mode algorithms in the frequency domain," *IEEE Transactions on Automatic Control*, vol. 49, (6), pp. 946–950, 2004.

[55] H. Lee and V. I. Utkin, "Chattering suppression methods in sliding mode control systems," *Annual Reviews in Control*, vol. 31, pp. 179–188, 2007.

[56] K. D. Young, V. I. Utkin, and Ümit Özgüner, "A control engineer's guide to sliding mode control," *IEEE Transactions on Control System Technology*, vol. 7, (3), pp. 328–342, 1999.

[57] H. Sira-Ramirez, "Non-linear discrete variable structure system in quasisliding mode," *International Journal of Control*, vol. 54, (5), pp. 1171–1187, 1991.

[58] J. J. Slotine and S. S. Sastry, "Tracking control of nonlinear systems using sliding surfaces with application to robot manipulators," *International Journal of Control*, vol. 38, pp. 465 – 492, 1983.

[59] S. K. Spurgeon and R. Davies, "A nonlinear control strategy for robust sliding mode performance in the presence of unmatched uncertainty," *International Journal of Control*, vol. 57, (5), pp. 1107–1123, 1993.

[60] H. Ashrafiuon, K. R. Muske, and L. C. M. R. A. Soltan, "Sliding-mode tracking control of surface vessels," *IEEE Transactions on Industrial Electronics*, vol. 55 (11), pp. 4004–4012, 2008.

[61] Q. Zong, Z. S. Zhao, and J. Zhang, "Higher order sliding mode control with selftuning law based on integral sliding mode," *IET Control Theory and Applications*, vol. 4(7), pp. 1282–1289, 2010.

[62] M. Defoort, T. Floquet, A. Kokosyd, and W. Perruquetti, "A novel higher order sliding mode control scheme," *System and Control Letters*, vol. 58, pp. 102 – 108, 2009.

[63] S. P. Bhat and D. S. Bernstein, "Geometric homogeneity with applications to finite-time stability," *Math. Control Signals Systems*, vol. 17, pp. 101–127, 2005.

[64] Y. Wang, X. Zhang, X. Yuan, and G. Liu, "Position-sensorless hybrid sliding-mode control of electric vehicles with brushless dc motor," *IEEE Transactions on Vehicular Technology*, vol. 60, (2), pp. 421–432, 2011.

[65] H. Li, X. Liao, C. Li, and C. Li, "Chaos control and synchronization via a novel chatter free sliding mode control strategy," *Neurocomputing*, vol. 74(17), pp. 3212–3222, 2011.

[66] N. Zhang, M. Yang, Y. Jing, and S. Zhang, "Congestion control for Diffserv network using second-order sliding mode control," *IEEE Transactions on Industrial Electronics*, vol. 56, (9), pp. 3330–3336, 2009.

[67] S. Mondal and C. Mahanta, "Nonlinear sliding surface based second order sliding mode controller for uncertain linear systems," *Communications in Nonlinear Science and Numerical Simulation*, vol. 16, pp. 3760–3769, 2011.

[68] V. I. Utkin and K. K. D. Young, "Methods for constructing discontinuity planes in multidimensional variable structure systems," *Automatic Remote Control*, vol. 39, pp. 1466–1470, 1978.

[69] R.-J. Wai and L.-J. Chang, "Adaptive stabilizing and tracking control for a nonlinear inverted-pendulum system via sliding-mode technique," *IEEE Transactions on Industrial Electronics*, vol. 53(2), pp. 674–692, 2006.

[70] Y. J. Huang, T.-C. Kuo, and S.-H. Chang, "Adaptive sliding-mode control for nonlinear systems with uncertain parameters," *IEEE Transactions on Systems, Man, And Cybernetics-Part B:Cybernetics*, vol. 38, (2), pp. 534–539, 2008.

[71] W.-D. Chang and S.-P. Shih, "PID controller design of nonlinear systems using an improved particle swarm optimization approach," *Communications in Nonlinear Science and Numerical Simulation*, vol. 15, pp. 3632–3639, 2010.

[72] B. R. Barmish and G. Leitmann, "On ultimate boundedness control of uncertain systems in the absence of matching assumptions," *IEEE Transactions on Automatic Control*, vol. 27, (1), pp. 153–158, 1982.

[73] S. N. Singh and A. R. C. Antonio, "Nonlinear control of mismatched uncertain linear systems and application to control of aircraft," *Journal of Dynamic Systems, Measurement, and Control*, vol. 106, (3), pp. 203–210, 1984.

[74] K.-K. Shyu, Y.-W. Tsai, and C.-K. Lai, "Sliding mode control for mismatched uncertain systems," *Electronics Letters*, vol. 34, (24), pp. 2359–2360, 1998.

[75] M. C. Pai and A. K. Sinha, "Sliding mode output feedback control of time-varying mismatched uncertain systems," in *Proceedings of IEEE International Conference on Systems, Man, and Cybernetics, vol. 2, pp. 1355-1360*, 2006.

[76] S. Xie, L. Xie, Y. Wang, and G. Guo, "Decentralized control of multimachine power systems with guaranteed performance," *IEE Proceedings Part D: Control Theory Application*, vol. 147, (3), pp. 355–365, 2000.

[77] X.-G. Yan, C. Edwards, S. Spurgeon, and J. Bleijs, "Decentralised sliding-mode control for multimachine power systems using only output information," *IEE Proceedings of Control Theory Application*, vol. 151, (5), pp. 627–635, 2004.

[78] X. Yan and L. Xie, "Reduced-order control for a class of nonlinear similar interconnected systems with mismatched uncertainty," *Automatica*, vol. 39, (1), pp. 91–99, 2003.

[79] P. Li and Z.-Q. Zheng, "Robust adaptive second-order sliding-mode control with fast transient performance," *IET Control Theory and Applications*, vol. 6, (2), pp. 305–312, 2012.

[80] J. G. Juang, K. T. Tu, and W. K. Liu, "Optimal fuzzy switching grey prediction with rga for trms control," in *Proceedings of IEEE International Conference on Systems, Man, and Cybernetics, pp, 681-686*, 2006.

[81] S. M. Ahmad, M. H. Shaheed, A. J. Chipperfield, and M. O. Tokhi, "Nonlinear modelling of a trms using radial basis function networks," in *Proceedings of National Aerospace and Electronics Conference, pp. 313-320*, 2000.

[82] G.-R. Yu and H.-T. Liu, "Sliding mode control of a two-degree-of-freedom helicopter via linear quadratic regulator," in *Proceedings of IEEE International Conference on Systems, Man and Cybernetics, vol. 4, pp. 3299 - 3304*, 2005.

[83] M. L. Martnez, C. Vivas, and M. G. Ortega, "A multivariable nonlinear h infinity controller for a laboratory helicopter," in *Proceedings of IEEE Conference on European Control, pp. 4065-4070*, 2005.

[84] J. G. Juang, M. T. Huang, and W. K. Liu, "PID control using presearched genetic algorithms for a mimo system," *IEEE Transactions on Systems, Man, and Cybernetics-Part C: Applications and Reviews*, vol. 38(5), pp. 716–727, 2008.

[85] P. Wen and T.-W. Lu, "Decoupling control of a twin rotor mimo system using robust deadbeat control technique," *IET Control Theory & Applications*, vol. 2(11), pp. 999–1007, 2008.

[86] S. Hui and S. H. Zak, "Robust control synthesis for uncertain/nonlinear dynamical systems," *Automatica*, vol. 28, (2), pp. 289–298, 1992.

[87] Y. Xia, Z. Zhu, M. Fu, and S. Wang, "Attitude tracking of rigid spacecraft with bounded disturbances," *IEEE Transactions on Industrial Electronics*, vol. 58, (2), pp. 647–659, 2011.

[88] *QNET vertical take off and landing kit user mannual*, Quanser.

[89] J. Han, "From PID to active disturbance rejection control," *IEEE Transactions on Industrial Electronics*, vol. 56, (3), pp. 900–906, 2009.

[90] S. E. Talole, J. P. Kolhe, and S. B. Phadke, "Extended-state-observer-based control offlexible-joint system with experimental validation," *IEEE Transactions on Industrial Electronics*, vol. 57, pp. 1411–1499, Apr. 2010.

[91] Z. Gao, "Active disturbance rejection control: A paradigm shift in feedback control system design," in *Proc. American Control Conference*, June 14-16 2006, pp. 2399–2405.

[92] B. Sridhar and D. P. Lindorff, "Pole-placement with constant gain output feedback," *International Journal of Control*, vol. 18, pp. 993–1003, 1973.

[93] M. Zhihong and X. H. Yu, "Terminal sliding mode control of MIMO linear systems," *IEEE Transactions on circuits and systems -I*, vol. 44(11), pp. 1065–1070, 1997.

[94] S. Yu, X. Yu, B. Shirinzadeh, and Z. Man, "Continuous finite-time control for robotic manipulators with terminal sliding mode," *Automatica*, vol. 41, pp. 1957–1964, 2005.

[95] X. Yu and M. Zhihong, "Fast terminal sliding-mode control design for nonlinear dynamical systems," *IEEE Transactions on Circuits and Systems-I: Fundamental Theory and Applications*, vol. 49(2), pp. 261–264, 2002.

[96] Y. Feng, J. Zheng, X. Yu, and N. V. Truong, "Hybrid terminal sliding-mode observer design method for a permanent-magnet synchronous motor control system," *IEEE Transactions on Industrial Electronics*, vol. 56(9), pp. 3424–3431, 2009.

[97] V. Nekoukar and A. Erfanian, "Adaptive fuzzy terminal sliding mode control for a class of mimo uncertain nonlinear systems," *Fuzzy Sets and Systems*, vol. 179, pp. 34–49, 2011.

[98] Y. Feng, X. Han, Y. Wang, and X. Yu, "Second-order terminal sliding mode control of uncertain multivariable systems," *International Journal of Control*, vol. 80, (6), pp. 856 – 862, 2007.

[99] F.-J. Chang, E.-C. Chang, T.-J. Liang, and J. F. Chen, "Digital-signal-processor-based DC/AC inverter with integral-compensation terminal sliding-mode control," *IET Power Electronics*, vol. 4, (1), pp. 159 –167, 2011.

[100] A. Al-khazraji, N. Essounbouli, A. Hamzaoui, F. Nollet, and JananZaytoon, "Type-2 fuzzy sliding mode control without reaching phase for nonlinear system," *Engineering Applications of Artificial Intelligence*, vol. 24 (1), pp. 23–38, 2011.

[101] S. Skogestad, "Simple analytic rules for model reduction and pid controller tuning," *Journal of Process Control*, vol. 13, pp. 291–309, 2003.

[102] B. M. Chen, T. H. Lee, K. Peng, and V. Venkataramanan, *Hard Disk Drive Servo Systems*, second, Ed. Springer, London, 2006.

[103] Z. Lin, M. Pachter, and S. Banda, "Toward improvement of tracking performance - nonlinear feedback for linear systems," *International Journal of Control*, vol. 70, pp. 1–11, 1998.

[104] B. M. Chen, G. Cheng, and T. H. Lee, "Modeling and compensation of nonlinearities and friction in a micro hard disk servo system with nonlinear control," *IEEE Transactions on Control Systems Technology*, vol. 13(5), pp. 708 – 721, 2005.

[105] S. Mondal and C. Mahanta, "Composite nonlinear feedback based discrete integral sliding mode controller for uncertain systems," *Communications in Nonlinear Science and Numerical Simulation*, vol. 17, pp. 1320–1331, 2012.

[106] B. Bandyopadhyay and D. Fulwani, "High performance tracking controller for discrete plant using nonlinear sliding surface," *IEEE Transactions on Industrial Electronics*, vol. 56, (9), pp. 3628 – 3637, 2009.

[107] B. Bandyopadhyay, D. Fulwani, and K. S. Kim, *Sliding mode control using novel sliding surfaces*. Springer, 2010.

[108] J. Fei and C. Batur, "A novel adaptive sliding mode control with application to mems gyroscope," *ISA Tracsactions*, vol. 48, pp. 73 –78, 2009.

[109] G. Cheng and K. Peng, "Robust composite nonlinear feedback control with application to a servo positioning system," *IEEE Transactions on Industrial Electronics*, vol. 54(2), pp. 1132 – 1140, 2007.

[110] W. Gao, Y. Wang, and A. Homaifa, "Discrete-time variable structure control systems," *IEEE Transactions on Industrial Electronics*, vol. 42(2), pp. 117–122, 1995.

[111] K. Furuta, "Sliding mode control of a discrete system," *System and Control Letters*, vol. 14(2), pp. 145 –152, 1990.

[112] A. Bartoszewicz, "Discrete-time quasi-sliding-mode control strategies," *IEEE Transactions on Industrial Electronics*, vol. 45, (1), pp. 633–637, 1998.

[113] ——, "Remarks on discrete-time variable structure control systems," *IEEE Transactions on Industrial Electronics*, vol. 43, (1), pp. 235–238, 1996.

[114] B. Bandyopadhyay, D. Fulwani, and Y. J. Park, "A robust algorithm against actuator saturation using integral sliding mode and composite nonlinear feedback," in *In Proc. 17th IFAC World Congress, pp. 14174-14179, Seoul, Korea*, 2008.

[115] S. Janardhanan and B. Bandyopadhyay, "Output feedback sliding-mode control for uncertain systems using fast output sampling technique," *IEEE Transactions on Industrial Electronics*, vol. 53, (5), pp. 1677–1682, 2006.

[116] K. Abidi and A. Śabanovic, "Sliding-mode control for high-precision motion of a piezostage," *IEEE Transactions on Industrial Electronics*, vol. 54 (1), pp. 629–637, 2007.

[117] C. M. Saaj, B. Bandyopadhyay, and H. Unbehauen, "A new algorithm for discrete-time sliding mode control using fast output sampling feedback," *IEEE Transactions on Industrial Electronics*, vol. 49, pp. 518–523, 2002.

[118] P. Ignaciuk and A. Bartoszewicz, "Linear quadratic optimal discrete-time sliding-mode controller for connection-oriented communication networks," *IEEE Transactions on Industrial Electronics*, vol. 55, (11), pp. 4013–4021, 2008.

[119] Z. Xi and T. Hesketh, "Discrete time integral sliding mode control for systems with matched and unmatched uncertainties," *IET Control Theory and Applications*, vol. 4(5), pp. 889–896, 2009.

[120] S. Laghrouche, F. Plestanb, and A. Glumineaub, "Higher order sliding mode control based on integral sliding mode," *Automatica*, vol. 43, pp. 531–537, 2007.

[121] W. C. Su, S. V. Drakunov, and U. Ozguner, "An O(T2) boundary layer in sliding mode for sampled-data systems," *IEEE Transactions on Automatic Control*, vol. 45, (3), pp. 482–485, 2000.

[122] B. M. Chen, T. H. Lee, K. Peng, and V. Venkataramanan, "Composite nonlinear feedback control for linear systems with input saturation: Theory and an application," *IEEE Transactions on Automatic Control*, vol. 48(3), pp. 427–439, 2003.

[123] W. Lan, C. K. Thum, and B. M. Chen, "A hard-disk-drive servo system design using composite nonlinear-feedback control with optimal nonlinear gain tuning methods," *IEEE Transactions on Industrial Electronics*, vol. 57, (5), pp. 1735–1745, 2010.